

Supplementary Information

There and back again: the role of hyperconjugation in the fluorine gauche effect

Vinícius C. Port,^a Rodrigo A. Cormanich^{*a}

University of Campinas, Institute of Chemistry, Department of Organic Chemistry, 13083-970 – Campinas, SP, Brazil.

*Corresponding author: cormanich@unicamp.br

Contents

Computational Details	11
Table S1. Atomic Coordinates for the <i>gauche</i> and <i>anti</i> conformers of XCH ₂ CH ₂ X molecules obtained at the M06-2X/6-311++G(3df,2p) level.....	12
Table S2. Atomic Coordinates for the <i>gauche</i> and <i>anti</i> conformers of XBH ₂ NH ₂ X molecules obtained at the M06-2X/6-311++G(3df,2p) level.....	13
Table S3. Atomic Coordinates for the <i>gauche</i> and <i>anti</i> conformers of XCH ₂ OX molecules obtained at the M06-2X/6-311++G(3df,2p) level.....	14
Table S4. Atomic Coordinates for the <i>gauche</i> and <i>anti</i> conformers of XCH ₂ SX molecules molecules obtained at the M06-2X/6-311++G(3df,2p) level.....	15
Table S5. Atomic Coordinates for the <i>gauche</i> and <i>anti</i> conformers of XOOX molecules obtained at the M06-2X/6-311++G(3df,2p) level.	16
Table S6. Atomic Coordinates for the <i>gauche</i> and <i>anti</i> conformers of XSSX molecules obtained at the M06-2X/6-311++G(3df,2p) level.	16
Table S7. Benchmarking study of methods/functionals (left) and basis sets (right) with respect to the CCSD(T)/CBS level. Mean absolute deviations are given in kcal mol ⁻¹	18
Table S8. Geometrical parameters of the XCH ₂ CH ₂ X systems obtained in the M06-2X/6-311++G(3df,2p) level, distances are given in Å and angles in degrees.	19
Table S9. Geometrical parameters of the XBH ₂ NH ₂ X systems obtained in the M06-2X/6-311++G(3df,2p) level, distances are given in Å and angles in degrees.	20

Table S10. Geometrical parameters of the XCH ₂ OX systems obtained in the M06-2X/6-311++G(3df,2p) level, distances are given in Å and angles in degrees.....	21
Table S11. Geometrical parameters of the XCH ₂ SX systems obtained in the M06-2X/6-311++G(3df,2p) level, distances are given in Å and angles in degrees.....	22
Table S12. Geometrical parameters of the XOOX systems obtained in the M06-2X/6-311++G(3df,2p) level, distances are given in Å and angles in degrees.....	23
Table S13. Geometrical parameters of the XSSX systems obtained in the M06-2X/6-311++G(3df,2p) level, distances are given in Å and angles in degrees.....	24
Figure S1. Potential energy curves for XCH ₂ CH ₂ X molecules calculated at the M06-2X/6-311++G(3df,2p) level.....	25
Figure S2. Potential energy curves for XBH ₂ NH ₂ X molecules calculated at the M06-2X/6-311++G(3df,2p) level.....	26
Figure S3. Potential energy curves for XCH ₂ OX molecules calculated at the M06-2X/6-311++G(3df,2p) level.....	27
Figure S4. Potential energy curves for XCH ₂ SX molecules calculated at the M06-2X/6-311++G(3df,2p) level.....	28
Figure S5. Potential energy curves for XOOX molecules calculated at the M06-2X/6-311++G(3df,2p) level.....	29
Figure S6. Potential energy curves for XSSX molecules calculated at the M06-2X/6-311++G(3df,2p) level.....	30
Figure S7. NBO deletion analysis calculated for FCH ₂ CH ₂ F at the M06-2X/6-311++G(3df,2p) level.....	31
Figure S8. NBO deletion analysis calculated for ClCH ₂ CH ₂ Cl at the M06-2X/6-311++G(3df,2p) level.....	32
Figure S9. NBO deletion analysis calculated for BrCH ₂ CH ₂ Br at the M06-2X/6-311++G(3df,2p) level.....	33
Figure S10. NBO deletion analysis calculated for FBH ₂ NH ₂ F at the M06-2X/6-311++G(3df,2p) level.....	34
Figure S11. NBO deletion analysis calculated for ClBH ₂ NH ₂ Cl at the M06-2X/6-311++G(3df,2p) level.....	35

Figure S12. NBO deletion analysis calculated for BrBH ₂ NH ₂ Br at the M06-2X/6-311++G(3df,2p) level.	36
Figure S13. NBO deletion analysis calculated for FCH ₂ OF at the M06-2X/6-311++G(3df,2p) level.	37
Figure S14. NBO deletion analysis calculated for ClCH ₂ OCl at the M06-2X/6-311++G(3df,2p) level.	38
Figure S15. NBO deletion analysis calculated for BrCH ₂ OB _r at the M06-2X/6-311++G(3df,2p) level.	39
Figure S16. NBO deletion analysis calculated for FCH ₂ SF at the M06-2X/6-311++G(3df,2p) level.	40
Figure S17. NBO deletion analysis calculated for ClCH ₂ SCl at the M06-2X/6-311++G(3df,2p) level.	41
Figure S18. NBO deletion analysis calculated for BrCH ₂ SBr at the M06-2X/6-311++G(3df,2p) level.	42
Figure S19. NBO deletion analysis calculated for FOOF at the M06-2X/6-311++G(3df,2p) level.	43
Figure S20. NBO deletion analysis calculated for ClOOCl at the M06-2X/6-311++G(3df,2p) level.	44
Figure S21. NBO deletion analysis calculated for BrOOBr at the M06-2X/6-311++G(3df,2p) level.	45
Figure S22. NBO deletion analysis calculated for FSSF at the M06-2X/6-311++G(3df,2p) level.	46
Figure S23. NBO deletion analysis calculated for ClSSCl at the M06-2X/6-311++G(3df,2p) level.	47
Figure S24. NBO deletion analysis calculated for BrSSBr at the M06-2X/6-311++G(3df,2p) level.	48
Figure S25. Hyperconjugation interaction energies for FCH ₂ CH ₂ F obtained at the M06-2X/6-311++G(3df,2p) level using NBO analysis.	49
Figure S26. Hyperconjugation interaction energies for ClCH ₂ CH ₂ Cl obtained at the M06-2X/6-311++G(3df,2p) level using NBO analysis.	50
Figure S27. Hyperconjugation interaction energies for BrCH ₂ CH ₂ Br obtained at the M06-2X/6-311++G(3df,2p) level using NBO analysis.	51

Figure S28. Hyperconjugation interaction energies for FBH ₂ NH ₂ F obtained at the M06-2X/6-311++G(3df,2p) level using NBO analysis.	52
Figure S29. Hyperconjugation interaction energies for ClBH ₂ NH ₂ Cl obtained at the M06-2X/6-311++G(3df,2p) level using NBO analysis.	53
Figure S30. Hyperconjugation interaction energies for BrBH ₂ NH ₂ Br obtained at the M06-2X/6-311++G(3df,2p) level using NBO analysis.	54
Figure S31. Hyperconjugation interaction energies for FCH ₂ OF obtained at the M06-2X/6-311++G(3df,2p) level using NBO analysis.	55
Figure S32. Hyperconjugation interaction energies for ClCH ₂ OCl obtained at the M06-2X/6-311++G(3df,2p) level using NBO analysis.	56
Figure S33. Hyperconjugation interaction energies for BrCH ₂ OBr obtained at the M06-2X/6-311++G(3df,2p) level using NBO analysis.	57
Figure S34. Hyperconjugation interaction energies for FCH ₂ SF obtained at the M06-2X/6-311++G(3df,2p) level using NBO analysis.	58
Figure S35. Hyperconjugation interaction energies for ClCH ₂ SCl obtained at the M06-2X/6-311++G(3df,2p) level using NBO analysis.	59
Figure S36. Hyperconjugation interaction energies for BrCH ₂ SBr obtained at the M06-2X/6-311++G(3df,2p) level using NBO analysis.	60
Figure S37. Hyperconjugation interaction energies for FOOF obtained at the M06-2X/6-311++G(3df,2p) level using NBO analysis..	61

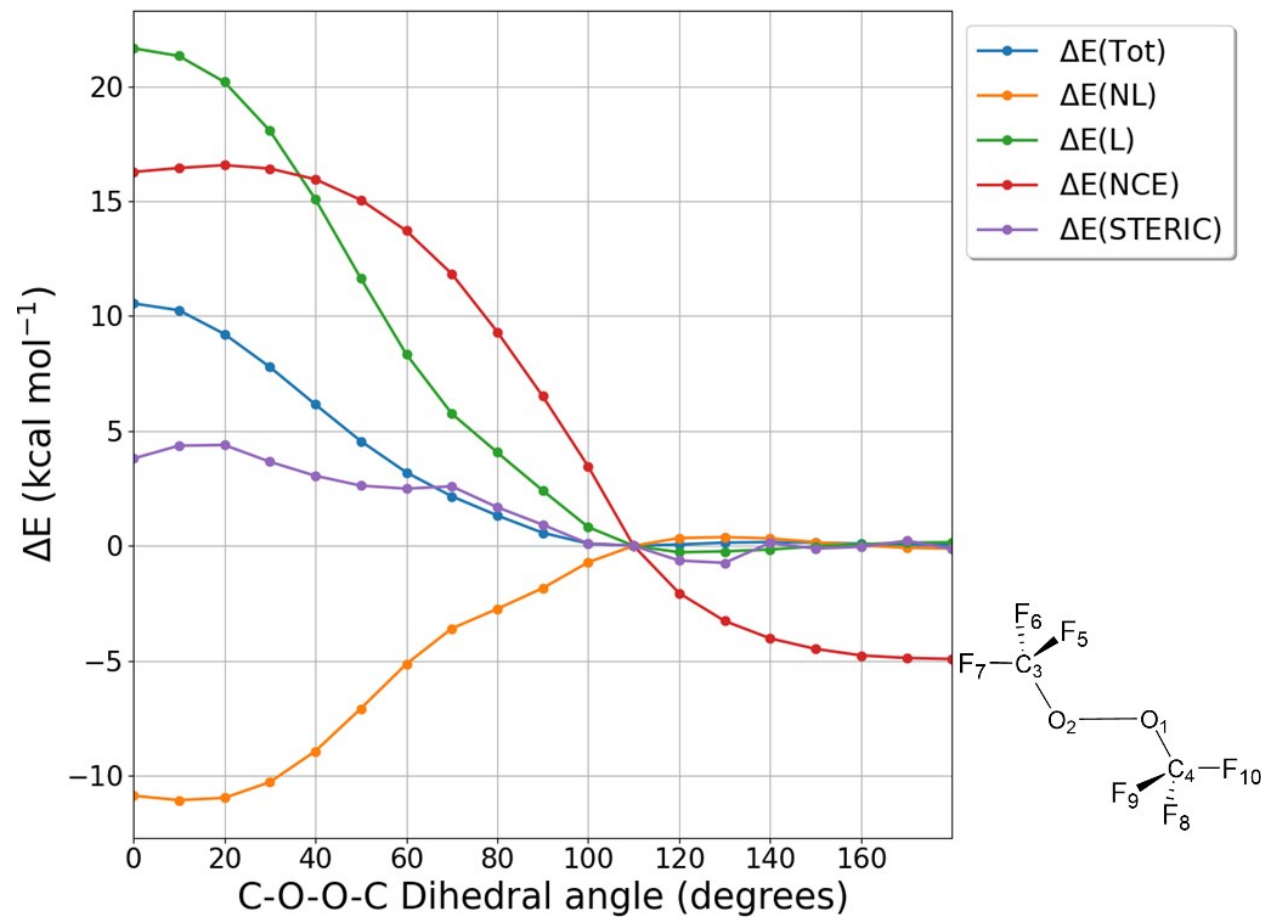
Figure S38. Hyperconjugation interaction energies for ClOOCl obtained at the M06-2X/6-311++G(3df,2p) level using NBO analysis.	62
Figure S39. Hyperconjugation interaction energies for BrOOBr obtained at the M06-2X/6-311++G(3df,2p) level using NBO analysis.	63
Figure S40. Hyperconjugation interaction energies for FSSF obtained at the M06-2X/6-311++G(3df,2p) level using NBO analysis.	64
Figure S41. Hyperconjugation interaction energies for ClSSCl obtained at the M06-2X/6-311++G(3df,2p) level using NBO analysis.	65
Figure S42. Hyperconjugation interaction energies for BrSSBr obtained at the M06-2X/6-311++G(3df,2p) level using NBO analysis.	66
Figure S43. Atomic charges and natural Coulomb electrostatic (NCE) energy curves for FCH ₂ CH ₂ F calculated at the M06-2X/6-311++G(3df,2p) level.	67
Figure S44. Atomic charges and natural Coulomb electrostatic (NCE) energy curves for ClCH ₂ CH ₂ Cl calculated at the M06-2X/6-311++G(3df,2p) level.	68
Figure S45. Atomic charges and natural Coulomb electrostatic (NCE) energy curves for BrCH ₂ CH ₂ Br calculated at the M06-2X/6-311++G(3df,2p) level.	69
Figure S46. Atomic charges and natural Coulomb electrostatic (NCE) energy curves for FBH ₂ NH ₂ F calculated at the M06-2X/6-311++G(3df,2p) level.	70
Figure S47. Atomic charges and natural Coulomb electrostatic (NCE) energy curves for ClBH ₂ NH ₂ Cl calculated at the M06-2X/6-311++G(3df,2p) level.	71

Figure S48. Atomic charges and natural Coulomb electrostatic (NCE) energy curves for BrBH ₂ NH ₂ Br calculated at the M06-2X/6-311++G(3df,2p) level	72
Figure S49. Atomic charges and natural Coulomb electrostatic (NCE) energy curves for FCH ₂ OF calculated at the M06-2X/6-311++G(3df,2p) level	73
Figure S50. Atomic charges and natural Coulomb electrostatic (NCE) energy curves for ClCH ₂ OCl calculated at the M06-2X/6-311++G(3df,2p) level	74
Figure S51. Atomic charges and natural Coulomb electrostatic (NCE) energy curves for BrCH ₂ OBr calculated at the M06-2X/6-311++G(3df,2p) level	75
Figure S52. Atomic charges and natural Coulomb electrostatic (NCE) energy curves for FCH ₂ SF calculated at the M06-2X/6-311++G(3df,2p) level	76
Figure S53. Atomic charges and natural Coulomb electrostatic (NCE) energy curves for ClCH ₂ SCl calculated at the M06-2X/6-311++G(3df,2p) level	77
Figure S54. Atomic charges and natural Coulomb electrostatic (NCE) energy curves for BrCH ₂ SBr calculated at the M06-2X/6-311++G(3df,2p) level	78
Figure S55. Atomic charges and natural Coulomb electrostatic (NCE) energy curves for FOOF calculated at the M06-2X/6-311++G(3df,2p) level	79
Figure S56. Atomic charges and natural Coulomb electrostatic (NCE) energy curves for ClOOCl calculated at the M06-2X/6-311++G(3df,2p) level	80
Figure S57. Atomic charges and natural Coulomb electrostatic (NCE) energy curves for BrOOBr calculated at the M06-2X/6-311++G(3df,2p) level	81

Figure S58. Atomic charges and natural Coulomb electrostatic (NCE) energy curves for FSSF calculated at the M06-2X/6-311++G(3df,2p) level	82
Figure S59. Atomic charges and natural Coulomb electrostatic (NCE) energy curves for ClSSCl calculated at the M06-2X/6-311++G(3df,2p) level	83
Figure S60. Atomic charges and natural Coulomb electrostatic (NCE) energy curves for BrSSBr calculated at the M06-2X/6-311++G(3df,2p) level	84
Figure S61. a) $\sigma_{\text{CH}} \rightarrow \sigma^*_{\text{CF}}$ and b) $\text{LP}(2)\text{F} \rightarrow \sigma^*_{\text{CH}}$ hyperconjugative interaction representations for the <i>gauche</i> and c) $\text{LP}(2)\text{F} \rightarrow \sigma^*_{\text{CH}}$ hyperconjugative interaction for the <i>anti</i> conformer of $\text{FCH}_2\text{CH}_2\text{F}$. All orbital isosurfaces were plotted with isovalues of 0.07 au.	85
Figure S62. a) $\sigma_{\text{CF}} \rightarrow \sigma^*_{\text{CF}}$, b) $\sigma_{\text{CCl}} \rightarrow \sigma^*_{\text{CCl}}$ and c) $\sigma_{\text{CBr}} \rightarrow \sigma^*_{\text{CBr}}$ hyperconjugative interaction representations for the <i>anti</i> conformers of $\text{FCH}_2\text{CH}_2\text{F}$, $\text{ClCH}_2\text{CH}_2\text{Cl}$ and $\text{BrCH}_2\text{CH}_2\text{Br}$, respectively. All orbital isosurfaces were plotted with isovalues of 0.07 au.....	86
Figure S63. a) $\text{LP}(2)\text{O} \rightarrow \sigma^*_{\text{CF}}$ b) $\sigma_{\text{CH}} \rightarrow \sigma^*_{\text{OF}}$ hyperconjugative interactions for the <i>gauche</i> conformer of FCH_2OF and c) $\text{LP}(2)\text{O} \rightarrow \sigma^*_{\text{OF}}$ for the <i>gauche</i> conformer of FOOF . All orbital isosurfaces were plotted with isovalues of 0.07 a.u.	87
Figure S64. Number of remaining hyperconjugative interactions and the amplitude of the “Others” curve <i>versus</i> the cutoff value for the decomposition of hyperconjugative interactions and electrostatics interactions for $\text{XCH}_2\text{CH}_2\text{X}$ molecules.	88
Figure S65. Number of remaining hyperconjugative interactions and the amplitude of the “Others” curve <i>versus</i> the cutoff value for the decomposition of hyperconjugative interactions and electrostatics interactions for $\text{XBH}_2\text{NH}_2\text{X}$ molecules.	89
Figure S66. Number of remaining hyperconjugative interactions and the amplitude of the “Others” curve <i>versus</i> the cutoff value for the decomposition of hyperconjugative interactions and electrostatics interactions for XCH_2OX molecules.	90
Figure S67. Number of remaining hyperconjugative interactions and the amplitude of the “Others” curve <i>versus</i> the cutoff value for the decomposition of hyperconjugative interactions and electrostatics interactions for XOOX molecules.	91

Figure S68. Number of remaining hyperconjugative interactions and the amplitude of the “Others” curve *versus* the cutoff value for the decomposition of hyperconjugative interactions and electrostatics interactions for XCH_2SX molecules.....92

Figure S69. Number of remaining hyperconjugative interactions and the amplitude of the “Others” curve *versus* the cutoff value for the decomposition of hyperconjugative interactions and electrostatics interactions for XSSX molecules.....93



94

9

Figure S70. NBO deletion analysis calculated for CF_3OOCF_3 at the M06-2X/6-311++G(3df,2p) level	94
Figure S71. Hyperconjugation interaction energies for CF_3OOCF_3 obtained at the M06-2X/6-311++G(3df,2p) level using NBO analysis.	95
Figure S72. Atomic charges and natural Coulomb electrostatic (NCE) energy curves for CF_3OOCF_3 calculated at the M06-2X/6-311++G(3df,2p) level.	96

Computational Details

All optimization, frequency and energy calculations were done using the Gaussian16 Rev C.01 software.²⁴ To determine the most accurate level of theory, the F-C-C-F dihedral angle was scanned from 0 to 180° in 10° increments in the M06-2X/6-311+G(d) level for **DFE**. On the obtained geometries, single point calculations were performed using several DFT functionals and *ab initio* methods as well as several basis sets. The energies of all resulting geometries from the scan calculations were then compared to that obtained from the CCSD(T)/CBS level of theory. The M06-2X/6-311++G(3df,2p) level showed the lowest mean absolute deviations and was used in all further calculations. Natural Bond Orbitals analysis calculations were run at the M06-2X/6-311++G(3df,2p) level using the NBO 7.0 program.²⁵ Likewise, NBodel analysis was done by excluding all Rydberg and non-Lewis orbitals. The Natural Coulomb Electrostatic analysis (NCE)¹⁰ was carried out for the optimized geometries for the classical Coulomb

equation: $E_{AB} = \frac{Q_A Q_B}{R_{AB}}$, where (R_{AB}) are the optimized interatomic distances and (Q_A, Q_B) are NPA atomic charges. The Natural Steric Analysis (NSA)²¹ was done using the STERIC keyword in the NBO 7.0 software. All the individual hyperconjugative interactions were obtained setting the threshold for printing an interaction to 0.0 kcal mol⁻¹ in the NBO 7.0 program.

Table S1. Atomic Coordinates for the *gauche* and *anti* conformers of XCH₂CH₂X molecules obtained at the M06-2X/6-311++G(3df,2p) level.

		<i>gauche</i>			<i>anti</i>		
FCH ₂ CH ₂ F	C	-0.2641	0.70313	-0.5121	C	0.42346	-0.6274
	H	0.02156	1.20849	-1.4374	H	1.05097	-0.6713
	H	-1.3506	0.70298	-0.4109	H	1.05046	-0.6724
	C	0.26414	-0.7031	-0.5121	C	-0.4235	0.62735
	H	-0.0216	-1.2085	-1.4374	H	-1.051	0.67131
	H	1.35063	-0.703	-0.4109	H	-1.0505	0.67237
	F	-0.2641	-1.4052	0.54677	F	0.42346	1.71347
	F	0.26414	1.40521	0.54677	F	-0.4235	-1.7135
	C	0.64737	0.88604	0.38762	C	0.4892	0.57607
	H	0.46602	0.8037	1.45567	H	0.37421	1.19087
ClCH ₂ CH ₂ Cl	H	1.19405	1.80352	0.17872	H	0.37416	1.18995
	C	-0.6473	0.88609	-0.3876	C	-0.489	-0.5759
	H	-1.1939	1.8036	-0.1787	H	-0.3738	-1.1907
	H	-0.4659	0.80377	-1.4556	H	-0.3738	-1.1896
	Cl	-1.7049	-0.4661	0.08271	Cl	-2.1521	0.07049
	Cl	1.70485	-0.4661	-0.0827	Cl	2.15197	-0.0706
	C	0.6315	1.17723	0.41451	C	0.46003	0.59638
BrCH ₂ CH ₂ Br	H	0.41738	1.09259	1.47544	H	0.33902	1.20488
	H	1.19616	2.08646	0.22127	H	0.33876	1.20438
	C	-0.6279	1.1776	-0.4144	C	-0.4601	-0.5963
	H	-1.1939	2.08577	-0.2224	H	-0.3386	-1.2045
	H	-0.4163	1.09142	-1.4754	H	-0.3388	-1.2046
	Br	-1.8141	-0.2923	0.03854	Br	-2.3068	0.03049
	Br	1.81334	-0.293	-0.0385	Br	2.30681	-0.0305

Table S2. Atomic Coordinates for the *gauche* and *anti* conformers of XBH₂NH₂X molecules obtained at the M06-2X/6-311++G(3df,2p) level.

		<i>gauche</i>			<i>anti</i>		
FBH ₂ NH ₂ F	B	-0.8479	0.5436	-0.3533	B	-0.7293	0.66927
	H	-1.2061	1.60125	0.12499	H	-0.5954	1.28378
	H	-0.6801	0.55065	-1.5425	H	-0.5954	1.28355
	N	0.65542	0.48265	0.28934	N	0.53769	-0.4197
	H	0.60414	0.31504	1.2958	H	0.5041	-1.0124
	H	1.17212	1.34333	0.10971	H	0.50391	-1.012
	F	1.45936	-0.5315	-0.1887	F	1.78097	0.15261
ClBH ₂ NH ₂ Cl	F	-1.4859	-0.5692	0.16128	F	-1.7737	-0.2583
	B	0.73555	0.98046	0.45134	B	0.5675	0.82227
	H	0.44759	0.97157	1.60748	H	0.38429	1.4116
	H	1.16211	2.01533	0.01778	H	0.38226	1.41179
	N	-0.6581	0.82792	-0.3782	N	-0.4799	-0.4312
	H	-0.4414	0.67448	-1.3632	H	-0.3182	-1.01
	H	-1.2064	1.68237	-0.2914	H	-0.3162	-1.012
BrBH ₂ NH ₂ Br	Cl	-1.6931	-0.4755	0.0996	Cl	-2.1487	0.01894
	Cl	1.75	-0.4681	-0.0749	Cl	2.17156	-0.1304
	B	0.68826	1.28326	0.48548	B	0.51355	0.89428
	H	0.37167	1.25604	1.63123	H	0.33362	1.47661
	H	1.15363	2.30713	0.07389	H	0.33197	1.47569
	N	-0.6534	1.12397	-0.4039	N	-0.4526	-0.4016
	H	-0.3973	0.97591	-1.3802	H	-0.2719	-0.9756

Table S3. Atomic Coordinates for the *gauche* and *anti* conformers of XCH₂OX molecules obtained at the M06-2X/6-311++G(3df,2p) level.

	<i>gauche</i>				<i>anti</i>			
FCH ₂ OF	O	-0.6073	0.58732	-0.3521	O	-0.4634	-0.5711	0.00036
	C	0.61104	0.49803	0.2875	C	0.49286	0.47659	0.0003
	H	0.47768	0.39622	1.36448	H	0.38842	1.07041	0.90892
	H	1.11373	1.42457	0.00487	H	0.38791	1.071	-0.9078
	F	1.32053	-0.5679	-0.1572	F	1.6725	-0.1687	-0.0003
	F	-1.3649	-0.4885	0.12643	F	-1.6754	0.12063	-0.0003
ClCH ₂ OCl	O	-0.6392	0.83731	-0.4185	O	-0.4469	-0.5343	0.00115
	C	0.54181	0.89842	0.30664	C	0.42919	0.57275	0.00071
	H	0.36192	0.87542	1.37883	H	0.29921	1.16917	0.90182
	H	1.02057	1.82031	-0.0108	H	0.29805	1.1695	-0.9
	Cl	1.65403	-0.4457	-0.0609	Cl	2.05271	-0.1027	-0.0004
	Cl	-1.6258	-0.424	0.06917	Cl	-2.029	0.01445	-0.0005
BrCH ₂ OBr	O	-0.6481	1.09948	-0.4362	O	-0.4334	-0.5108	0.00152
	C	0.50197	1.1789	0.31959	C	0.39579	0.62035	0.00088
	H	0.31245	1.1487	1.38929	H	0.27037	1.21586	0.90234
	H	0.99831	2.09454	0.01227	H	0.26926	1.21577	-0.9004
	Br	1.77106	-0.2736	-0.0274	Br	2.20242	-0.0548	-0.0003
	Br	-1.7464	-0.2725	0.03227	Br	-2.1866	-0.0042	-0.0003

Table S4. Atomic Coordinates for the *gauche* and *anti* conformers of XCH_2SX molecules molecules obtained at the M06-2X/6-311++G(3df,2p) level.

		<i>gauche</i>				<i>anti</i>		
FCH ₂ SF	S	0.68524	-0.58	-0.1841	S	0.53684	-0.6	-0.0002
	C	-0.9131	-0.2579	0.4906	C	-0.8134	0.61227	-0.0005
	H	-0.8018	0.29366	1.42364	H	-0.7673	1.22258	-0.9006
	H	-1.3565	-1.2396	0.6731	H	-0.7662	1.22375	0.89874
	F	-1.7349	0.45065	-0.3448	F	-1.9637	-0.1213	0.00052
	F	1.36523	0.85751	0.11211	F	1.72204	0.50804	0.00039
ClCH ₂ SCl	S	-0.7067	0.9806	-0.2737	S	-0.4379	0.73912	-0.0009
	C	0.82574	0.69038	0.58897	C	0.66804	-0.6881	-0.0022
	H	0.63036	0.36472	1.60557	H	0.5293	-1.2798	-0.9013
	H	1.335	1.65266	0.5914	H	0.52693	-1.283	0.89452
	Cl	1.89885	-0.5088	-0.1667	Cl	2.3089	-0.0258	0.00107
	Cl	-1.6407	-0.7764	0.0872	Cl	-2.1946	-0.2762	0.0009
BrCH ₂ SBr	S	-0.6991	1.33471	-0.3051	S	-0.4106	0.81874	-0.0012
	C	0.77195	1.00722	0.63994	C	0.60432	-0.6665	-0.0029
	H	0.53176	0.71096	1.65456	H	0.45382	-1.2512	-0.9036
	H	1.32668	1.94281	0.63631	H	0.45147	-1.2549	0.895
	Br	1.95591	-0.3588	-0.0785	Br	2.43425	-0.04	0.00068
	Br	-1.8218	-0.4998	0.04281	Br	-2.376	-0.1484	0.00059

Table S5. Atomic Coordinates for the *gauche* and *anti* conformers of xOOX molecules obtained at the M06-2X/6-311++G(3df,2p) level.

	<i>gauche</i>				<i>anti</i>			
FOOF	O	-0.2948	-0.5734	0.54923	O	-0.452	-0.5557	0
	O	0.29478	0.57339	0.54923	O	0.45196	0.55566	0
	F	0.29478	-1.3305	-0.4882	F	0.45196	-1.5822	0
	F	-0.2948	1.33054	-0.4882	F	-0.452	1.58215	0
ClOOC _l	O	0.55386	0.82551	0.40996	O	0.43851	-0.5785	-0.0004
	O	-0.5539	0.82552	-0.41	O	-0.4385	0.57845	-0.0004
	Cl	1.62461	-0.3885	-0.0658	Cl	1.96601	0.06072	0.00018
	Cl	-1.6246	-0.3885	0.06577	Cl	-1.966	-0.0607	0.00018
BrOOBr	O	0.53594	1.07271	0.42555	O	0.41168	-0.5926	-0.0005
	O	-0.5359	1.07271	-0.4255	O	-0.4117	0.59261	-0.0005
	Br	1.74194	-0.2452	-0.0299	Br	2.11199	0.0264	0.00012
	Br	-1.7419	-0.2452	0.02993	Br	-2.112	-0.0264	0.00012

Table S6. Atomic Coordinates for the *gauche* and *anti* conformers of XSSX molecules obtained at the M06-2X/6-311++G(3df,2p) level.

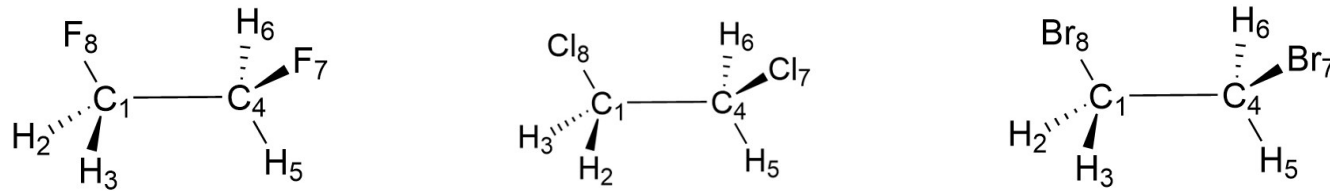
	<i>gauche</i>				<i>anti</i>			
FSSF	S	-0.8143	0.67388	-0.0003	S	-0.8529	-0.3951	0.41739

	S	0.81434	-0.6739	-0.0003	S	0.85288	-0.3952	-0.4174
	F	-1.9096	-0.5109	0.00061	F	-1.769	0.70249	-0.3578
	F	1.90963	0.51089	0.00061	F	1.76902	0.7025	0.35774
ClSSCl	S	-0.8196	-0.776	0.53356	S	0.00012	-1.0519	0
	S	0.82016	-0.775	-0.5339	S	0	1.05163	0
	Cl	-1.999	0.72984	-0.2059	Cl	-2.0077	-1.2413	0
	Cl	1.99843	0.72987	0.20622	Cl	2.00758	1.2416	0
BrSSBr	S	0.78124	1.11286	0.59081	S	0	1.04974	0
	S	-0.7811	1.11273	-0.5909	S	-5E-06	-1.05	0
	Br	2.12416	-0.5087	-0.0993	Br	2.16626	1.25868	0
	Br	-2.1242	-0.5087	0.09934	Br	-2.1663	-1.2585	0

Table S7. Benchmarking study of methods/functionals (left) and basis sets (right) with respect to the CCSD(T)/CBS level. Mean absolute deviations are given in kcal mol⁻¹

Method	MAD	Basis set	MAD
B3LYP/aug-cc-pVTZ	0.1035	M06-2X/6-311++G(3df,2p)	0.0314
B3LYP-D3/aug-cc-pVTZ	0.1040	M06-2X/cc-pVDZ	0.2242
M06/aug-cc-pVTZ	0.1240	M06-2X/cc-pVTZ	0.0391
M06L/aug-cc-pVTZ	0.2407	M06-2X/cc-pVQZ	0.0149
M06-2X/aug-cc-pVTZ	0.0566	M06-2X/cc-pV5Z	0.0050
M11/aug-cc-pVTZ	0.1856	M06-2X/aug-cc-pVDZ	0.0640
MP2/aug-cc-pVTZ	0.1691	M06-2X/aug-cc-pVTZ	0.0633
MP3/aug-cc-pVTZ	0.0169	M06-2X/aug-cc-pVQZ	0.0149
MP4(SDQ)/aug-cc-pVTZ	0.0182	-	-
CCSD(<i>T</i>)/CBS	0.0000	CCSD(<i>T</i>)/CBS	0.0000

Table S8. Geometrical parameters of the XCH₂CH₂X systems obtained in the M06-2X/6-311++G(3df,2p) level, distances are given in Å and angles in degrees.

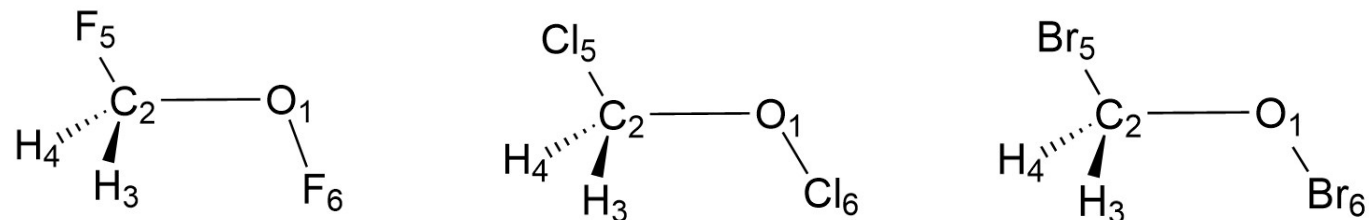


Parameter	<i>syn</i>	<i>gauche</i>	<i>anticlinal</i>	<i>anti</i>	<i>syn</i>	<i>gauche</i>	<i>anticlinal</i>	<i>anti</i>	<i>syn</i>	<i>gauche</i>	<i>anticlinal</i>	<i>anti</i>
$\phi^{[a]}$	0	70	120	180	0	70	120	180	0	70	120	180
<i>r</i> (1-2)	1.091	1.092	1.090	1.091	1.086	1.086	1.085	1.086	1.085	1.086	1.083	1.085
<i>r</i> (1-3)	1.091	1.091	1.090	1.090	1.086	1.088	1.086	1.086	1.085	1.088	1.085	1.085
<i>r</i> (1-4)	1.546	1.502	1.522	1.514	1.545	1.509	1.528	1.511	1.539	1.508	1.525	1.506
<i>r</i> (1-8)	1.369	1.376	1.380	1.377	1.775	1.780	1.785	1.784	1.938	1.940	1.948	1.950
<i>r</i> (4-5)	1.091	1.092	1.090	1.091	1.086	1.088	1.086	1.086	1.084	1.087	1.085	1.085
<i>r</i> (4-6)	1.091	1.091	1.090	1.090	1.086	1.086	1.085	1.086	1.084	1.085	1.083	1.085
<i>r</i> (4-7)	1.369	1.376	1.380	1.377	1.774	1.780	1.785	1.784	1.938	1.942	1.949	1.950
\angle (2-1-3)	109.0	109.8	109.7	109.6	108.7	109.7	109.3	109.7	109.0	110.0	109.6	110.3
\angle (2-1-4)	110.8	109.9	112.2	110.8	109.5	111.2	111.1	111.3	109.8	111.9	112.3	112.1
\angle (2-1-8)	107.9	108.4	107.2	108.8	106.1	107.5	106.8	107.7	104.8	106.8	105.6	106.6
\angle (3-1-4)	110.8	110.5	109.1	110.8	109.5	109.4	111.2	111.2	109.8	109.6	111.5	112.1
\angle (3-1-8)	107.9	108.1	108.5	108.7	106.1	106.9	106.6	107.7	104.8	106.0	105.8	106.6
\angle (4-1-8)	110.5	110.0	110.1	108.0	116.5	112.0	111.7	109.1	118.2	112.4	111.8	108.9
\angle (1-4-5)	110.8	109.9	112.2	110.8	109.6	109.4	111.2	111.3	109.8	109.8	111.5	112.1
\angle (1-4-6)	110.8	110.5	109.1	110.8	109.6	111.2	111.1	111.2	109.8	112.0	112.3	112.1
\angle (1-4-7)	110.5	110.0	110.1	108.0	116.5	112.0	111.7	109.1	118.2	112.4	111.8	108.9
\angle (5-4-6)	109.0	109.8	109.7	109.6	108.7	109.7	109.3	109.7	108.9	109.9	109.5	110.2
\angle (5-4-7)	107.9	108.4	107.2	108.8	106.1	106.9	106.6	107.7	104.8	105.8	105.8	106.6
\angle (6-4-7)	107.9	108.1	108.5	108.7	106.1	107.5	106.8	107.7	104.8	106.7	105.5	106.6

Table S9. Geometrical parameters of the $\text{XBH}_2\text{NH}_2\text{X}$ systems obtained in the M06-2X/6-311++G(3df,2p) level, distances are given in Å and angles in degrees.

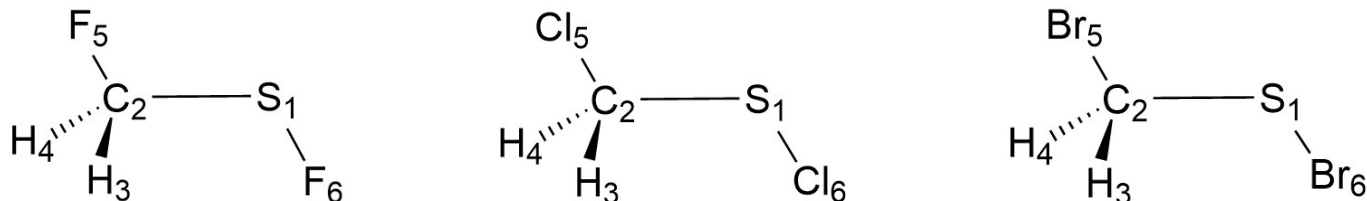
Parameter	<i>syn</i>	<i>gauche</i>	<i>anticlinal</i>	<i>anti</i>	<i>syn</i>	<i>gauche</i>	<i>anticlinal</i>	<i>anti</i>	<i>syn</i>	<i>gauche</i>	<i>anticlinal</i>	<i>anti</i>
	0	70	120	180		0	70	120		0	70	120
$r(1-2)$	1.205	1.215	1.204	1.200	1.195	1.191	1.188	1.191	1.193	1.189	1.186	1.189
$r(1-3)$	1.205	1.201	1.198	1.200	1.195	1.200	1.194	1.191	1.193	1.198	1.191	1.188
$r(1-4)$	1.741	1.636	1.685	1.671	1.702	1.629	1.665	1.633	1.679	1.618	1.650	1.616
$r(1-8)$	1.370	1.382	1.392	1.397	1.827	1.845	1.860	1.866	2.001	2.021	2.037	2.045
$r(4-5)$	1.019	1.022	1.022	1.021	1.017	1.020	1.021	1.020	1.017	1.020	1.021	1.019
$r(4-6)$	1.019	1.020	1.019	1.021	1.017	1.019	1.018	1.020	1.017	1.019	1.018	1.019
$r(4-7)$	1.371	1.380	1.375	1.369	1.725	1.732	1.727	1.728	1.888	1.890	1.887	1.893
$\angle(2-1-3)$	116.0	115.2	116.8	116.8	116.2	116.3	117.1	117.5	116.8	117.0	117.7	118.3
$\angle(2-1-4)$	101.6	98.6	103.2	104.4	102.3	106.7	106.9	106.3	103.2	107.9	108.3	107.6
$\angle(2-1-8)$	115.5	114.7	113.6	115.0	112.7	113.8	112.7	112.7	111.1	112.5	111.1	111.4
$\angle(3-1-4)$	101.6	105.1	103.7	104.4	102.3	101.6	104.5	106.3	103.2	102.6	105.5	107.6
$\angle(3-1-8)$	115.5	116.0	115.8	115.0	112.8	112.2	111.8	112.7	111.2	110.8	110.8	111.4
$\angle(4-1-8)$	103.5	104.4	100.8	97.7	109.1	104.6	102.3	99.2	110.7	104.8	102.2	98.6
$\angle(1-4-5)$	111.7	110.3	107.3	110.7	107.7	108.9	107.3	109.5	107.7	109.4	108.1	110.2
$\angle(1-4-6)$	111.7	111.4	113.6	110.7	107.7	109.8	110.4	109.5	107.7	109.9	110.7	110.2
$\angle(1-4-7)$	114.1	115.3	115.9	114.6	121.3	116.2	117.2	114.8	123.4	116.7	117.2	114.7
$\angle(5-4-6)$	109.1	109.7	109.6	108.9	107.8	108.8	108.4	107.6	107.4	108.6	108.2	107.4
$\angle(5-4-7)$	104.9	104.5	105.6	105.8	105.9	106.3	106.8	107.6	104.9	105.8	106.1	107.0
$\angle(6-4-7)$	104.9	105.3	104.6	105.8	105.9	106.6	106.5	107.6	104.9	106.1	106.1	107.0

Table S10. Geometrical parameters of the XCH₂OX systems obtained in the M06-2X/6-311++G(3df,2p) level, distances are given in Å and angles in degrees.



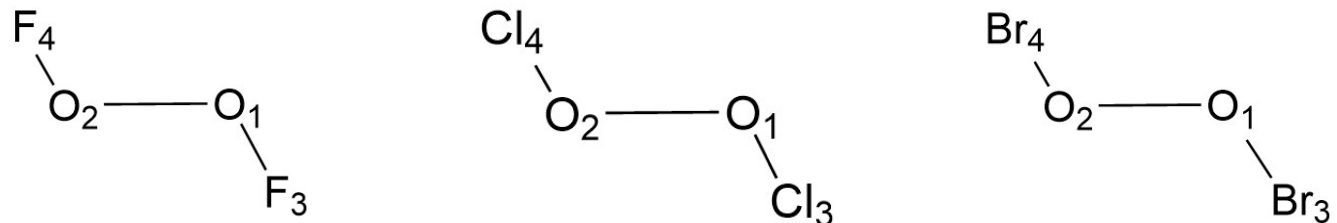
Parameter	<i>syn</i>	<i>gauche</i>	<i>anticlinal</i>	<i>anti</i>	<i>syn</i>	<i>gauche</i>	<i>anticlinal</i>	<i>anti</i>	<i>syn</i>	<i>gauche</i>	<i>anticlinal</i>	<i>anti</i>
ϕ	0	80	120	180	0	80	120	180	0	80	120	180
$r(1-2)$	1.439	1.377	1.399	1.418	1.422	1.387	1.402	1.412	1.408	1.378	1.392	1.403
$r(1-6)$	1.387	1.401	1.398	1.396	1.661	1.674	1.671	1.675	1.806	1.819	1.817	1.825
$r(2-3)$	1.091	1.089	1.087	1.090	1.087	1.087	1.085	1.088	1.086	1.087	1.084	1.088
$r(2-4)$	1.091	1.091	1.091	1.090	1.087	1.086	1.087	1.088	1.086	1.086	1.086	1.088
$r(2-5)$	1.339	1.358	1.356	1.345	1.763	1.783	1.777	1.758	1.937	1.960	1.952	1.929
$\angle(2-1-6)$	108.5	106.1	106.9	102.7	119.4	112.5	113.5	109.2	122.4	114.0	114.6	110.1
$\angle(1-2-3)$	106.9	110.8	109.4	109.7	107.0	111.9	112.1	110.8	107.8	113.1	113.6	111.9
$\angle(1-2-4)$	106.9	103.7	107.9	109.7	107.0	105.1	108.3	110.8	107.8	105.9	109.0	111.9
$\angle(1-2-5)$	111.6	111.2	108.7	103.7	117.0	113.0	109.7	105.8	118.5	113.6	109.8	105.8
$\angle(3-2-4)$	112.6	113.0	112.9	112.8	111.8	112.3	111.8	111.7	112.0	112.4	111.9	111.9
$\angle(3-2-5)$	109.4	109.0	110.6	110.2	107.1	106.9	108.1	108.7	105.4	105.5	106.7	107.5
$\angle(4-2-5)$	109.4	109.1	107.3	110.2	107.1	107.7	106.7	108.7	105.4	106.2	105.4	107.5

Table S11. Geometrical parameters of the XCH_2SX systems obtained in the M06-2X/6-311++G(3df,2p) level, distances are given in Å and angles in degrees.



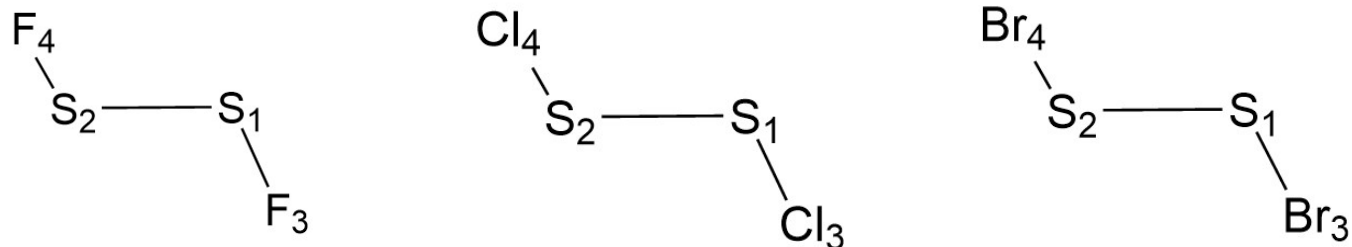
Parameter	<i>syn</i>	<i>gauche</i>	<i>anticlinal</i>	<i>anti</i>	<i>syn</i>	<i>gauche</i>	<i>anticlinal</i>	<i>anti</i>	<i>syn</i>	<i>gauche</i>	<i>anticlinal</i>	<i>anti</i>
ϕ	0	80	120	180	0	80	120	180	0	80	120	180
r (1-2)	1.850	1.765	1.792	1.815	1.846	1.782	1.805	1.806	1.837	1.779	1.802	1.799
r (1-6)	1.610	1.618	1.622	1.623	2.011	2.022	2.027	2.029	2.172	2.179	2.185	2.191
r (2-3)	1.088	1.090	1.090	1.088	1.085	1.085	1.084	1.085	1.084	1.084	1.083	1.084
r (2-4)	1.088	1.093	1.089	1.088	1.085	1.089	1.085	1.085	1.084	1.088	1.084	1.084
r (2-5)	1.354	1.369	1.369	1.364	1.755	1.778	1.778	1.769	1.919	1.945	1.945	1.934
\angle (2-1-6)	97.9	98.5	98.2	95.0	105.1	99.7	100.6	97.7	107.3	100.7	101.2	98.1
\angle (1-2-3)	108.8	109.1	106.0	110.1	106.8	110.3	108.6	110.7	106.9	111.4	109.8	111.6
\angle (1-2-4)	108.8	105.5	110.2	110.1	106.7	105.0	109.0	110.7	106.9	105.2	109.5	111.6
\angle (1-2-5)	109.4	113.9	111.8	105.6	116.7	115.0	112.8	105.8	118.7	115.9	112.9	105.4
\angle (3-2-4)	111.3	110.7	111.0	111.5	110.8	110.3	110.5	111.7	111.0	110.6	110.9	112.1
\angle (3-2-5)	109.2	108.8	110.7	109.7	107.9	107.7	109.0	108.9	106.7	106.8	107.7	107.9
\angle (4-2-5)	109.3	108.9	107.2	109.8	107.9	108.3	107.0	108.9	106.7	107.0	106.1	107.9

Table S12. Geometrical parameters of the XOOX systems obtained in the M06-2X/6-311++G(3df,2p) level, distances are given in Å and angles in degrees.



Parameter	<i>syn</i>	<i>gauche</i>	<i>anticlinal</i>	<i>anti</i>	<i>syn</i>	<i>gauche</i>	<i>anticlinal</i>	<i>anti</i>	<i>syn</i>	<i>gauche</i>	<i>anticlinal</i>	<i>anti</i>
ϕ	0	90	120	180	0	90	120	180	0	90	120	180
r (1-2)	1.455	1.287	1.329	1.433	1.473	1.378	1.406	1.452	1.448	1.369	1.396	1.443
r (1-3)	1.362	1.415	1.400	1.368	1.646	1.688	1.674	1.656	1.802	1.844	1.829	1.809
r (2-4)	1.362	1.415	1.400	1.368	1.646	1.688	1.674	1.656	1.802	1.844	1.829	1.809
\angle (2-1-3)	108.2	106.6	104.9	99.5	116.3	109.5	107.8	104.5	118.9	110.3	108.6	104.8
\angle (1-2-4)	108.2	106.6	104.9	99.5	116.3	109.5	107.8	104.5	118.9	110.3	108.6	104.8

Table S13. Geometrical parameters of the XSSX systems obtained in the M06-2X/6-311++G(3df,2p) level, distances are given in Å and angles in degrees.



Parameter	<i>syn</i>	<i>gauche</i>	<i>anticlinal</i>	<i>anti</i>	<i>syn</i>	<i>gauche</i>	<i>anticlinal</i>	<i>anti</i>	<i>syn</i>	<i>gauche</i>	<i>anticlinal</i>	<i>anti</i>
ϕ	0	90	120	180	0	90	120	180	0	90	120	180
r (1-2)	1.759	1.899	1.924	2.114	2.156	1.955	1.986	2.104	2.150	1.955	1.987	2.100
r (1-3)	1.767	1.626	1.629	1.613	1.999	2.053	2.047	2.017	2.157	2.218	2.211	2.176
r (2-4)	1.759	1.899	1.924	2.114	2.156	1.955	1.986	2.104	2.150	1.955	1.987	2.100
\angle (2-1-3)	115.1	107.2	105.7	93.1	105.4	106.9	105.3	95.4	107.7	107.6	105.9	95.5
\angle (1-2-4)	115.1	107.2	105.7	93.1	105.4	107.0	105.4	95.4	107.7	107.6	105.9	95.5

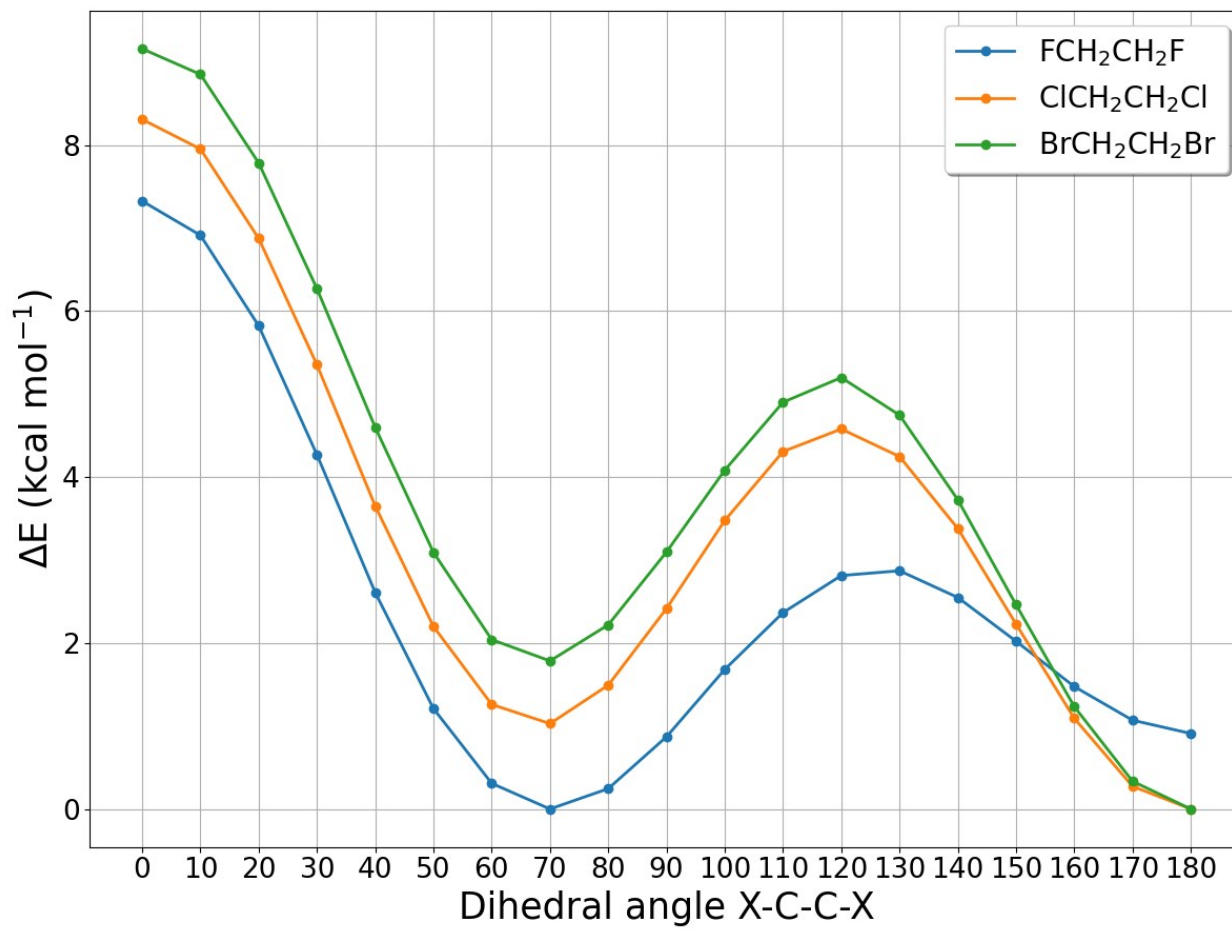


Figure S1. Potential energy curves for XCH_2CH_2X molecules calculated at the M06-2X/6-311++G(3df,2p) level.

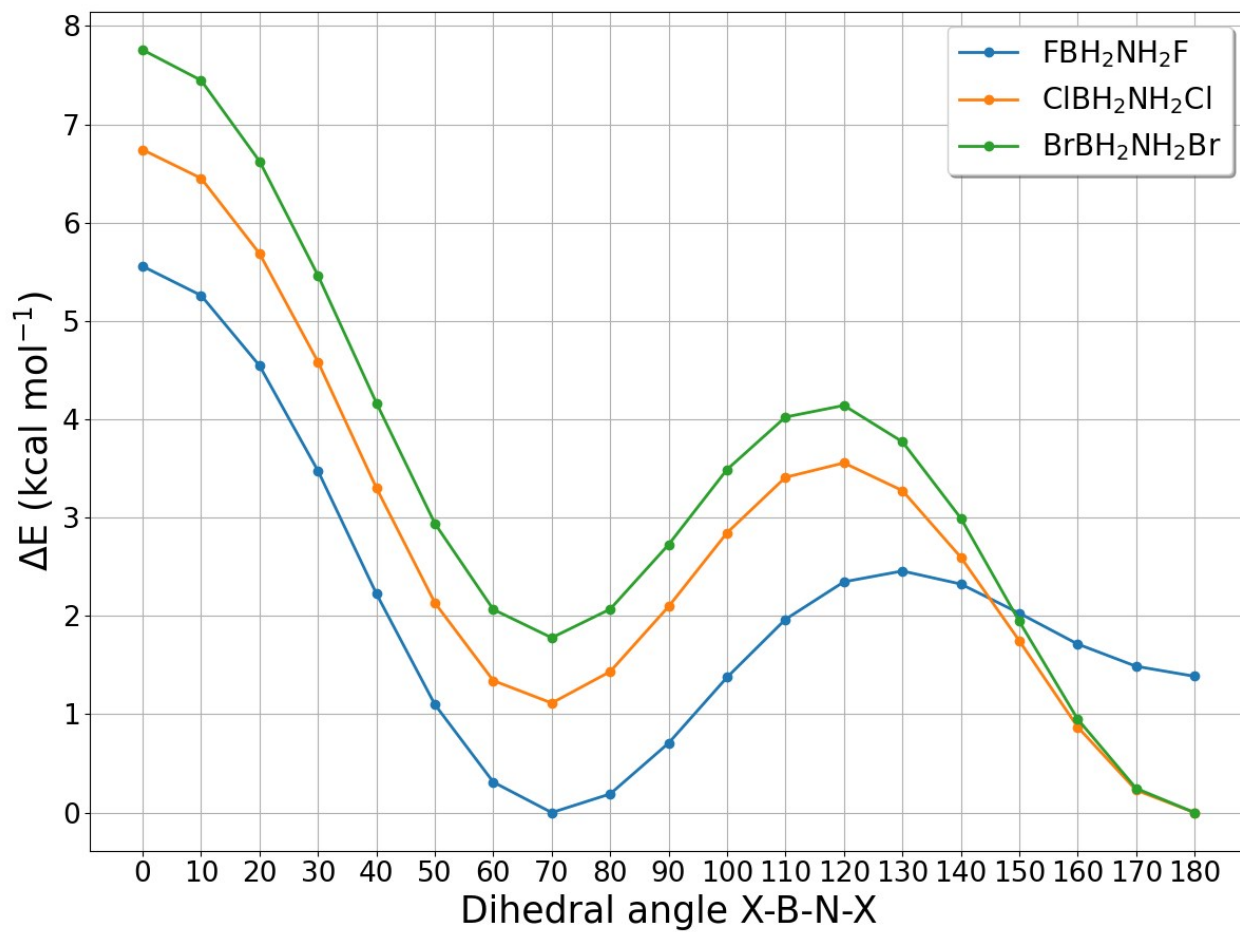


Figure S2. Potential energy curves for $X\text{BH}_2\text{NH}_2\text{X}$ molecules calculated at the M06-2X/6-311++G(3df,2p) level.

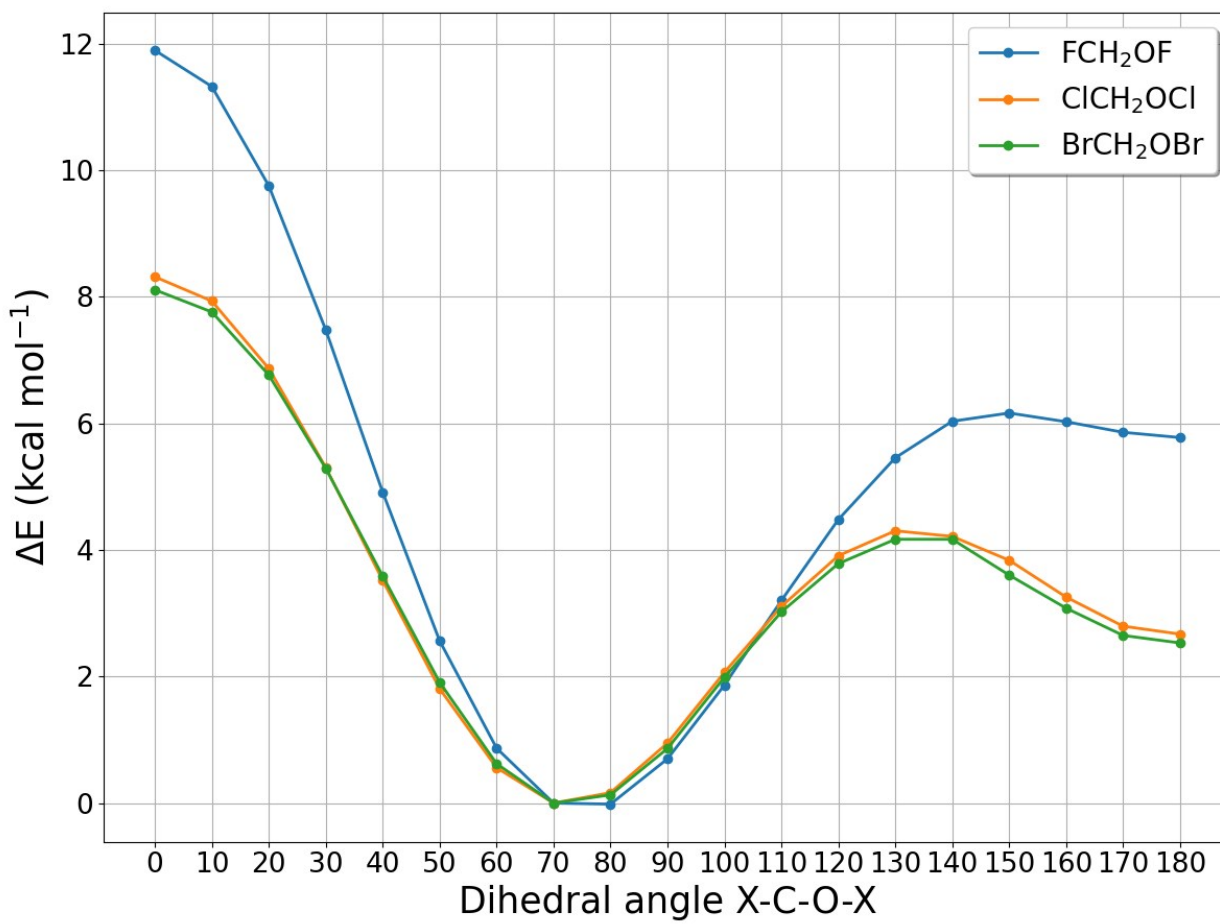


Figure S3. Potential energy curves for $X\text{CH}_2\text{OX}$ molecules calculated at the M06-2X/6-311++G(3df,2p) level.

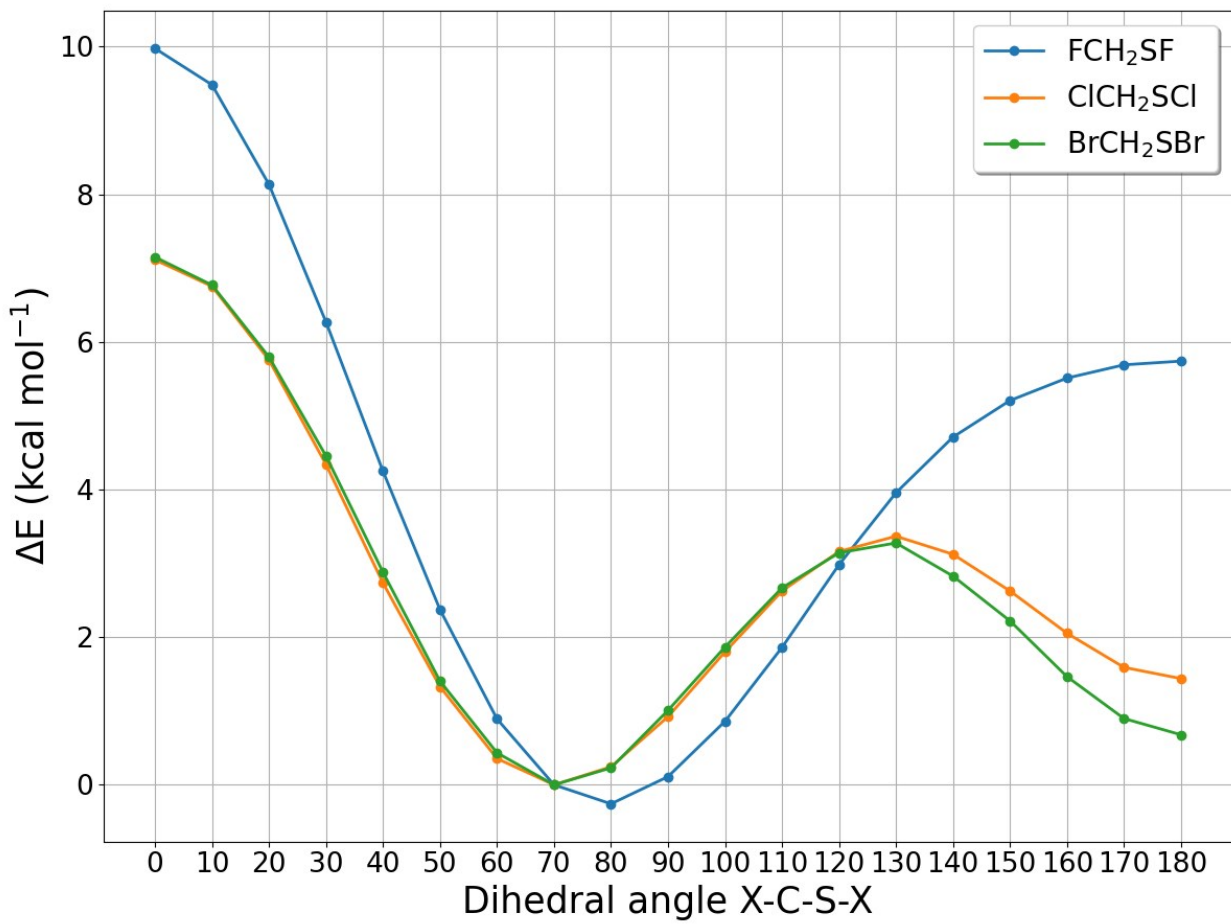


Figure S4. Potential energy curves for $X\text{CH}_2\text{SX}$ molecules calculated at the M06-2X/6-311++G(3df,2p) level.

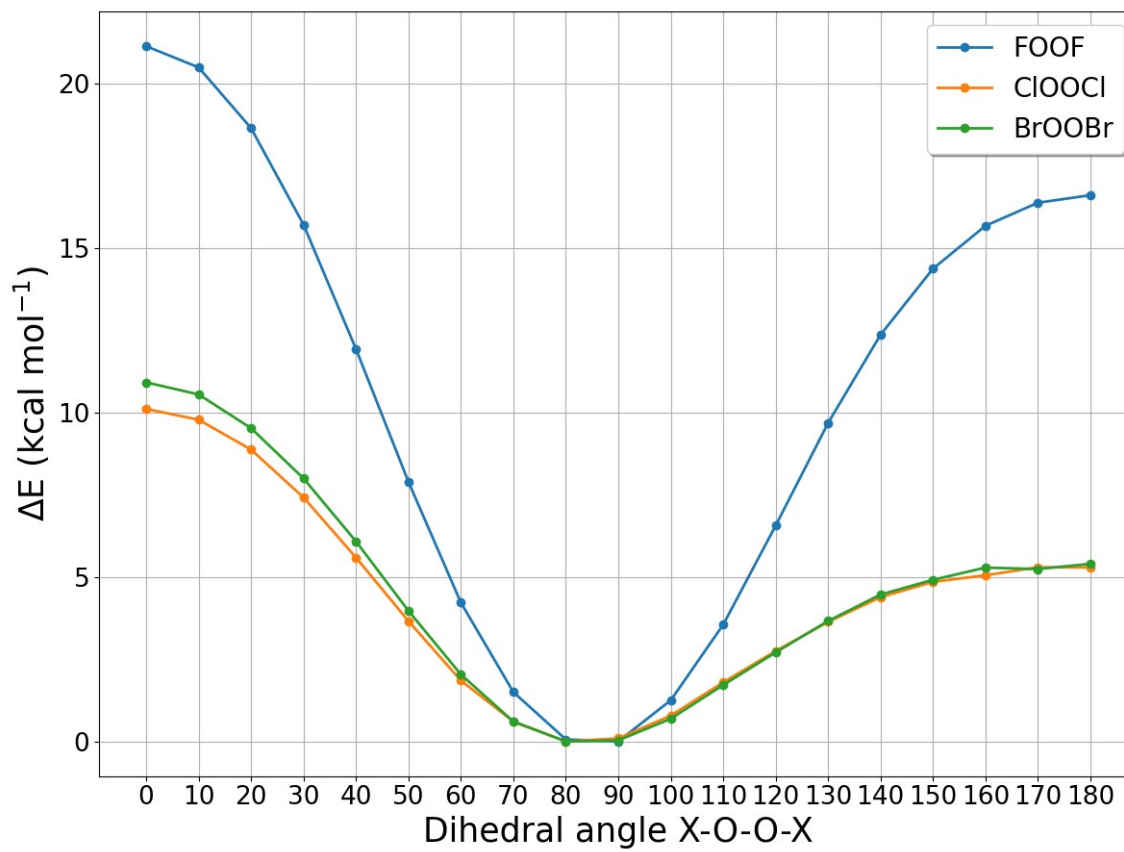


Figure S5. Potential energy curves for XOOX molecules calculated at the M06-2X/6-311++G(3df,2p) level.

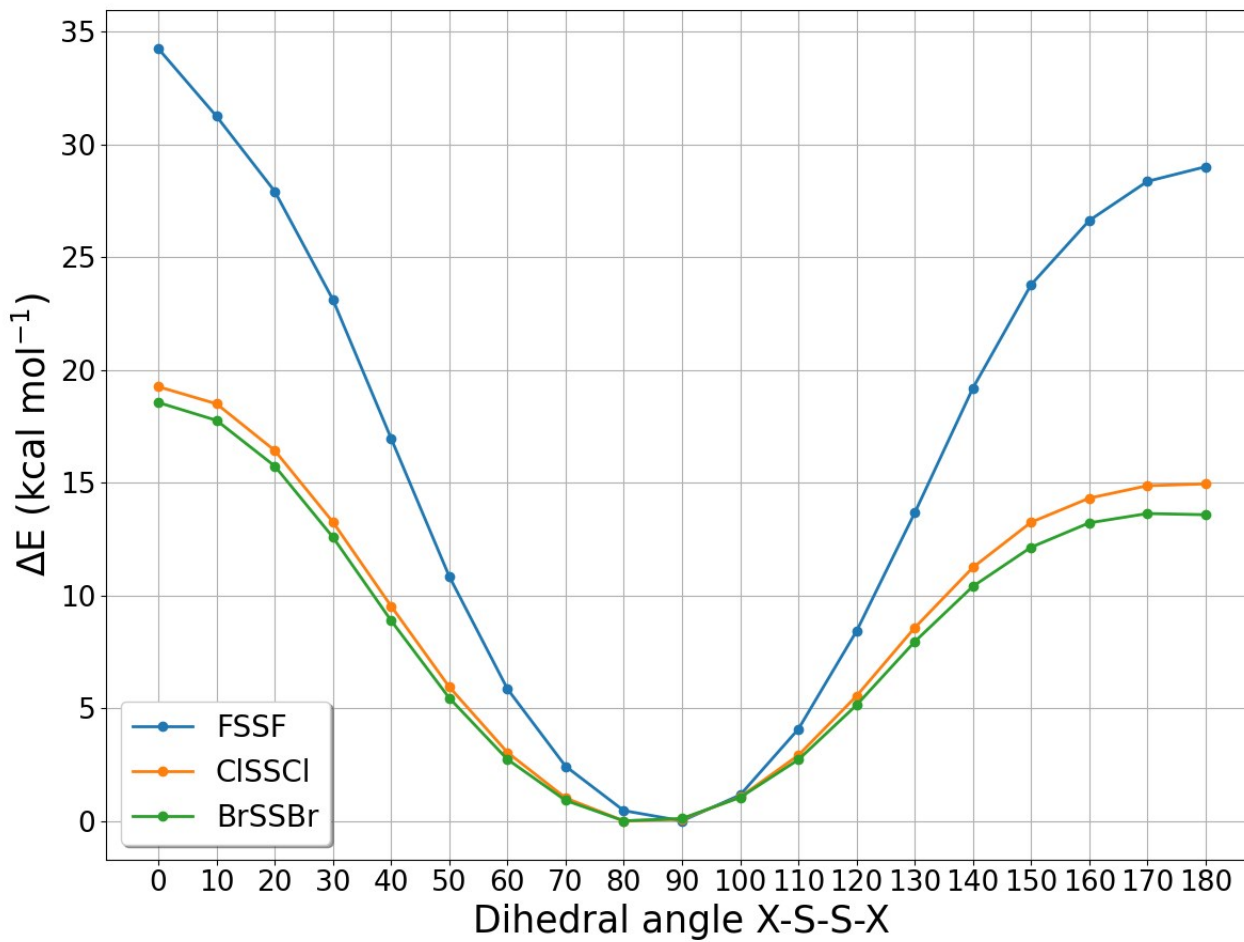


Figure S6. Potential energy curves for XSSX molecules calculated at the M06-2X/6-311++G(3df,2p) level.

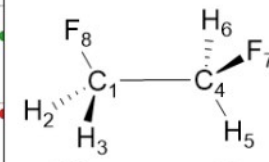
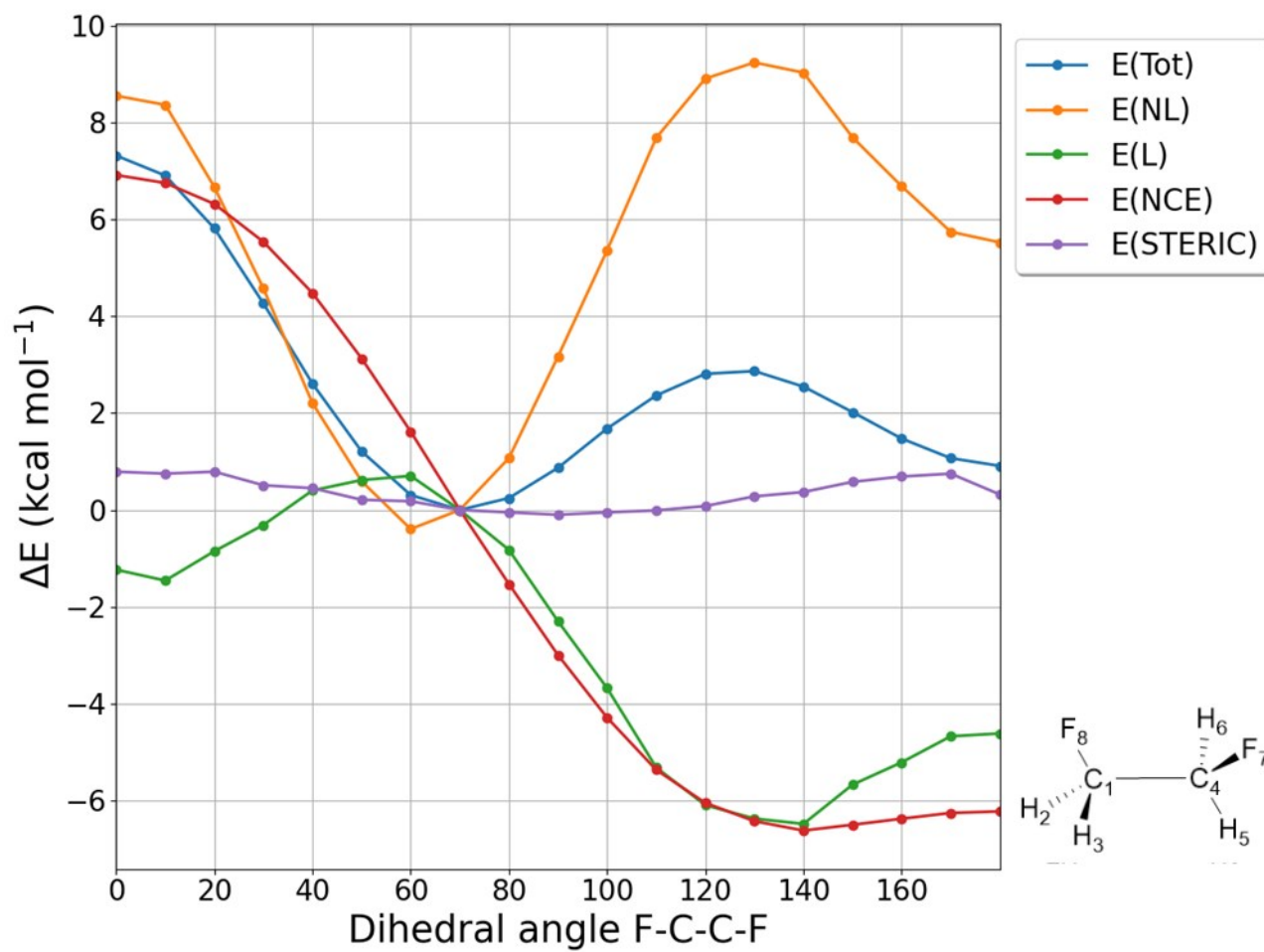


Figure S7. NBO deletion analysis calculated for $\text{FCH}_2\text{CH}_2\text{F}$ at the M06-2X/6-311++G(3df,2p) level.

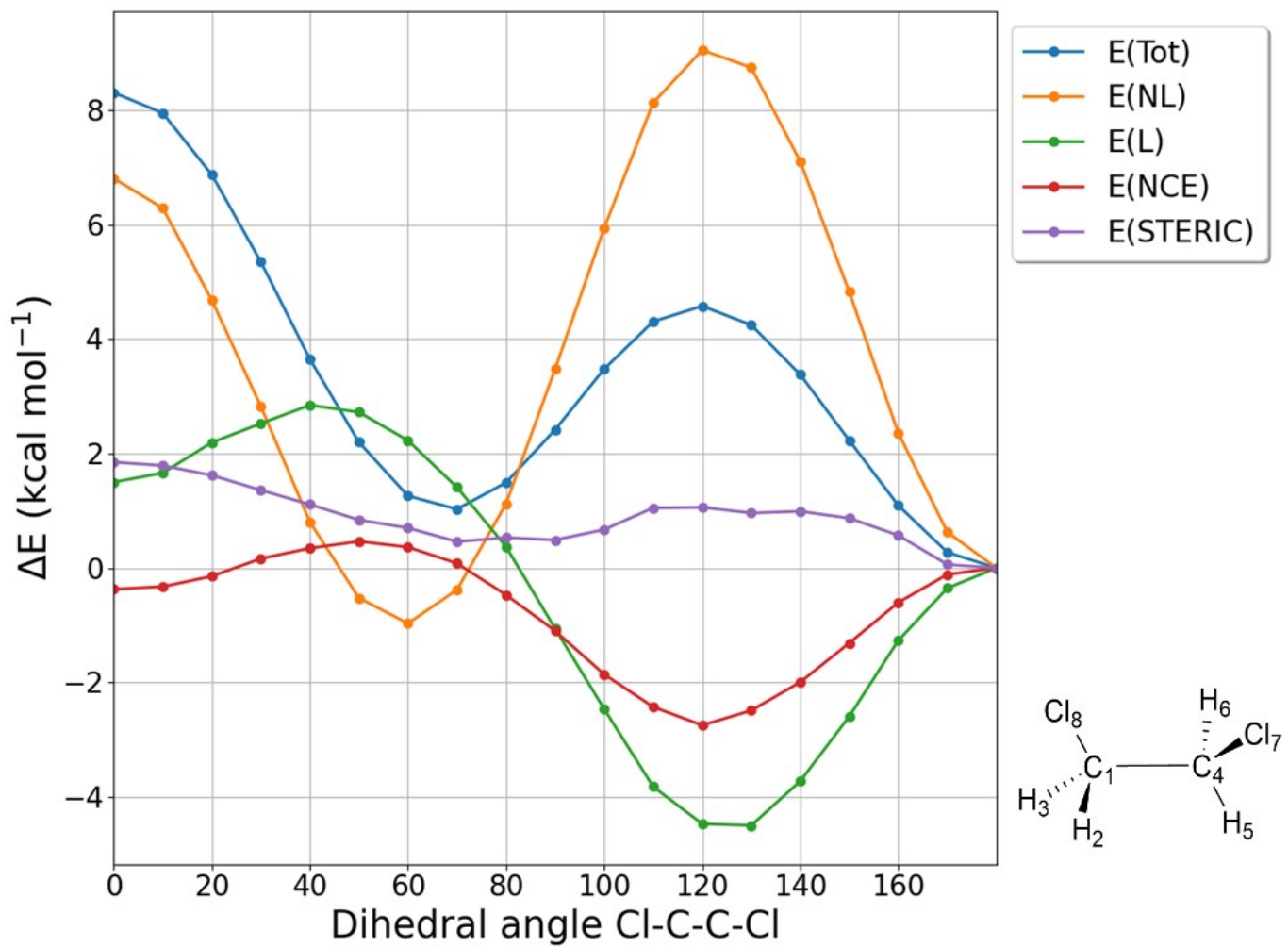


Figure S8. NBO deletion analysis calculated for $\text{ClCH}_2\text{CH}_2\text{Cl}$ at the M06-2X/6-311++G(3df,2p) level.

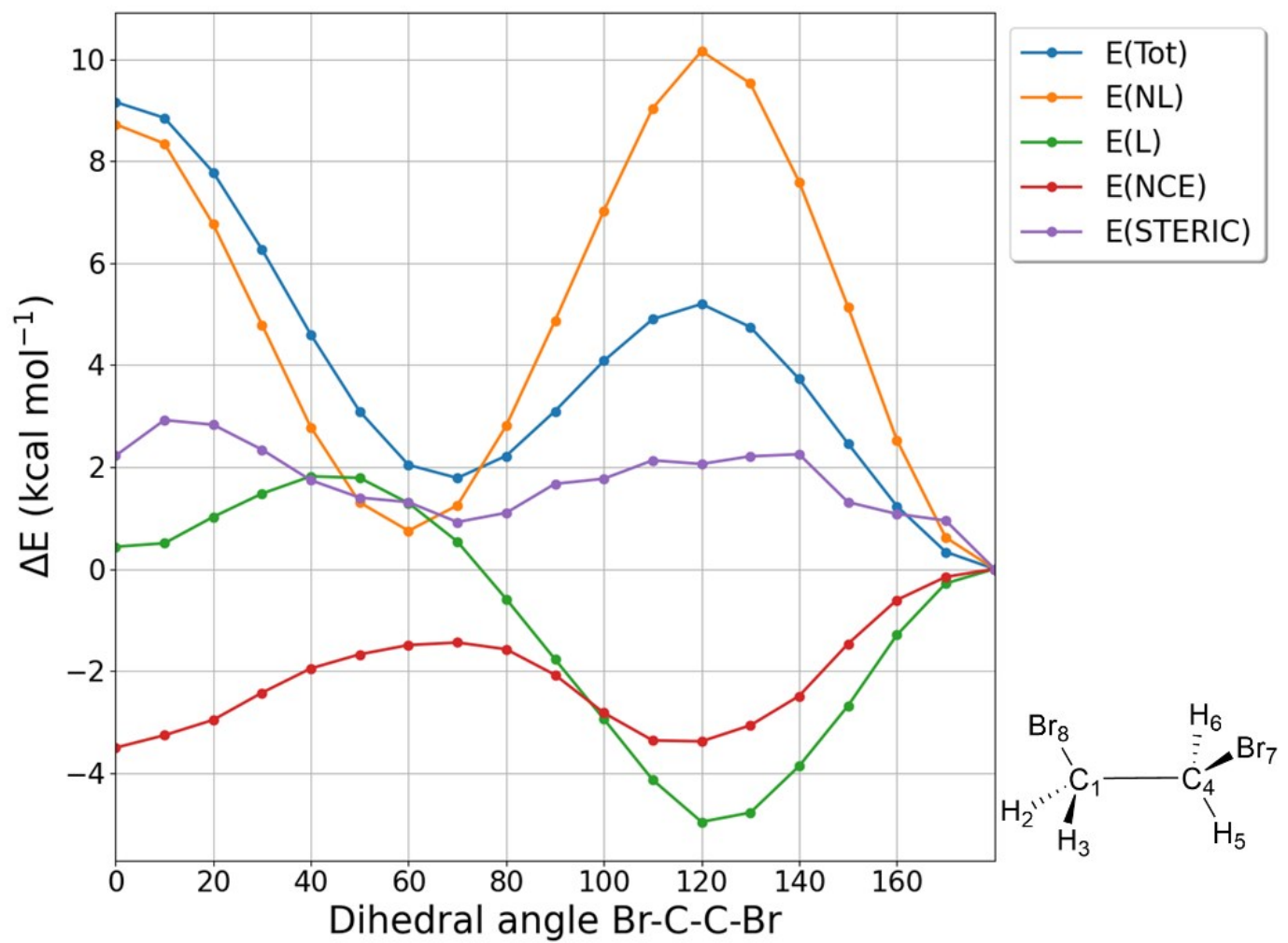


Figure S9. NBO deletion analysis calculated for $\text{BrCH}_2\text{CH}_2\text{Br}$ at the M06-2X/6-311++G(3df,2p) level.

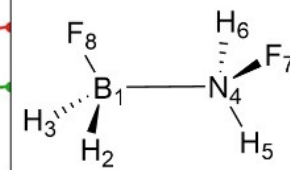
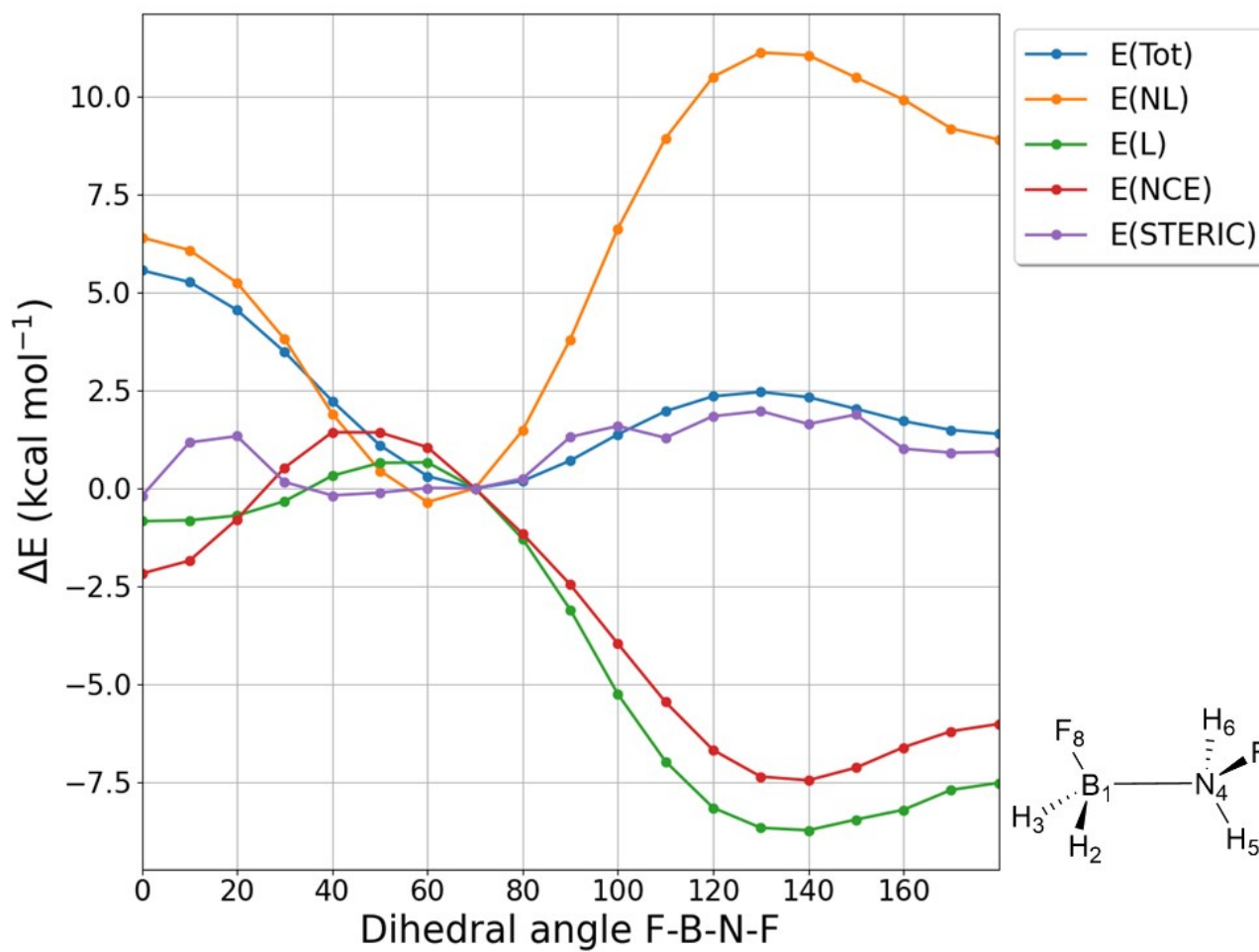


Figure S10. NBO deletion analysis calculated for $\text{FBH}_2\text{NH}_2\text{F}$ at the M06-2X/6-311++G(3df,2p) level.

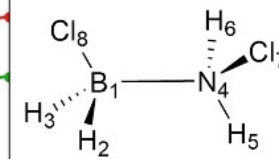
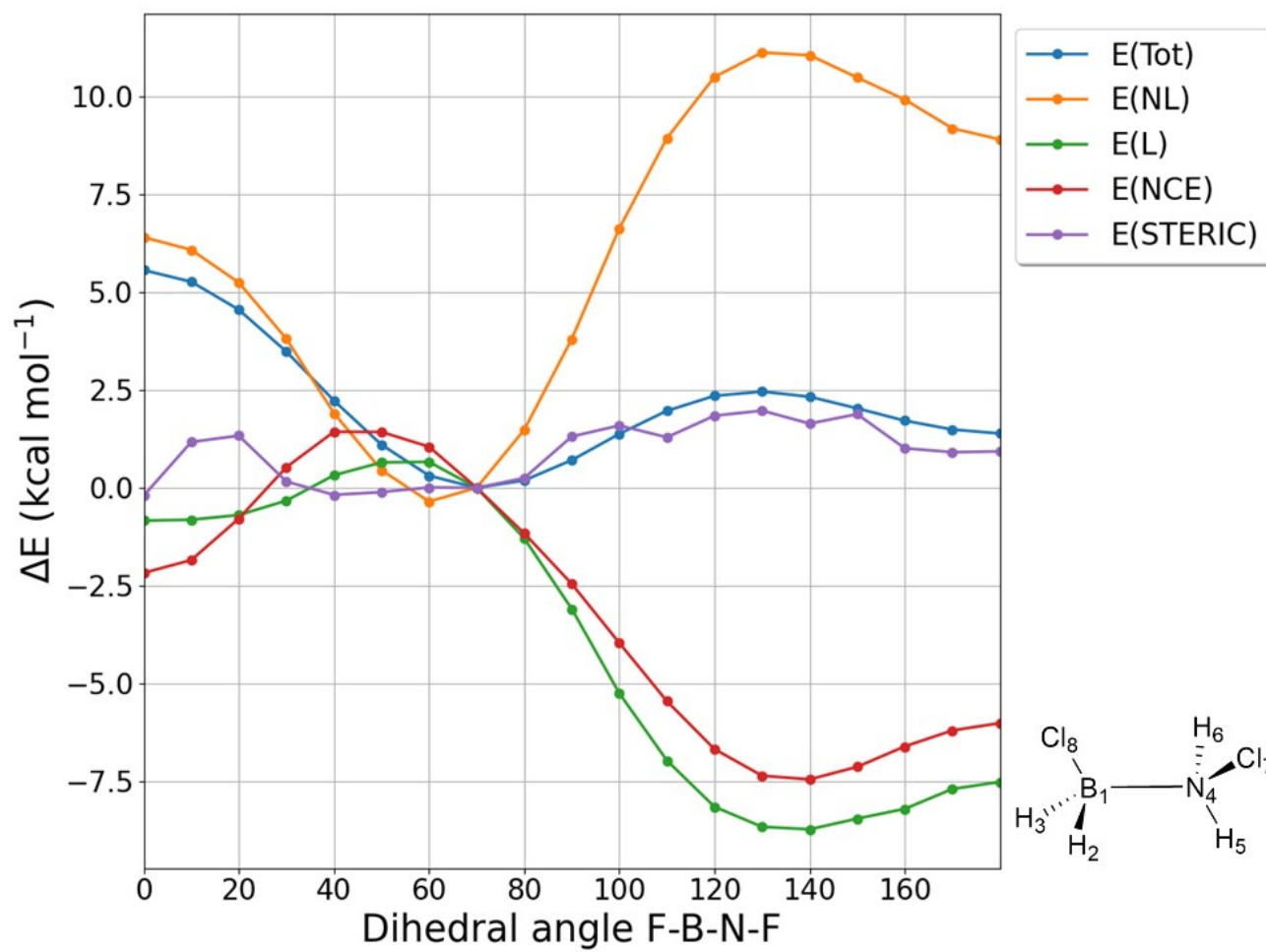


Figure S11. NBO deletion analysis calculated for $\text{ClBH}_2\text{NH}_2\text{Cl}$ at the M06-2X/6-311++G(3df,2p) level.

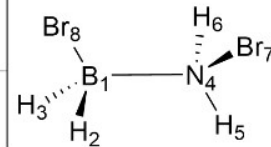
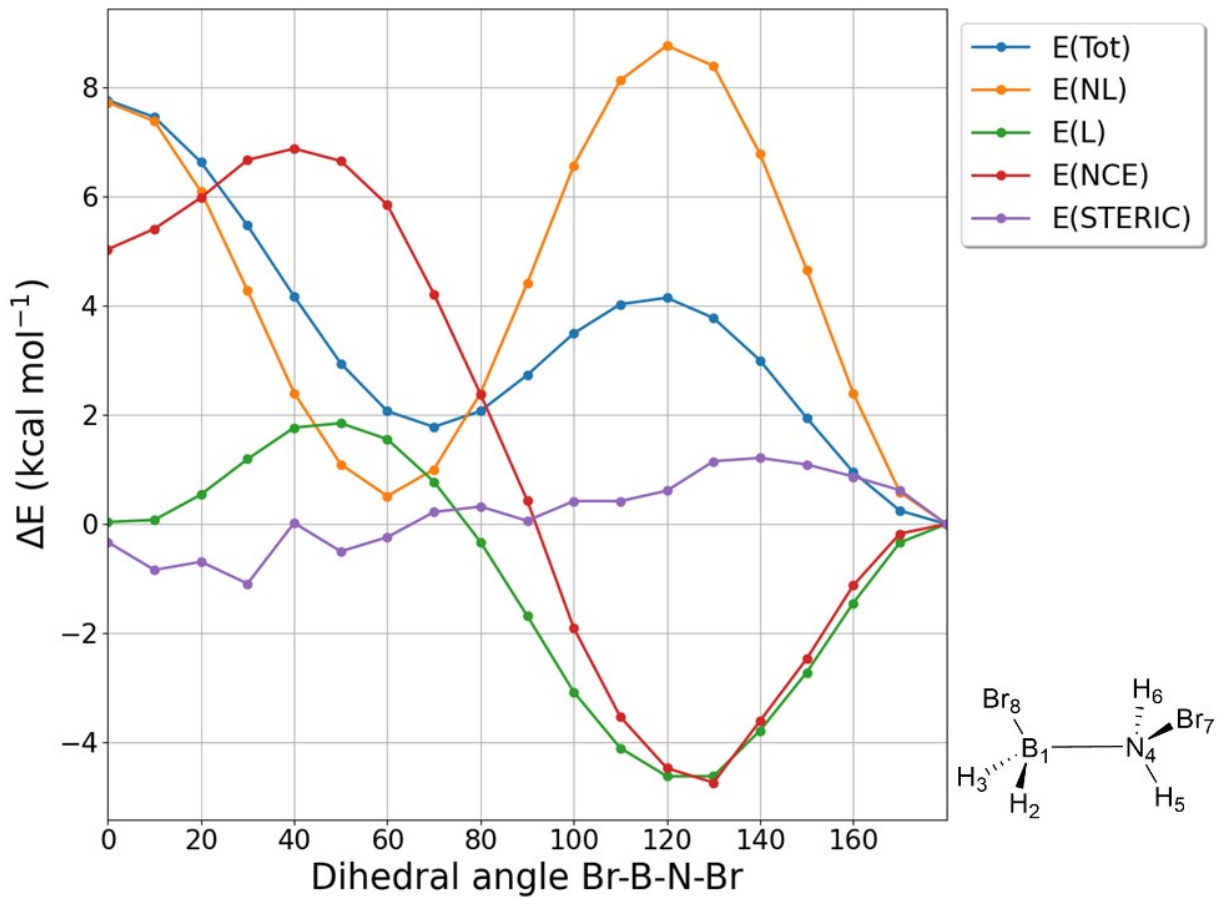


Figure S12. NBO deletion analysis calculated for $\text{BrBH}_2\text{NH}_2\text{Br}$ at the M06-2X/6-311++G(3df,2p) level.

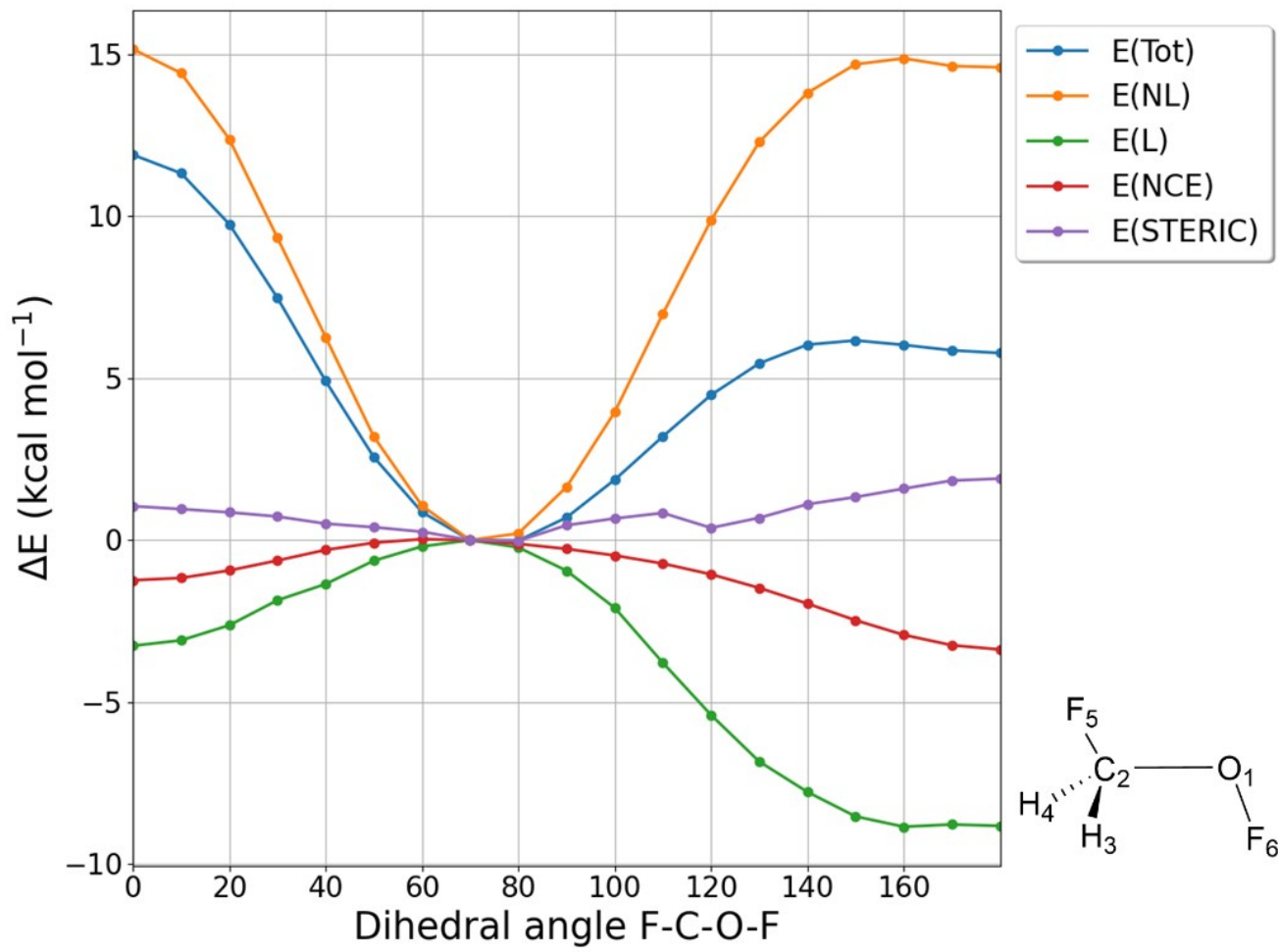


Figure S13. NBO deletion analysis calculated for FCH_2OF at the M06-2X/6-311++G(3df,2p) level.

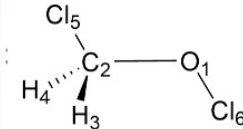
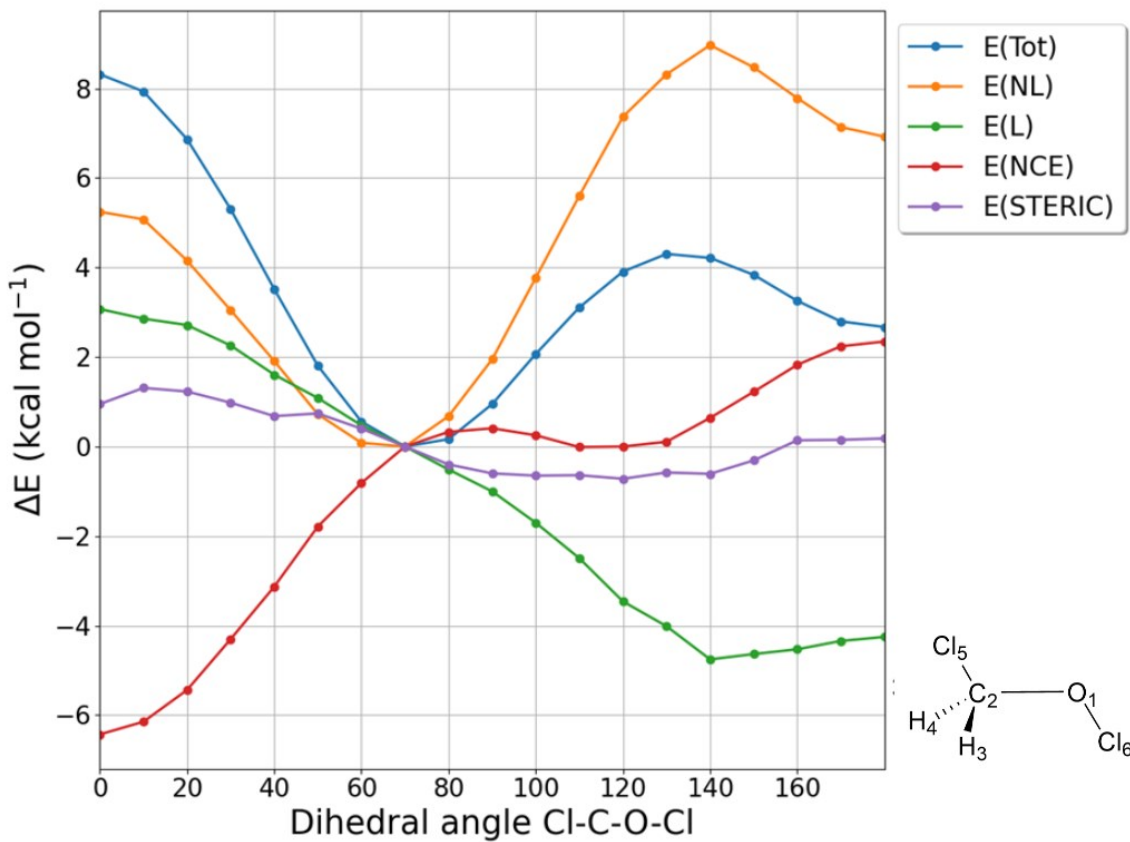


Figure S14. NBO deletion analysis calculated for ClCH_2OCl at the M06-2X/6-311++G(3df,2p) level.

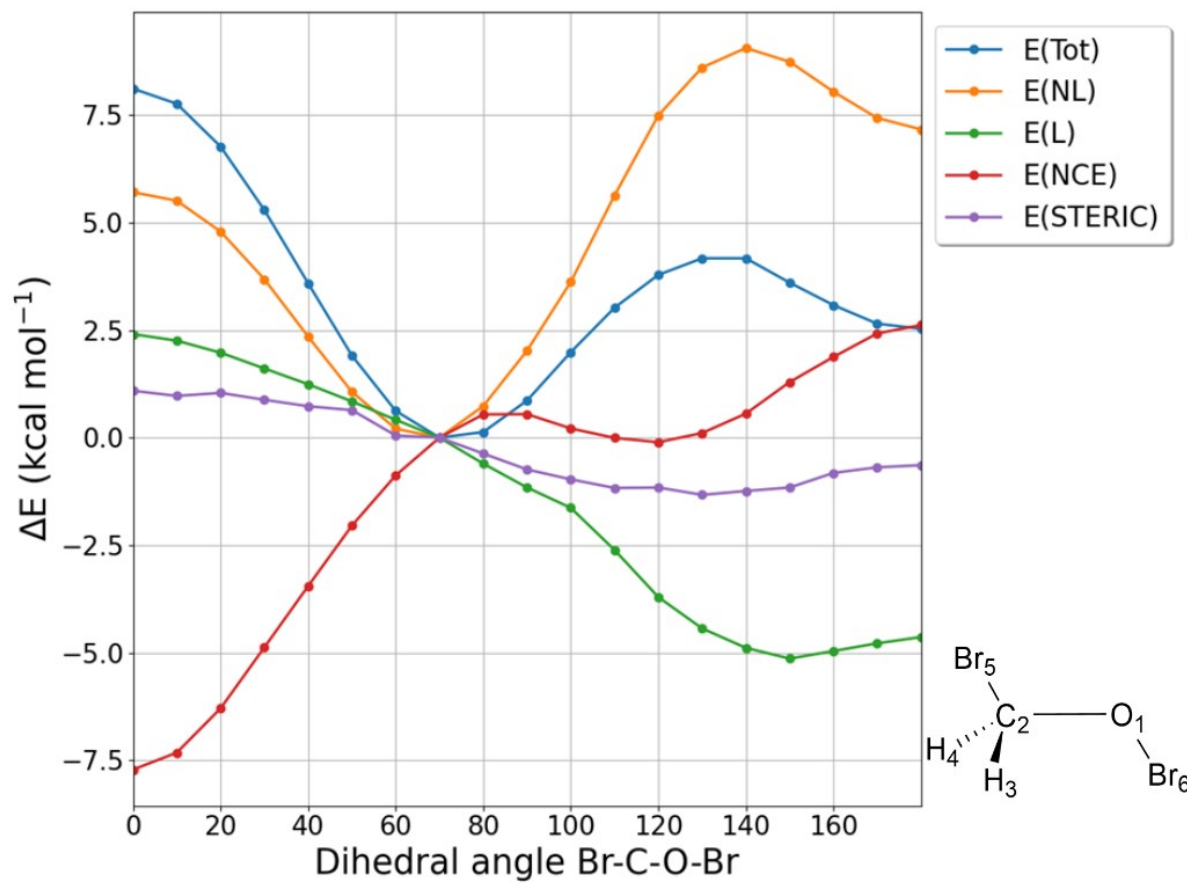


Figure S15. NBO deletion analysis calculated for BrCH_2OBr at the M06-2X/6-311++G(3df,2p) level.

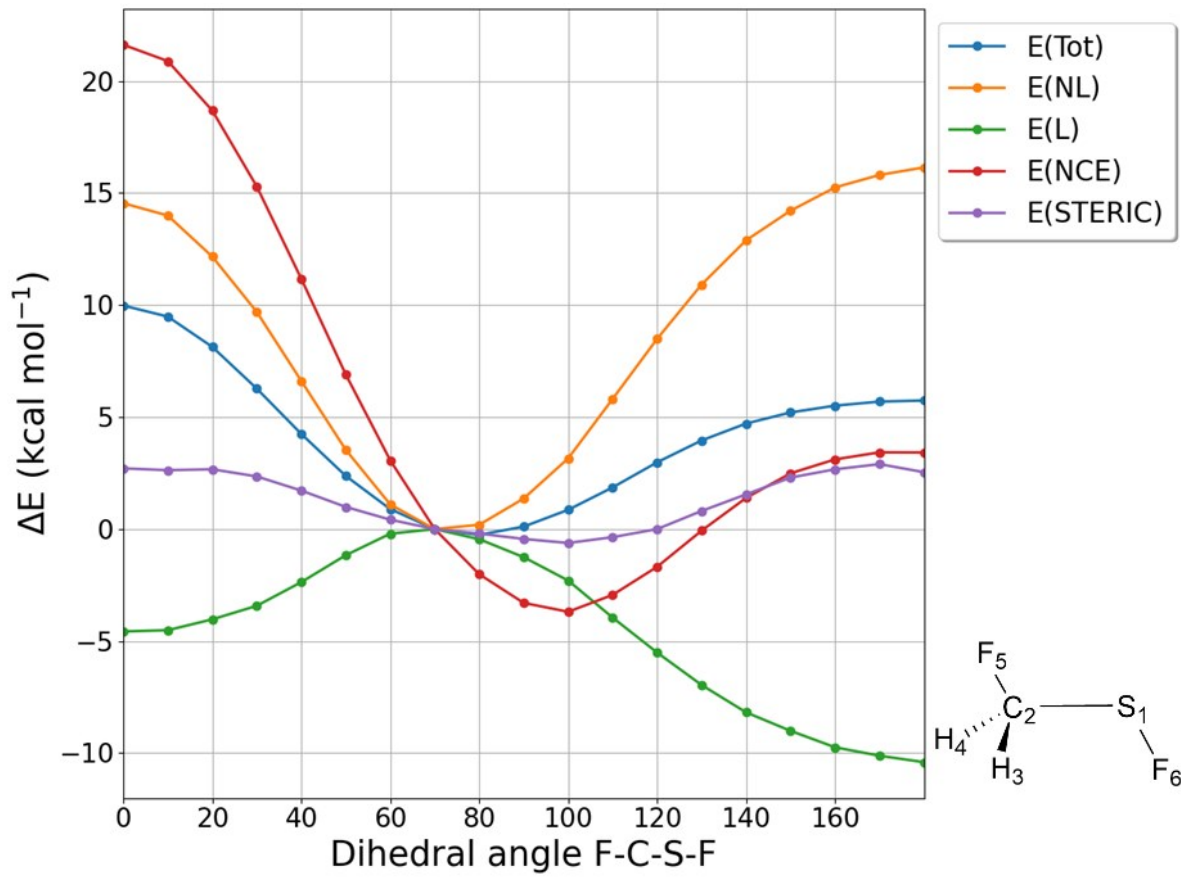


Figure S16. NBO deletion analysis calculated for FCH_2SF at the M06-2X/6-311++G(3df,2p) level.

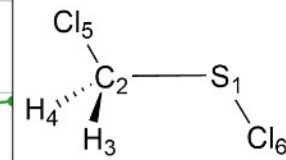
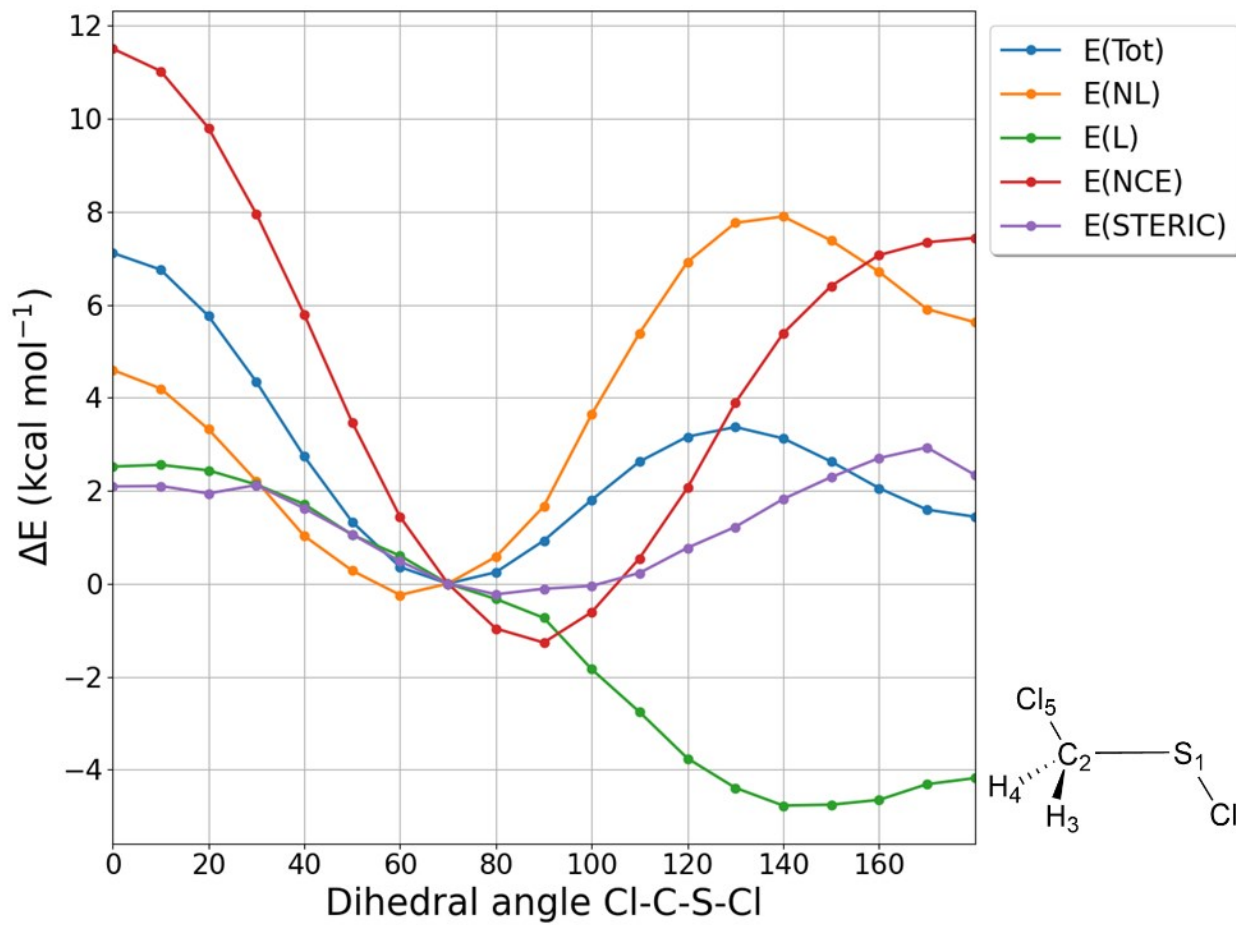


Figure S17. NBO deletion analysis calculated for ClCH_2SCl at the M06-2X/6-311++G(3df,2p) level.

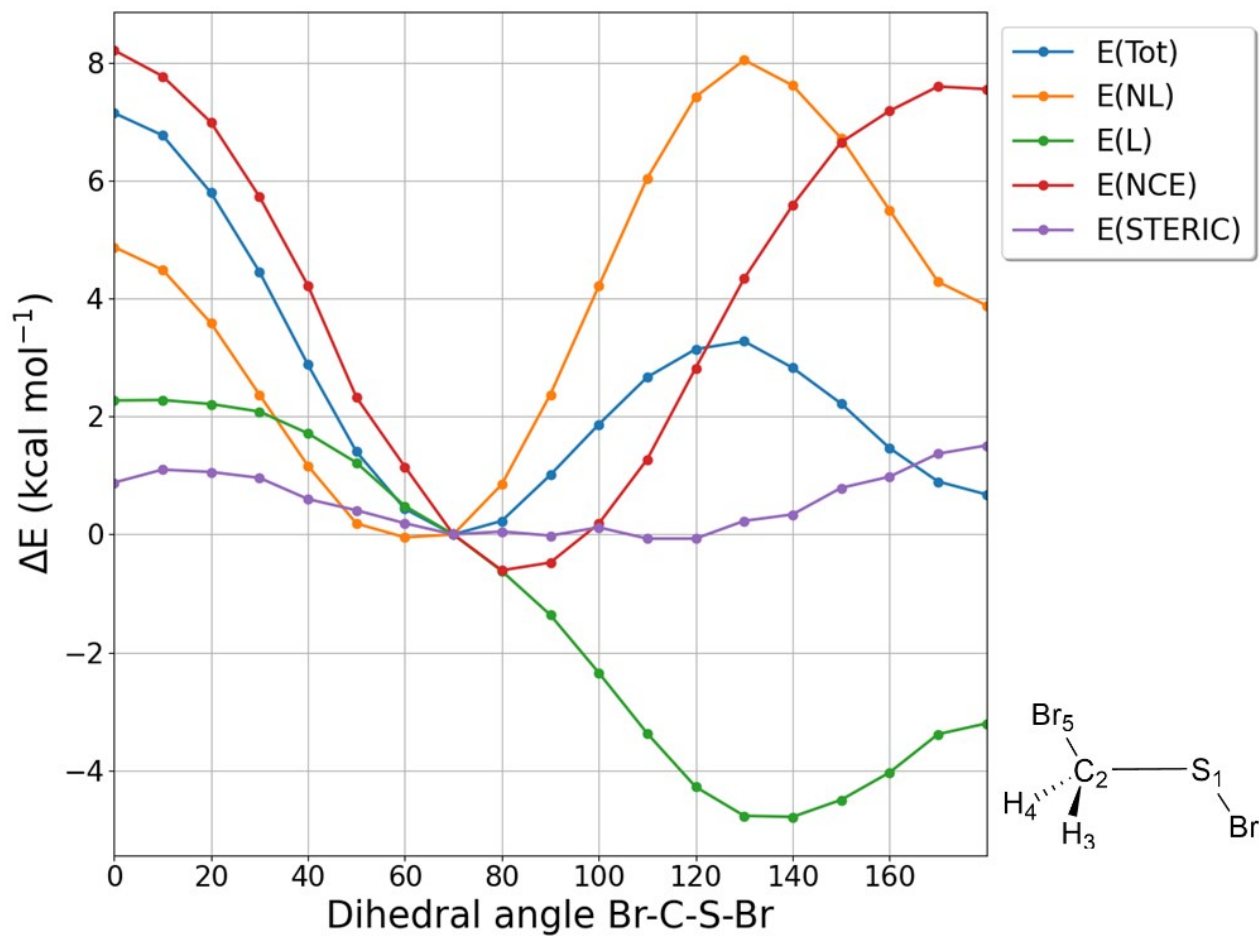


Figure S18. NBO deletion analysis calculated for BrCH_2SBr at the M06-2X/6-311++G(3df,2p) level.

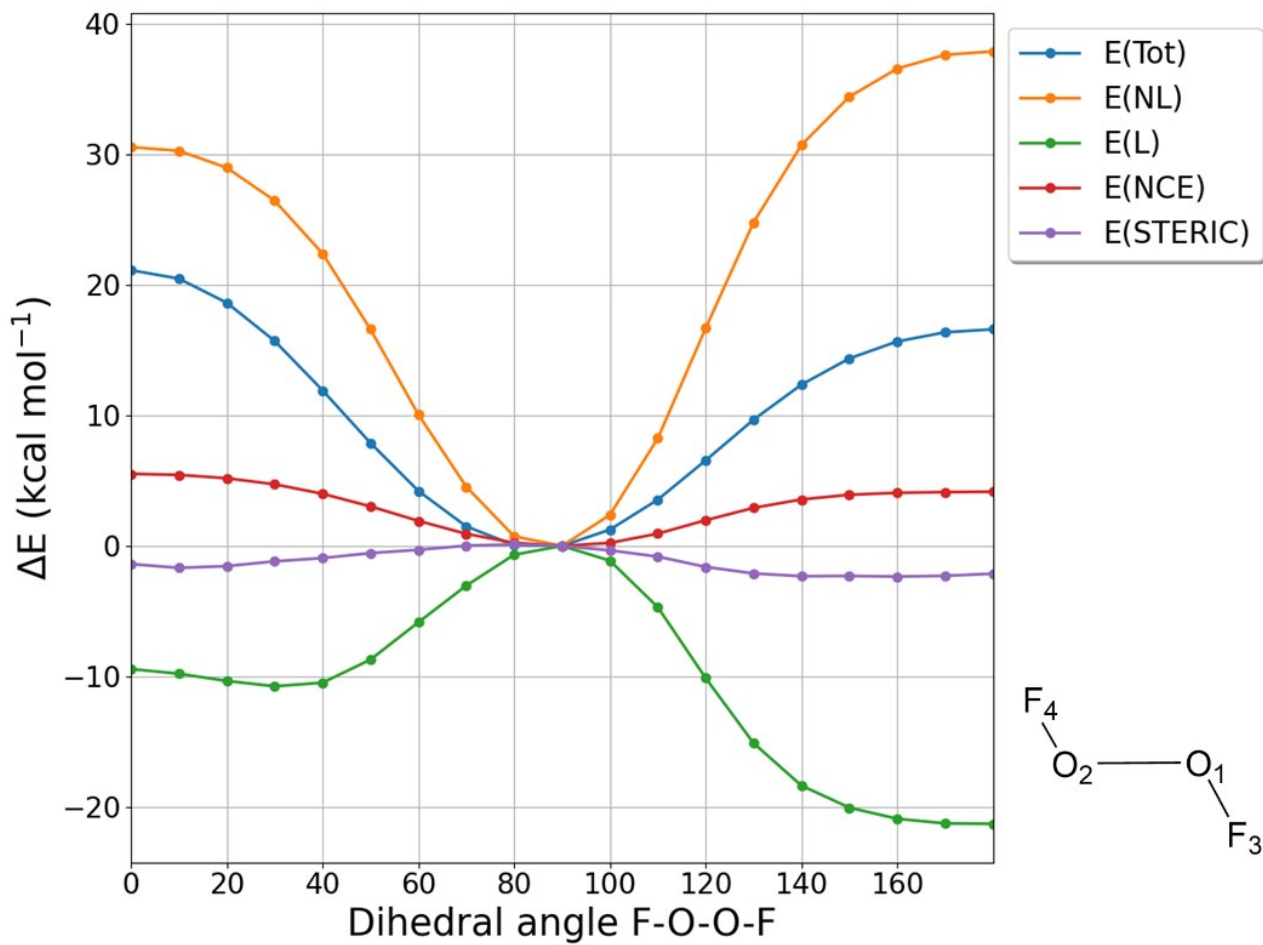


Figure S19. NBO deletion analysis calculated for FOOF at the M06-2X/6-311++G(3df,2p) level.

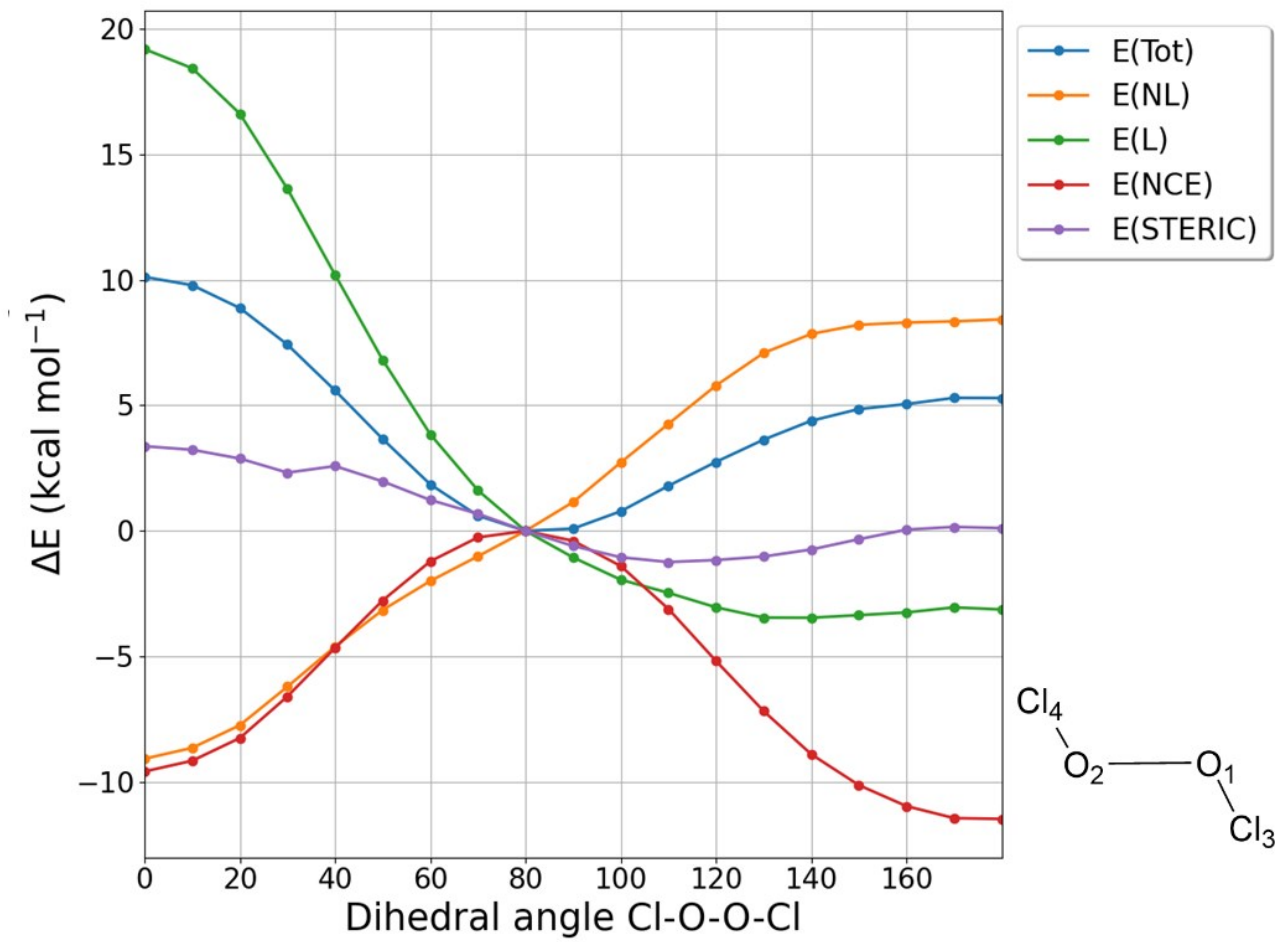


Figure S20. NBO deletion analysis calculated for ClOOCl at the M06-2X/6-311++G(3df,2p) level.

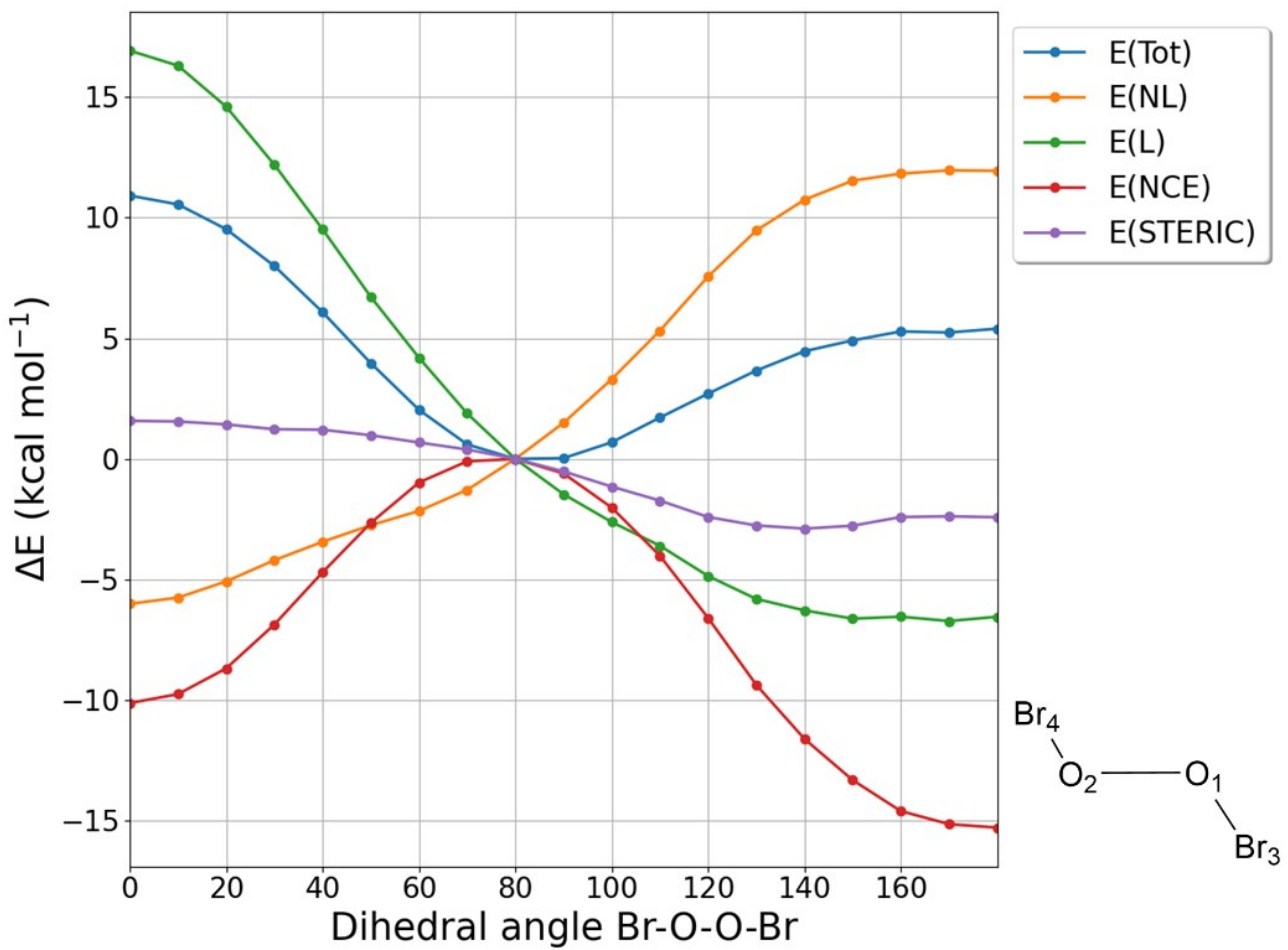


Figure S21. NBO deletion analysis calculated for BrOOBr at the M06-2X/6-311++G(3df,2p) level.

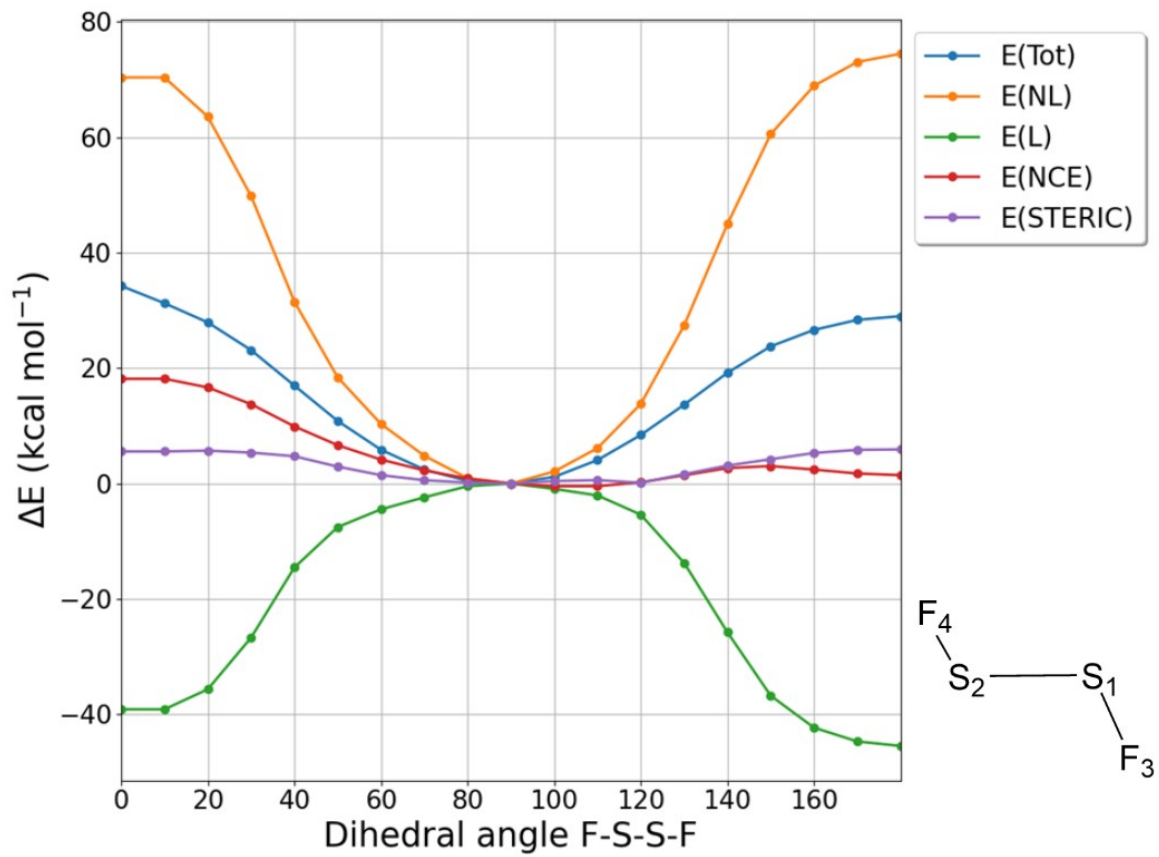


Figure S22. NBO deletion analysis calculated for FSSF at the M06-2X/6-311++G(3df,2p) level.

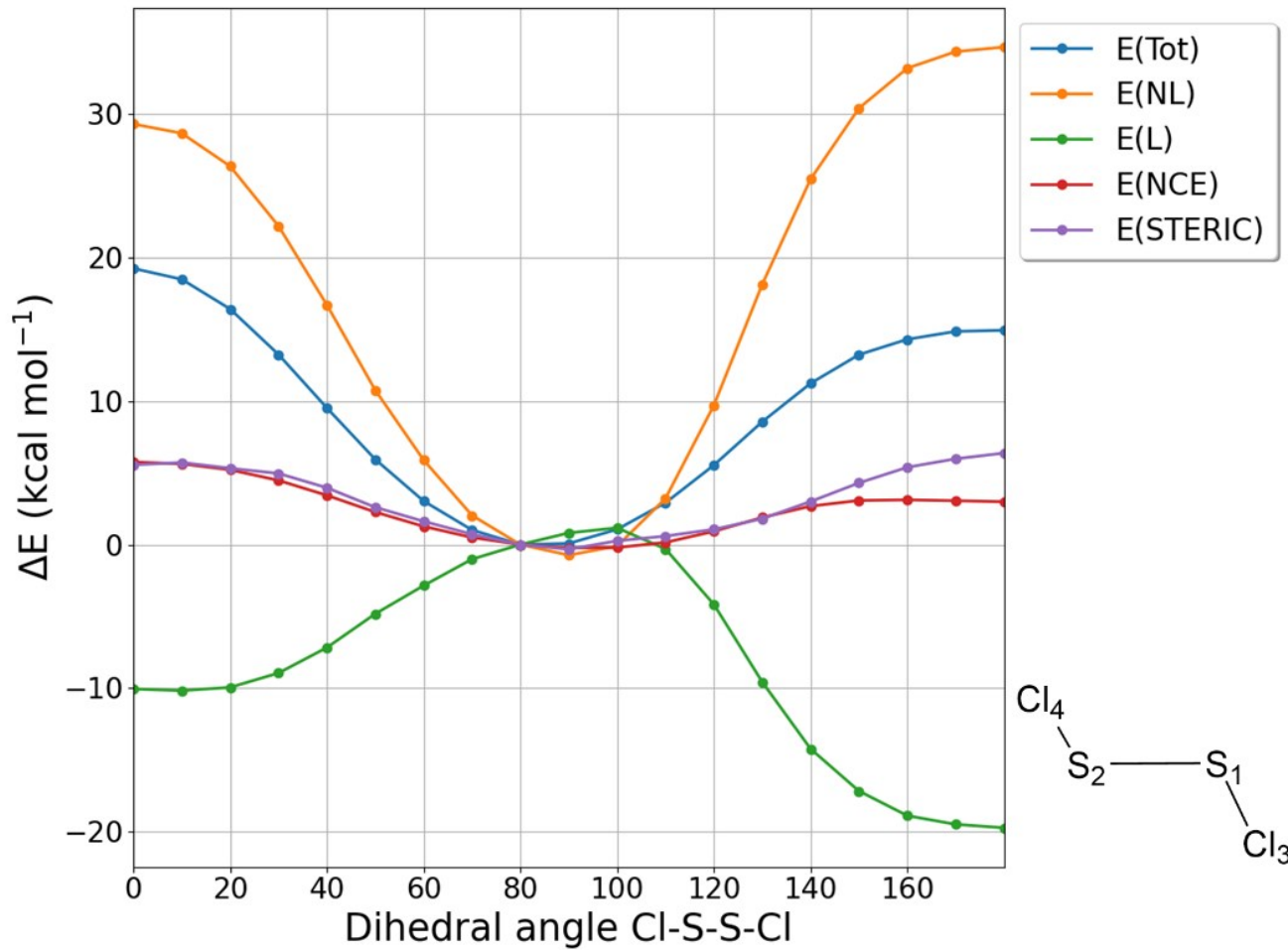


Figure S23. NBO deletion analysis calculated for ClSSCl at the M06-2X/6-311++G(3df,2p) level.

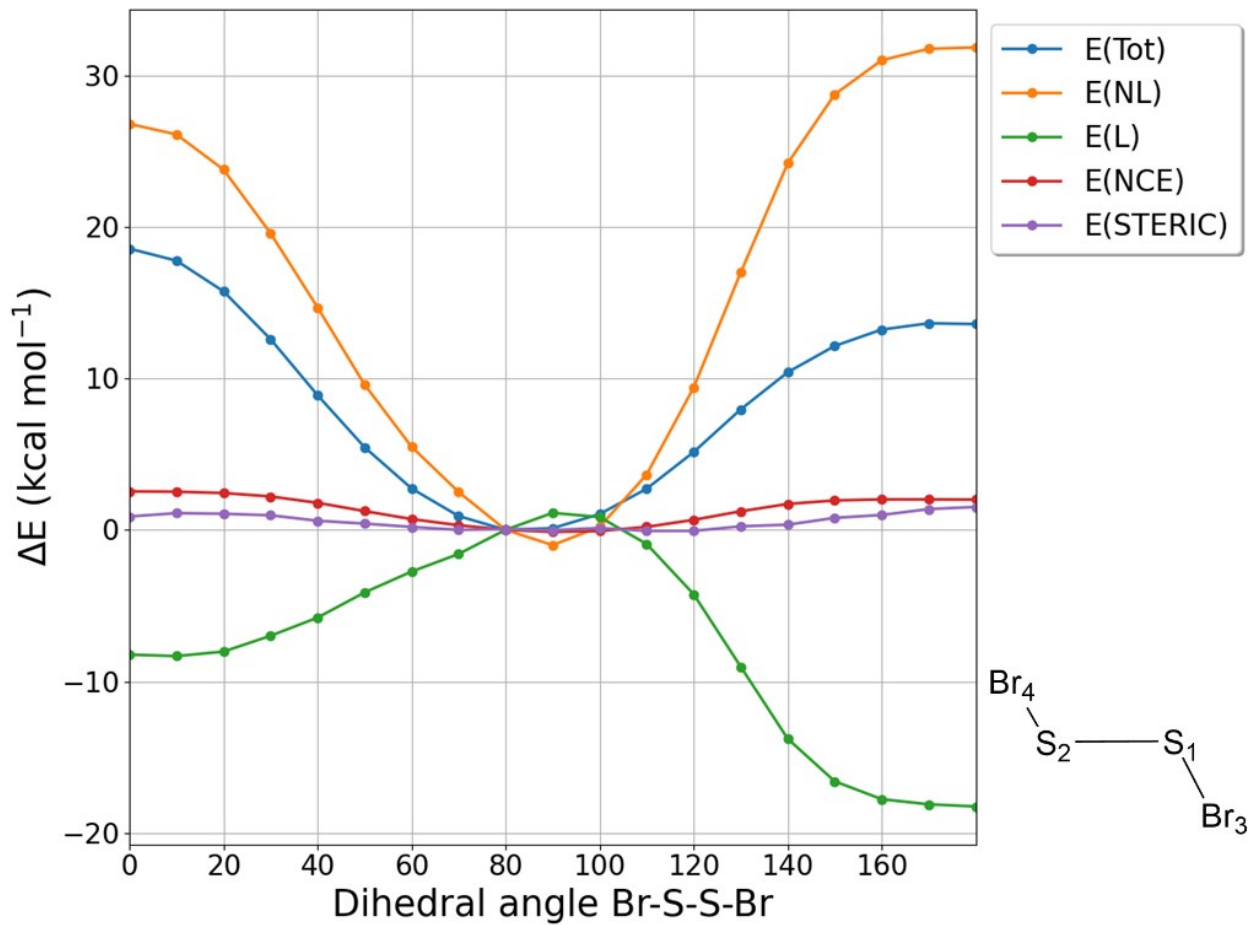


Figure S24. NBO deletion analysis calculated for BrSSBr at the M06-2X/6-311++G(3df,2p) level.

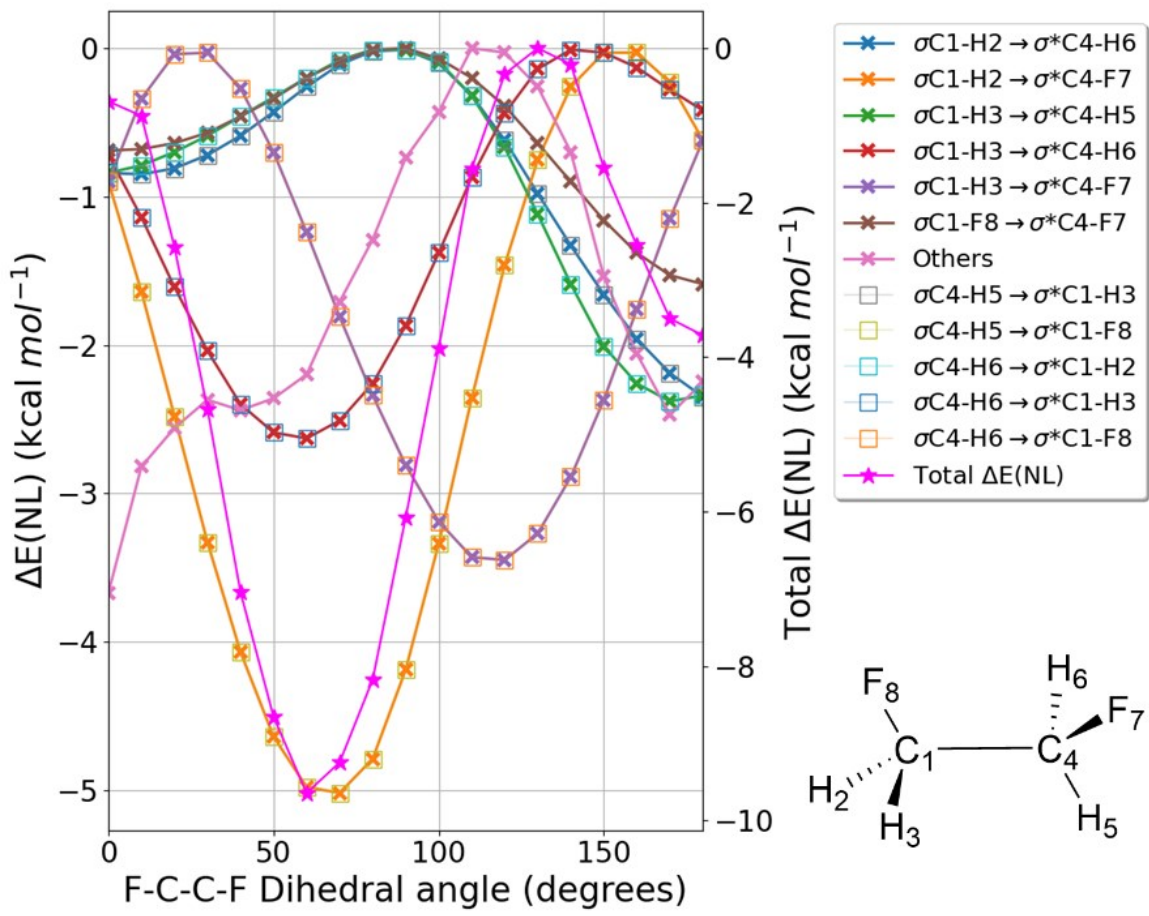


Figure S25. Hyperconjugation interaction energies for $\text{FCH}_2\text{CH}_2\text{F}$ obtained at the M06-2X/6-311++G(3df,2p) level using NBO analysis.

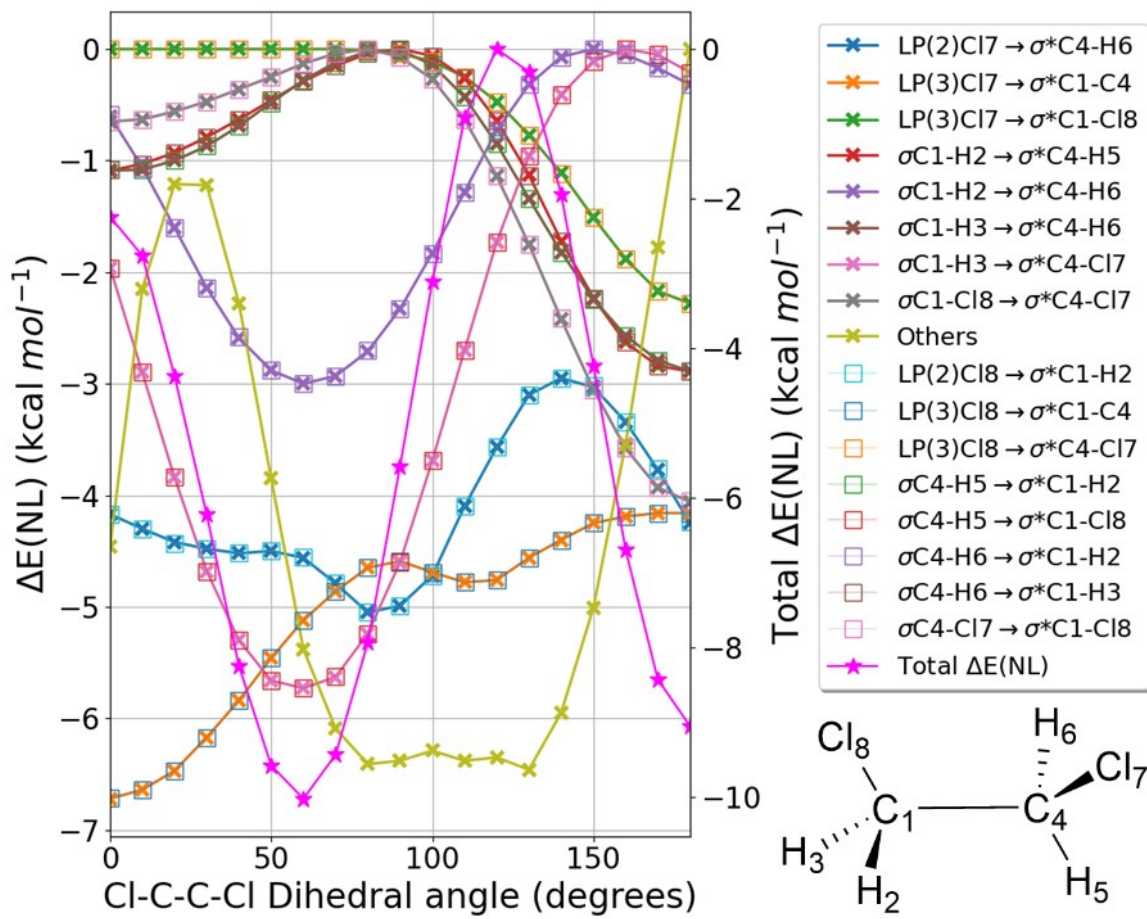


Figure S26. Hyperconjugation interaction energies for $\text{ClCH}_2\text{CH}_2\text{Cl}$ obtained at the M06-2X/6-311++G(3df,2p) level using NBO analysis.

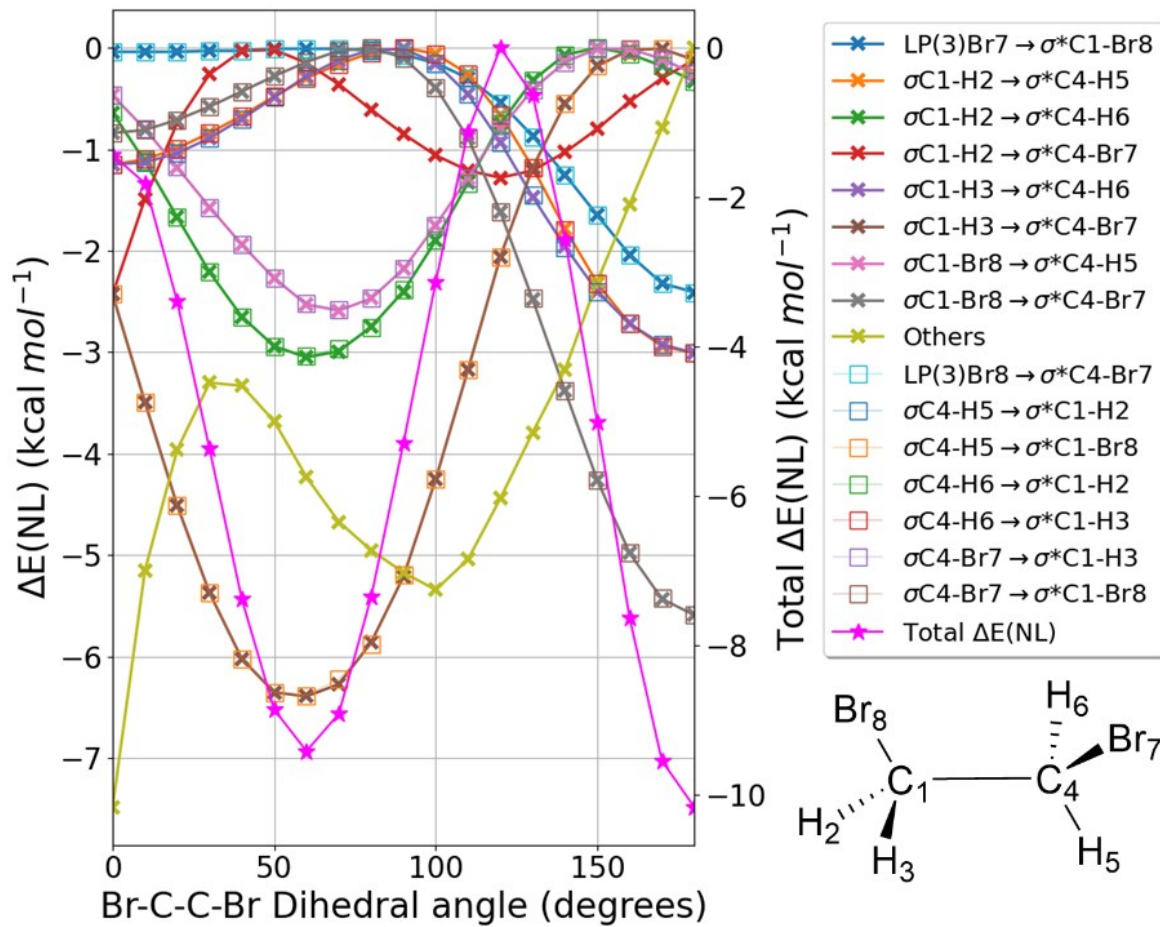


Figure S27. Hyperconjugation interaction energies for $\text{BrCH}_2\text{CH}_2\text{Br}$ obtained at the M06-2X/6-311++G(3df,2p) level using NBO analysis.

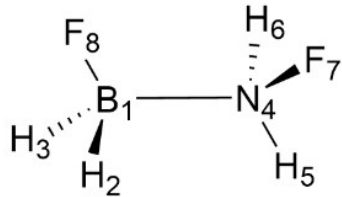
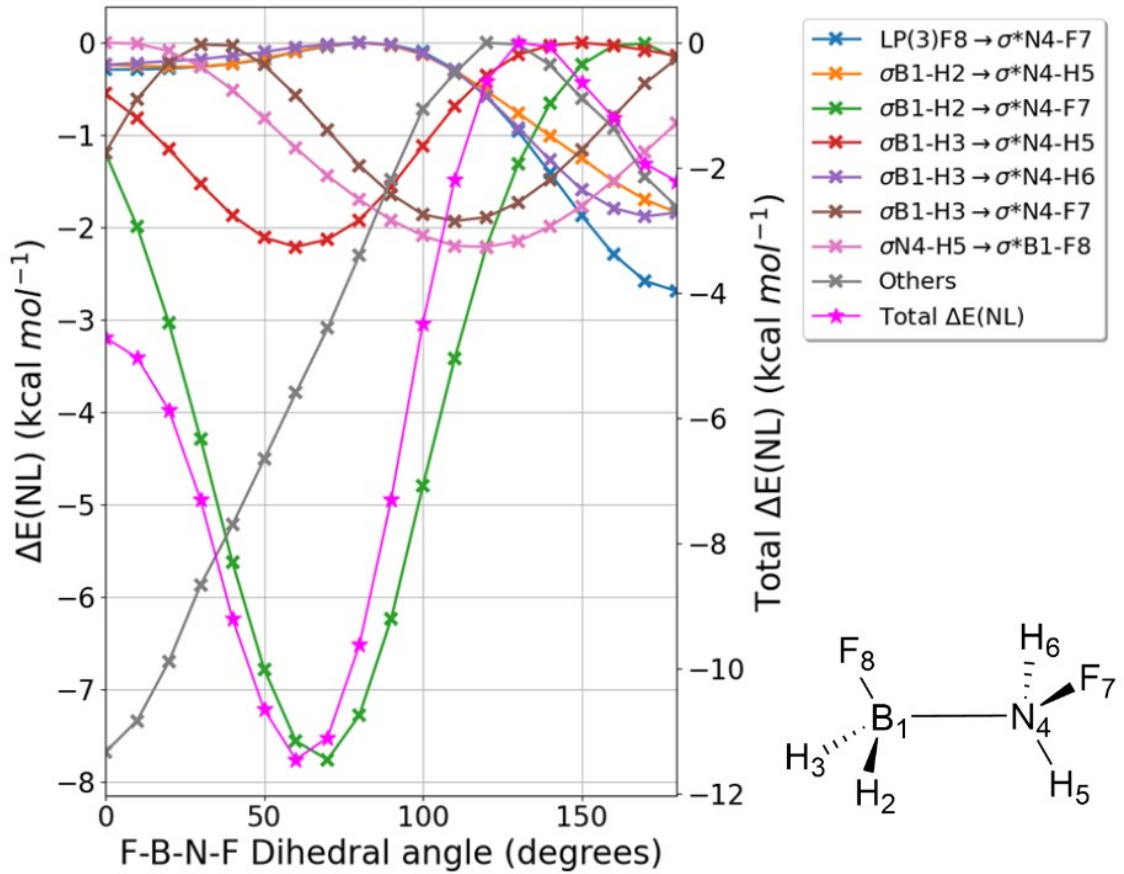


Figure S28. Hyperconjugation interaction energies for $\text{FBH}_2\text{NH}_2\text{F}$ obtained at the M06-2X/6-311++G(3df,2p) level using NBO analysis.

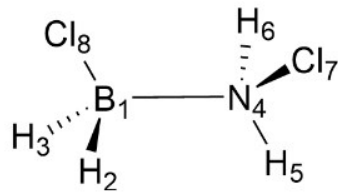
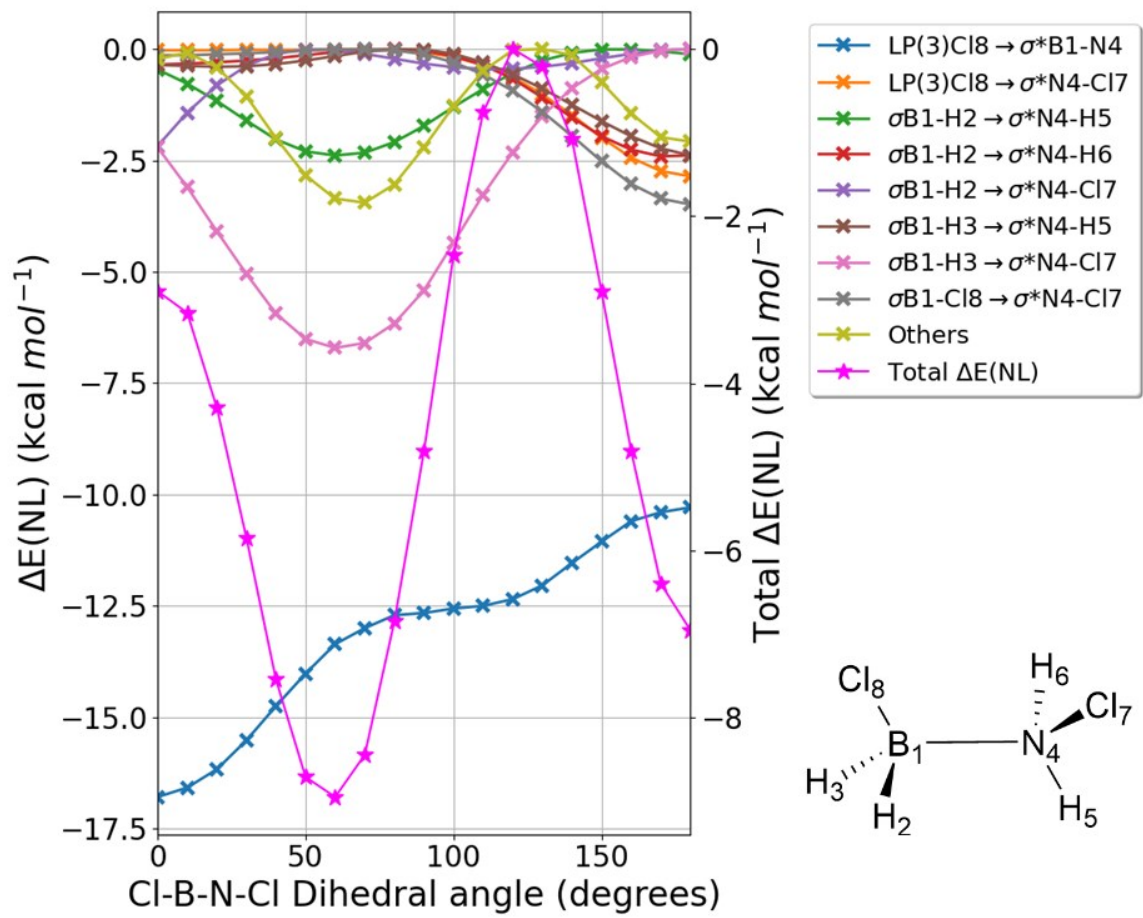


Figure S29. Hyperconjugation interaction energies for $\text{CIBH}_2\text{NH}_2\text{Cl}$ obtained at the M06-2X/6-311++G(3df,2p) level using NBO analysis.

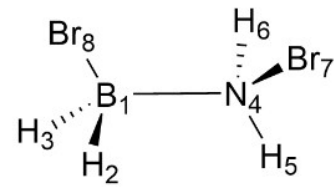
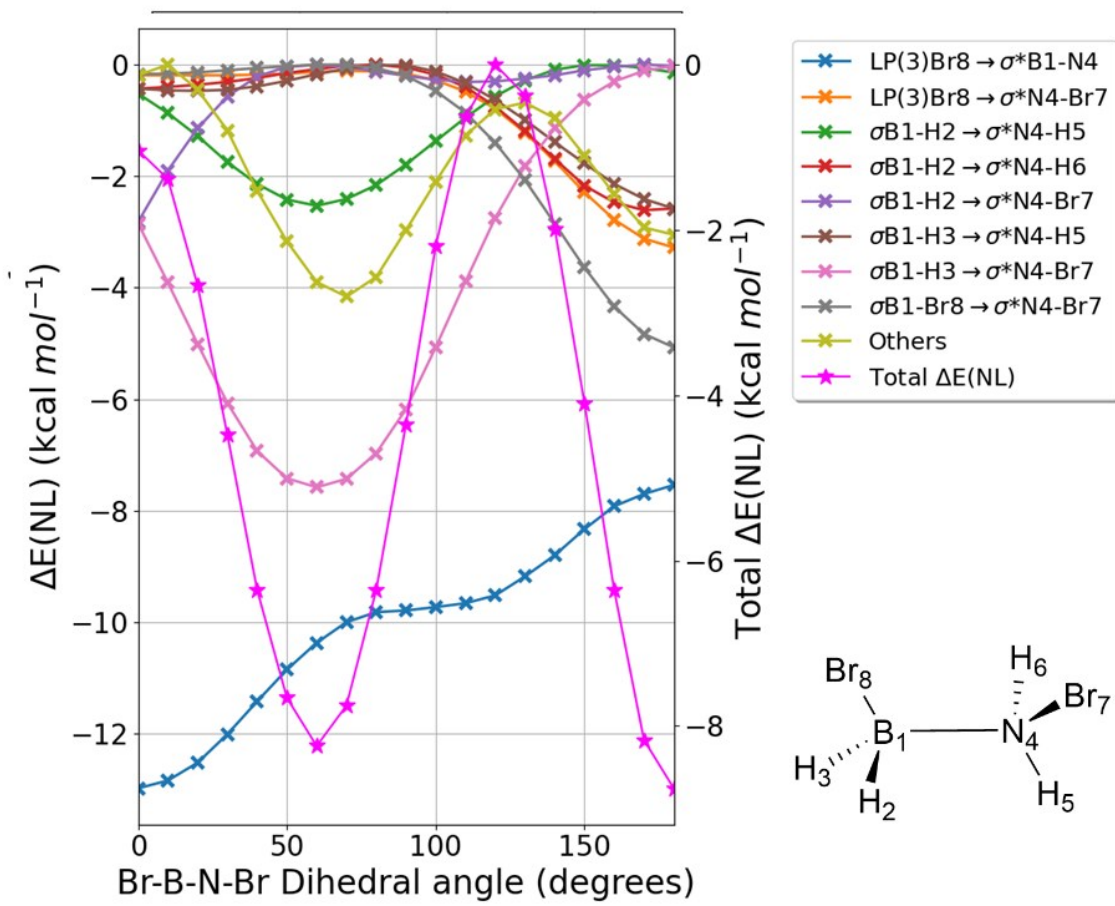


Figure S30. Hyperconjugation interaction energies for $\text{BrBH}_2\text{NH}_2\text{Br}$ obtained at the M06-2X/6-311++G(3df,2p) level using NBO analysis.

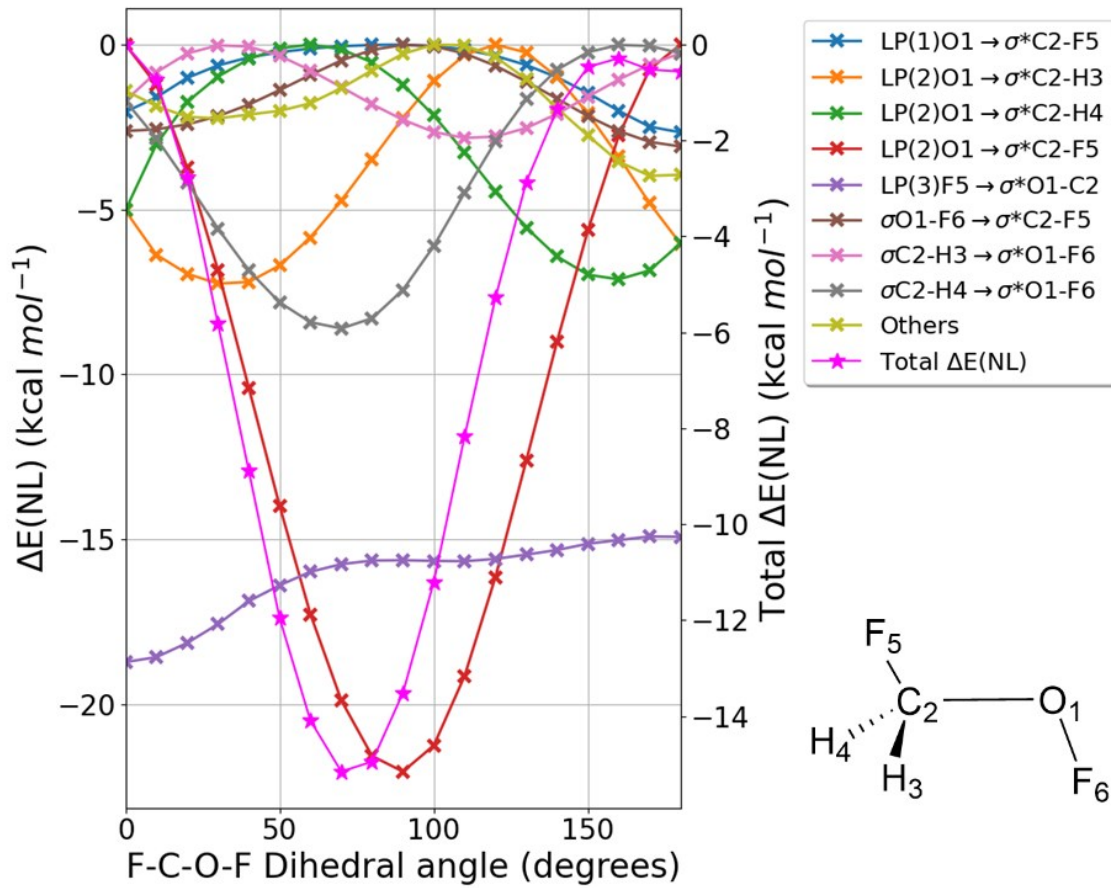


Figure S31. Hyperconjugation interaction energies for FCH_2OF obtained at the M06-2X/6-311++G(3df,2p) level using NBO analysis.

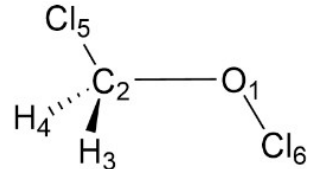
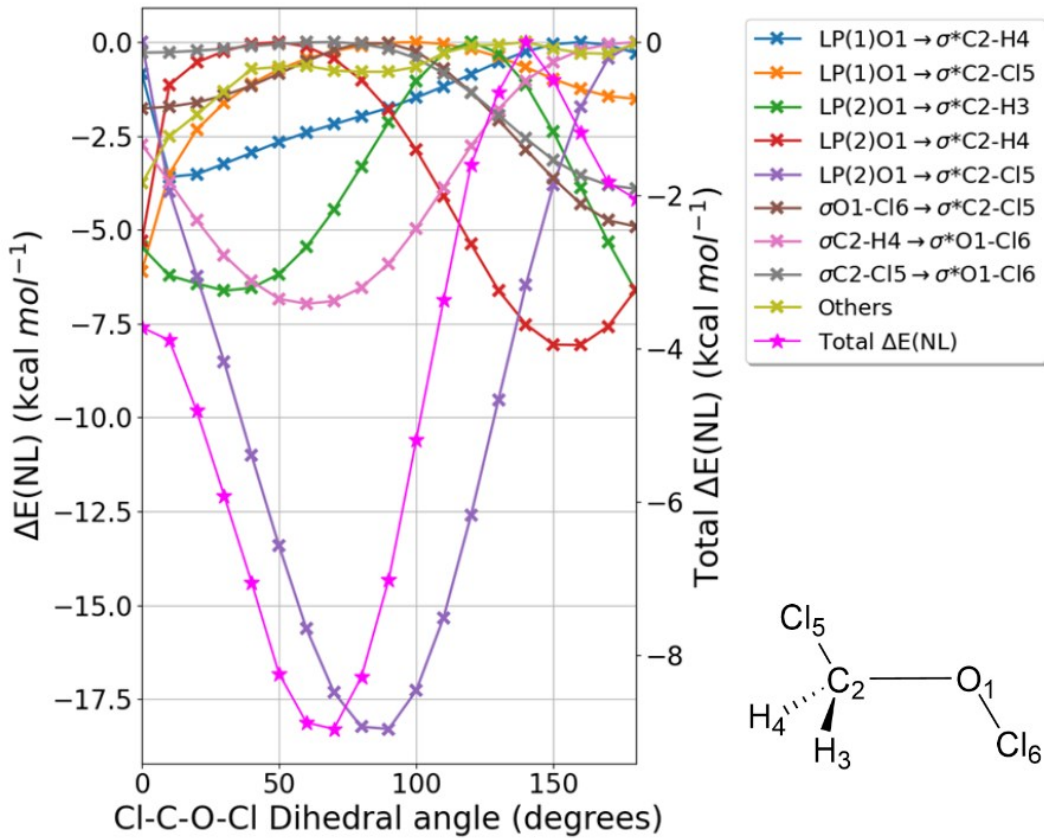


Figure S32. Hyperconjugation interaction energies for ClCH_2OCl obtained at the M06-2X/6-311++G(3df,2p) level using NBO analysis.

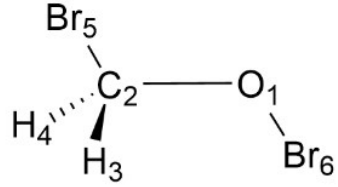
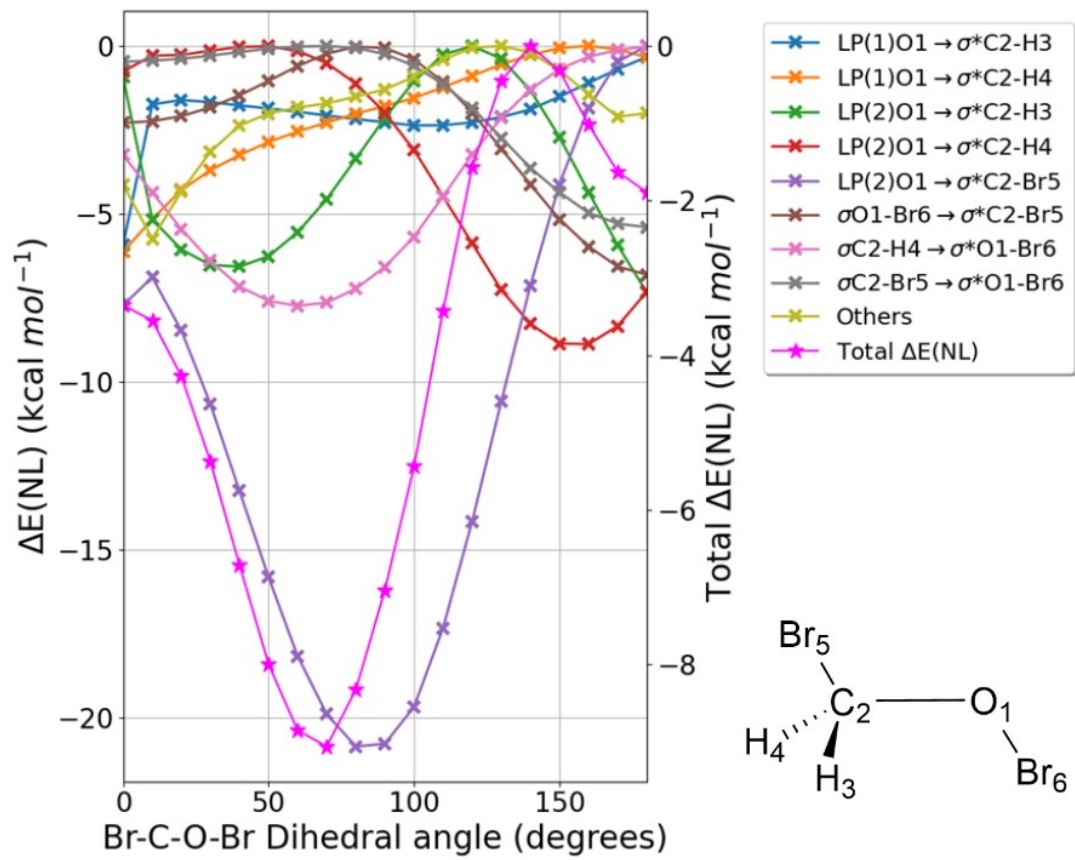


Figure S33. Hyperconjugation interaction energies for BrCH_2OBr obtained at the M06-2X/6-311++G(3df,2p) level using NBO analysis.

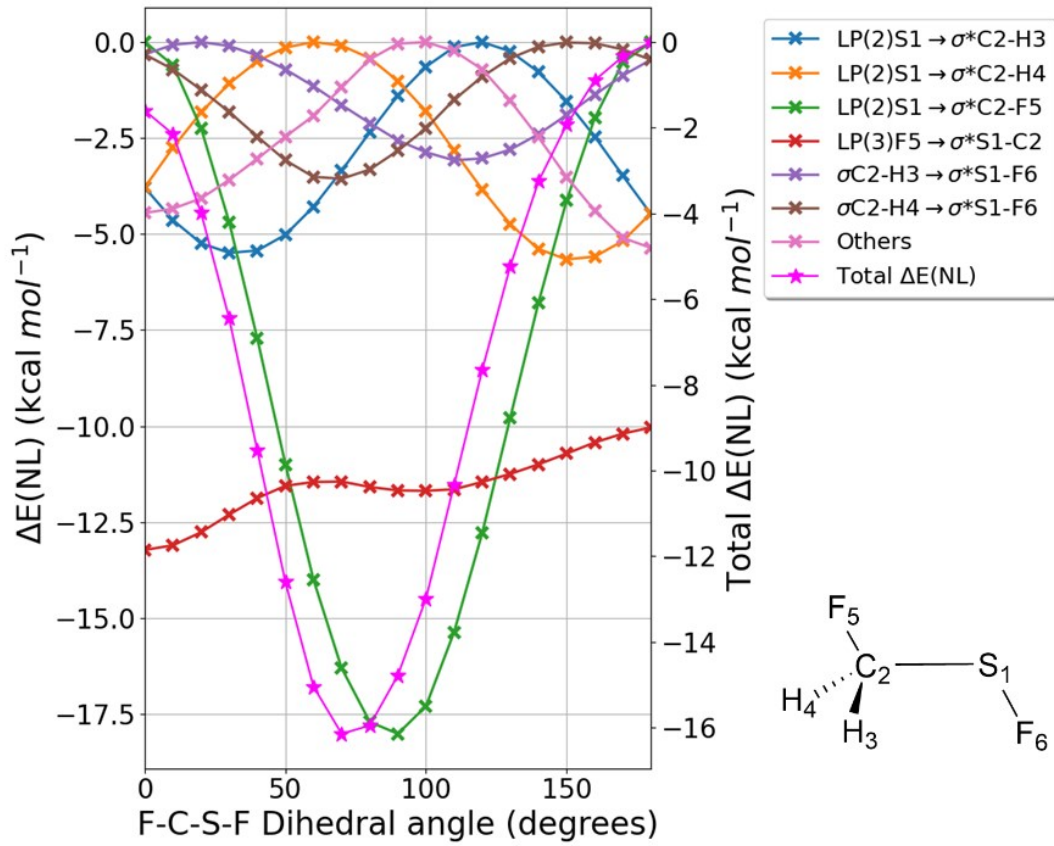


Figure S34. Hyperconjugation interaction energies for FCH_2SF obtained at the M06-2X/6-311++G(3df,2p) level using NBO analysis.

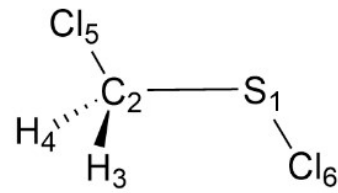
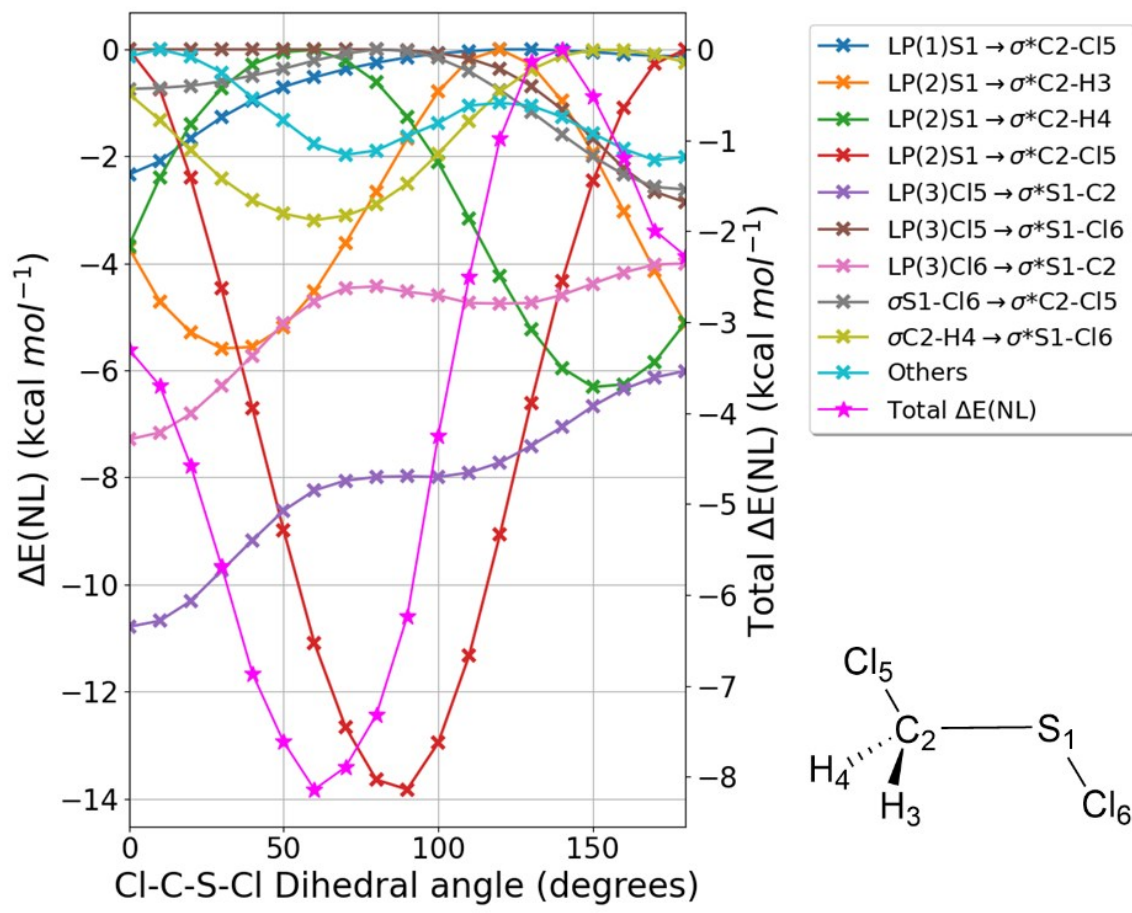


Figure S35. Hyperconjugation interaction energies for ClCH_2SCl obtained at the M06-2X/6-311++G(3df,2p) level using NBO analysis.

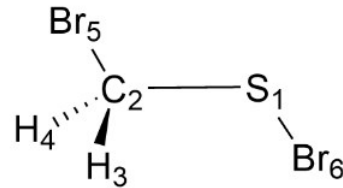
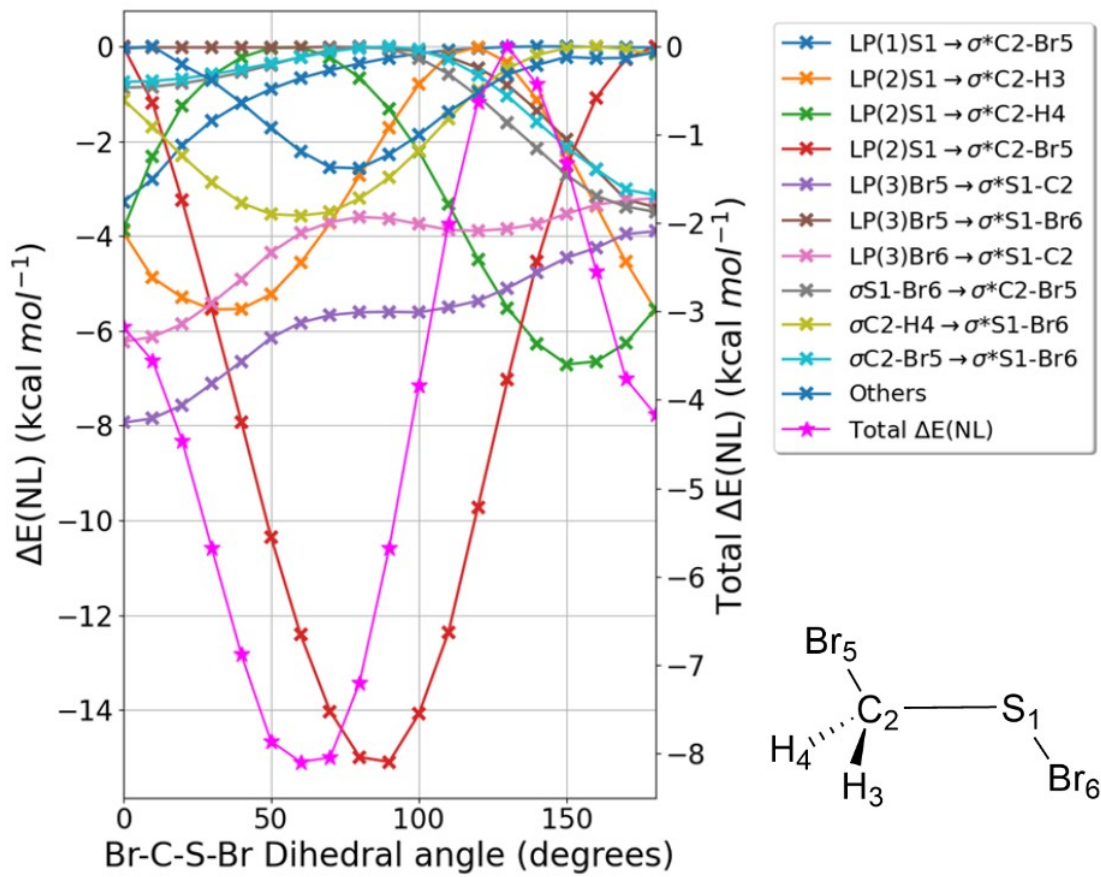


Figure S36. Hyperconjugation interaction energies for BrCH_2SBr obtained at the M06-2X/6-311++G(3df,2p) level using NBO analysis.

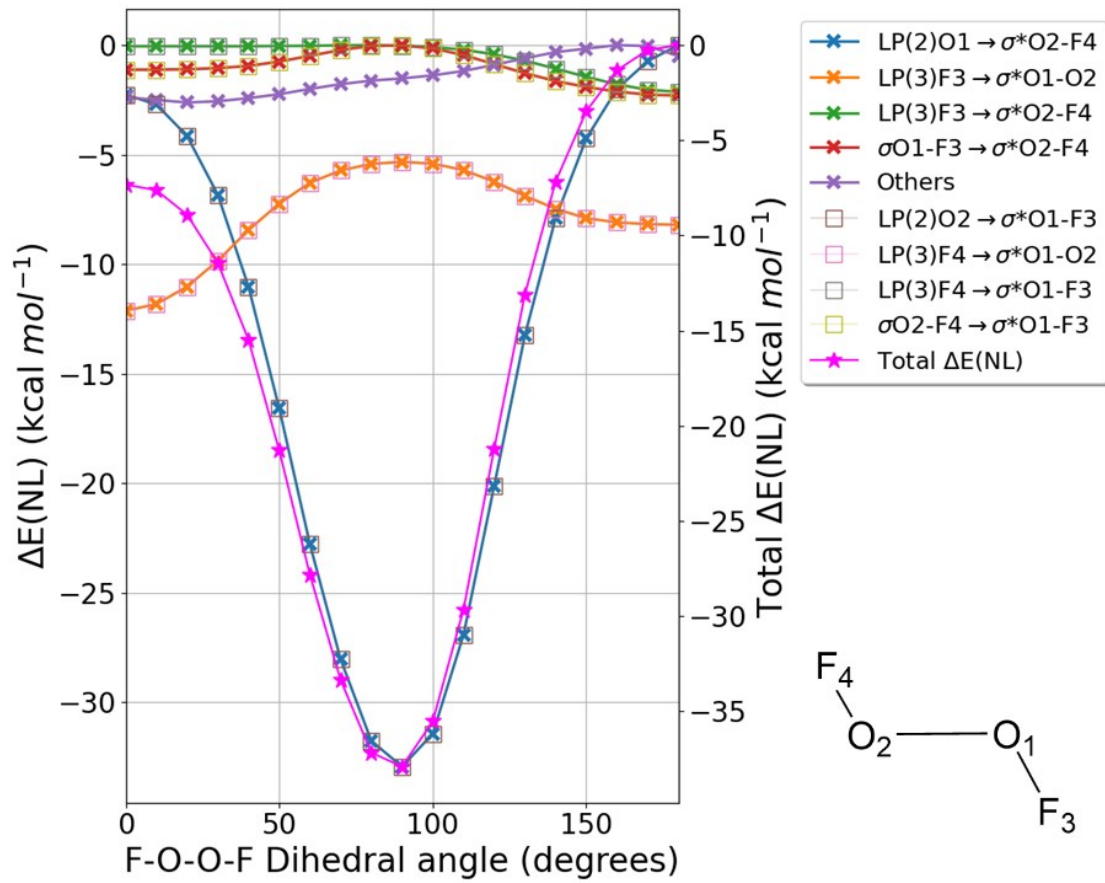


Figure S37. Hyperconjugation interaction energies for FOOF obtained at the M06-2X/6-311++G(3df,2p) level using NBO analysis.

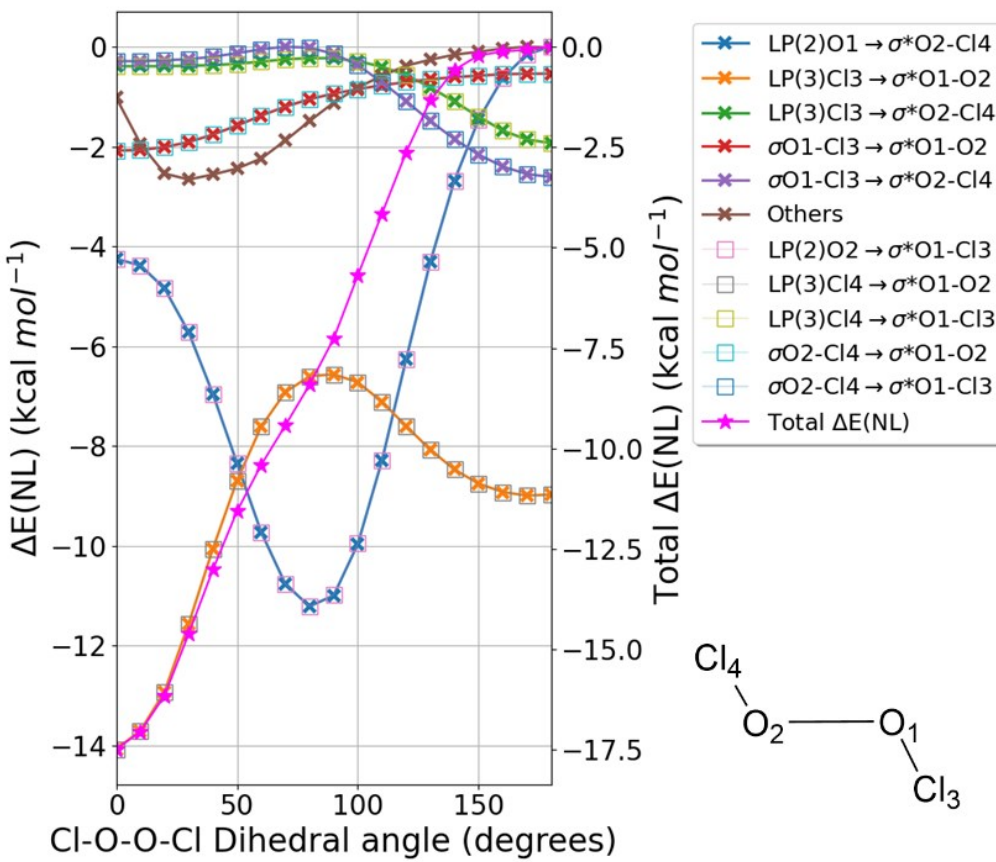


Figure S38. Hyperconjugation interaction energies for CLOOCl obtained at the M06-2X/6-311++G(3df,2p) level using NBO analysis.

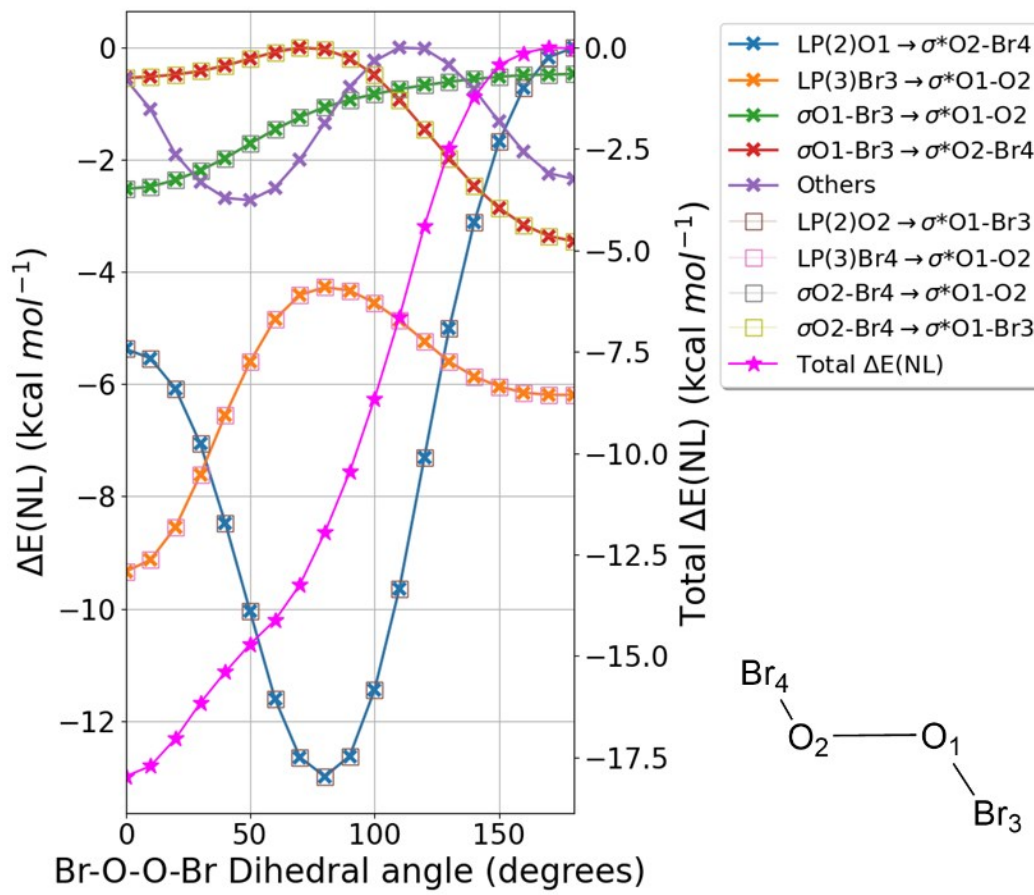


Figure S39. Hyperconjugation interaction energies for BrOOBr obtained at the M06-2X/6-311++G(3df,2p) level using NBO analysis.

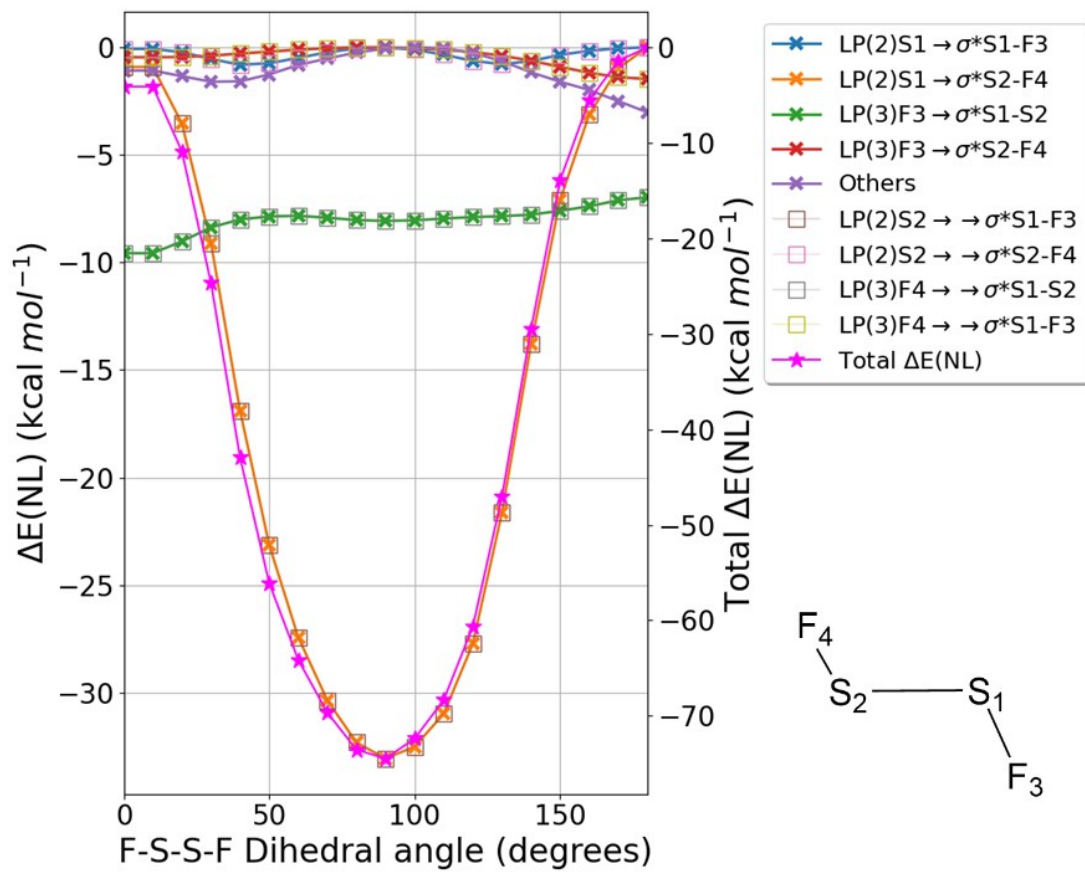


Figure S40. Hyperconjugation interaction energies for FSSF obtained at the M06-2X/6-311++G(3df,2p) level using NBO analysis.

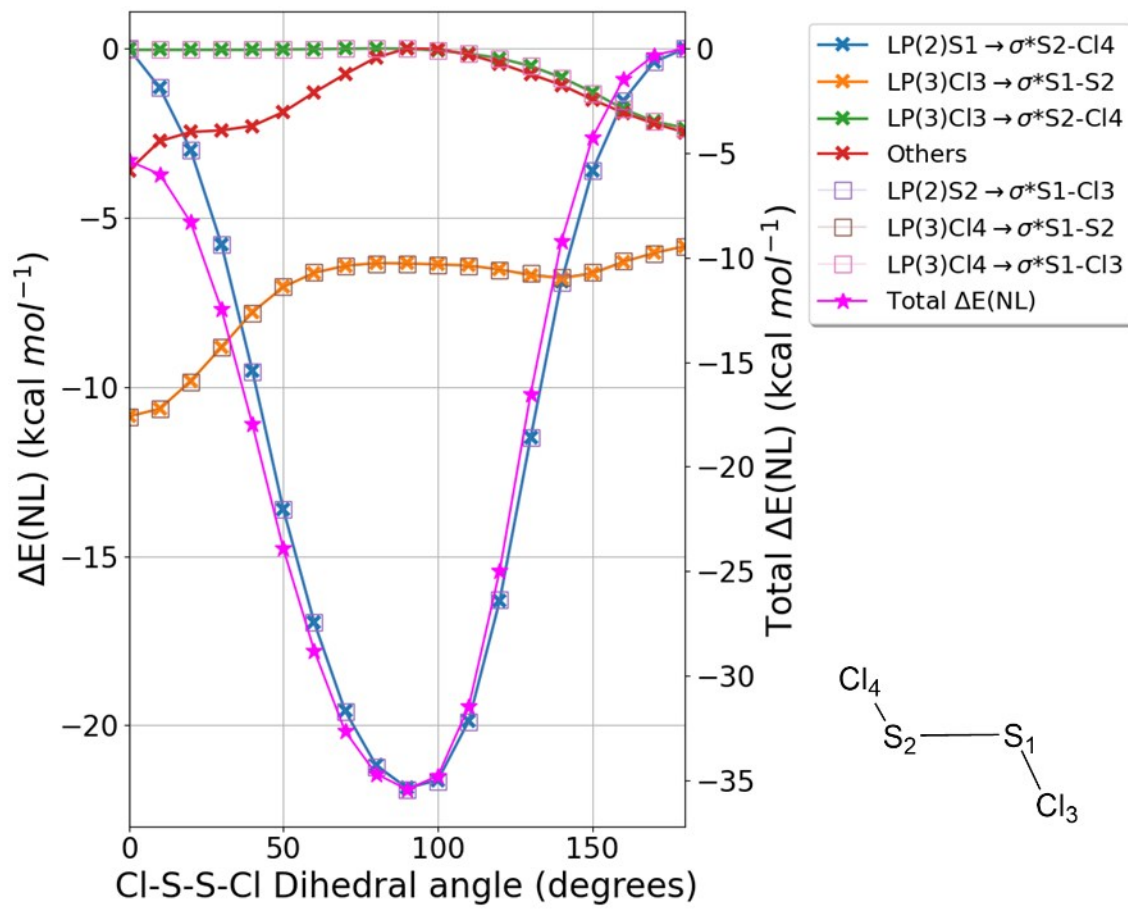


Figure S41. Hyperconjugation interaction energies for CISSCl obtained at the M06-2X/6-311++G(3df,2p) level using NBO analysis.

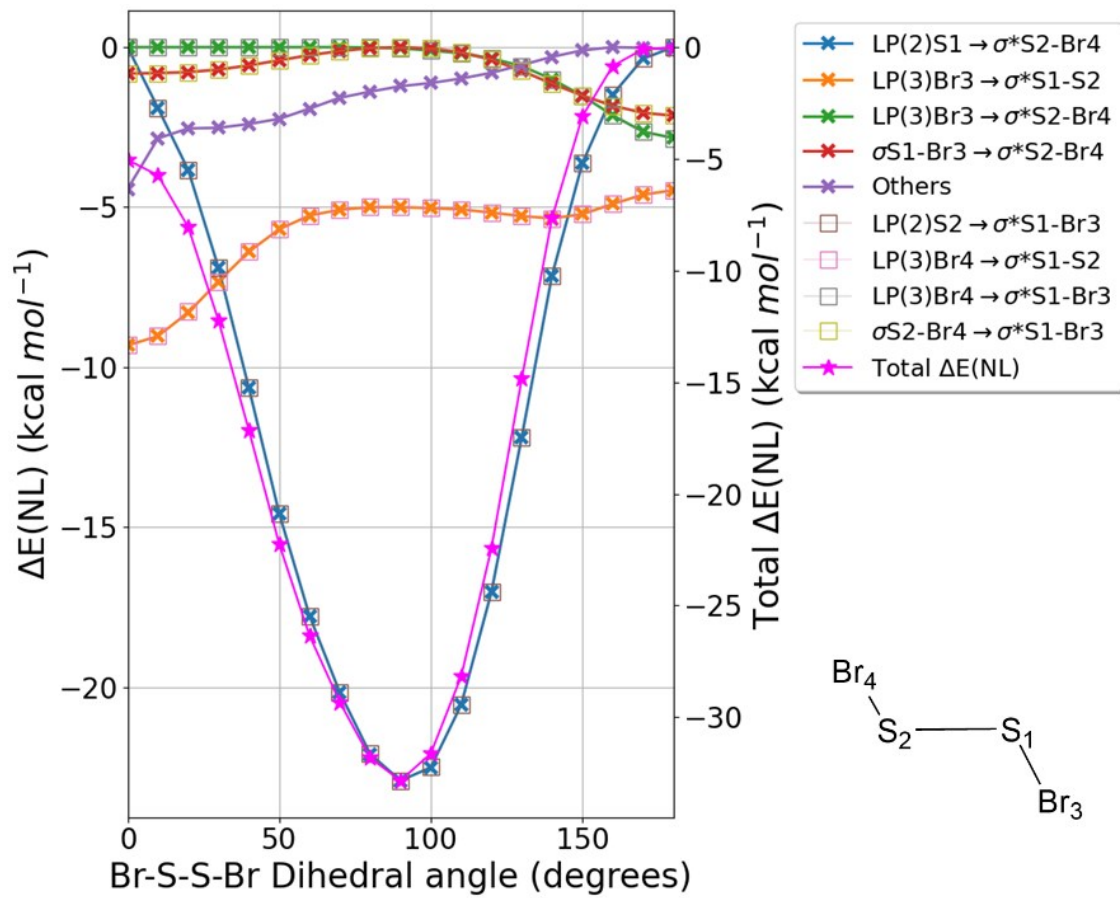


Figure S42. Hyperconjugation interaction energies for BrSSBr obtained at the M06-2X/6-311++G(3df,2p) level using NBO analysis.

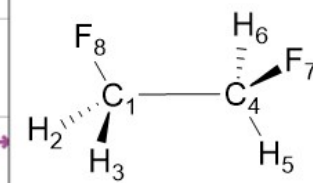
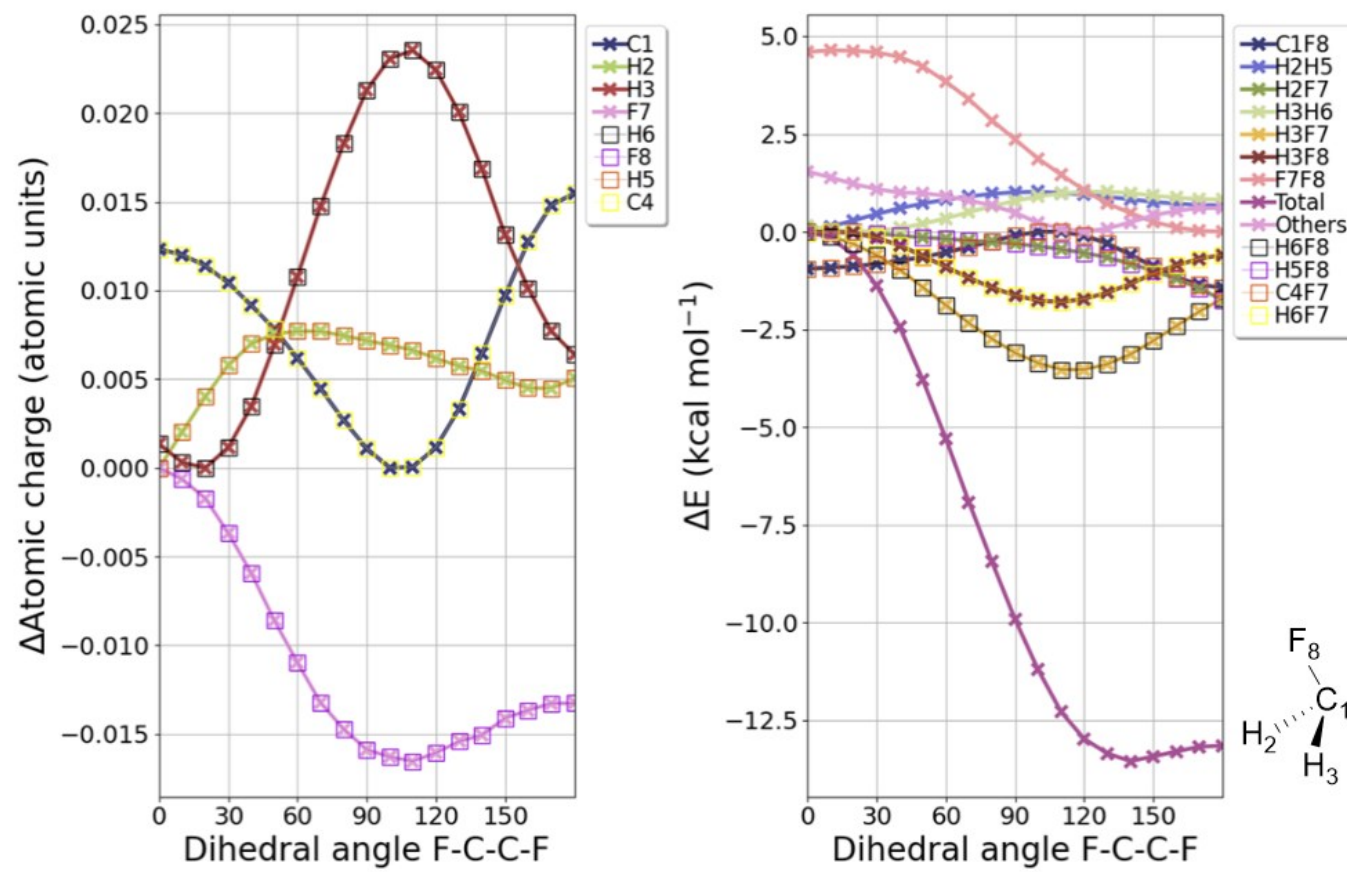


Figure S43. Atomic charges and natural Coulomb electrostatic (NCE) energy curves for $\text{FCH}_2\text{CH}_2\text{F}$ calculated at the M06-2X/6-311++G(3df,2p) level.

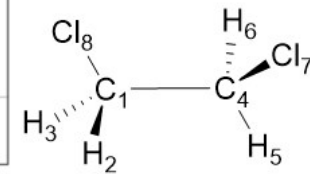
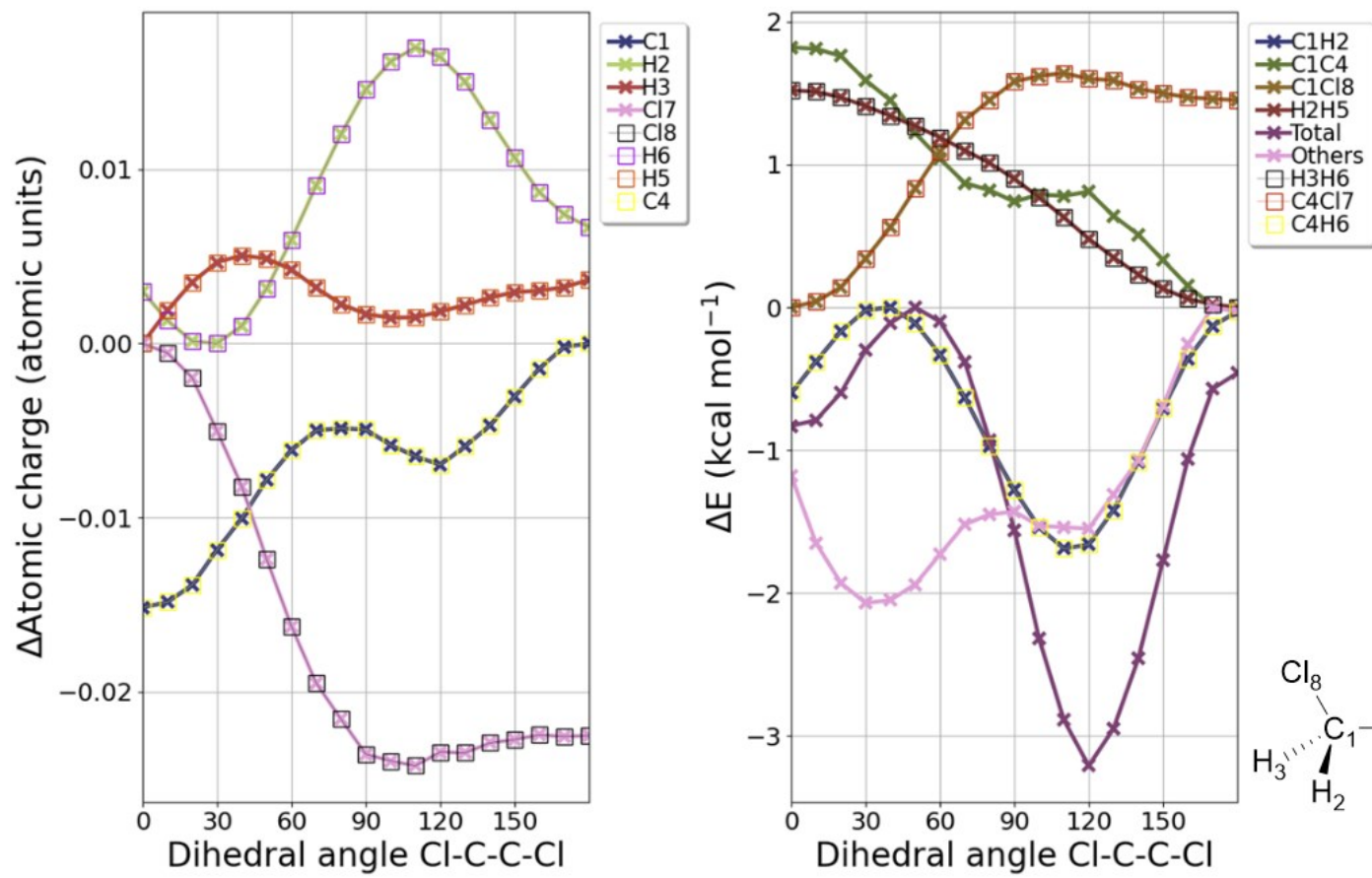


Figure S44. Atomic charges and natural Coulomb electrostatic (NCE) energy curves for $\text{ClCH}_2\text{CH}_2\text{Cl}$ calculated at the M06-2X/6-311++G(3df,2p) level.

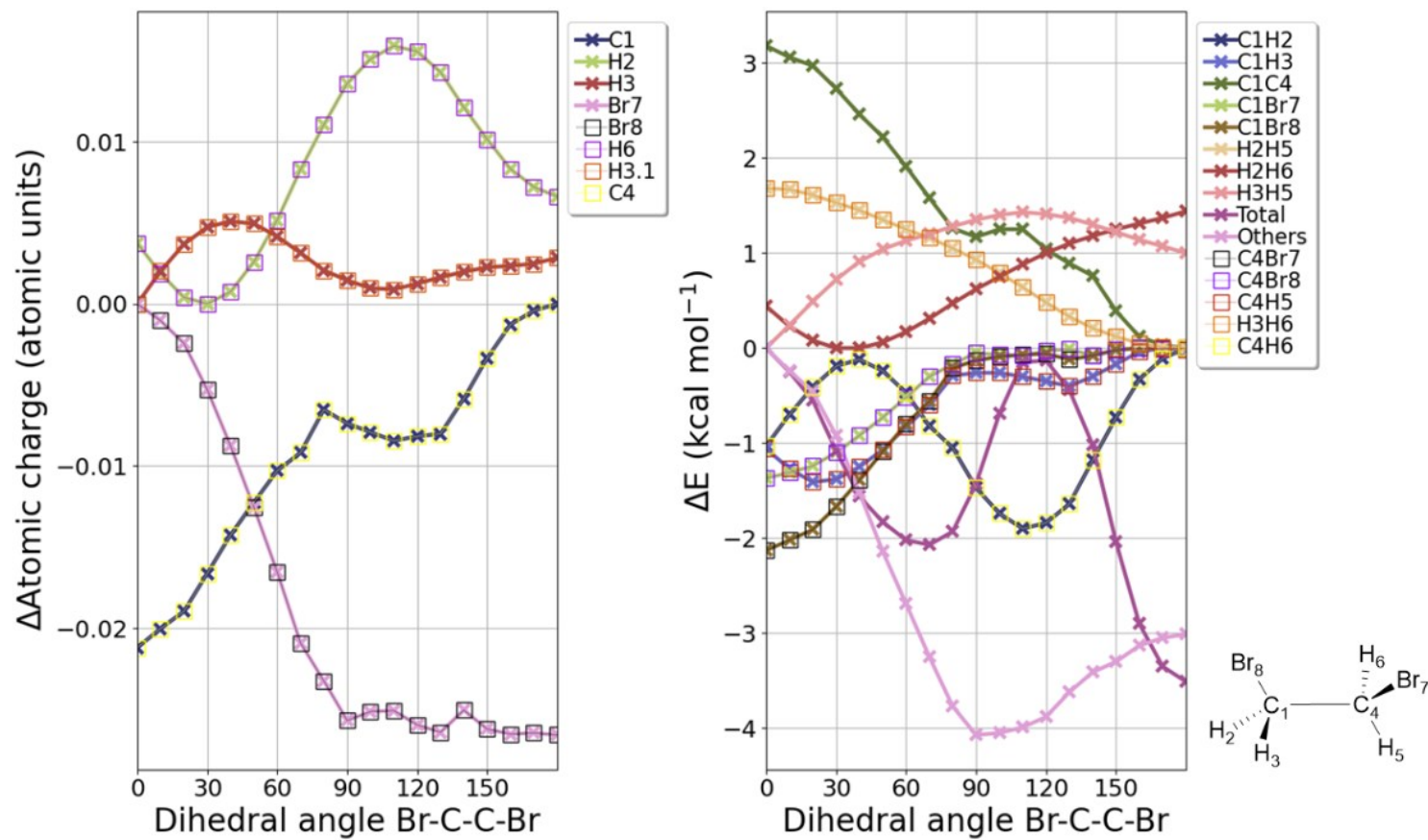


Figure S45. Atomic charges and natural Coulomb electrostatic (NCE) energy curves for $\text{BrCH}_2\text{CH}_2\text{Br}$ calculated at the M06-2X/6-311++G(3df,2p) level.

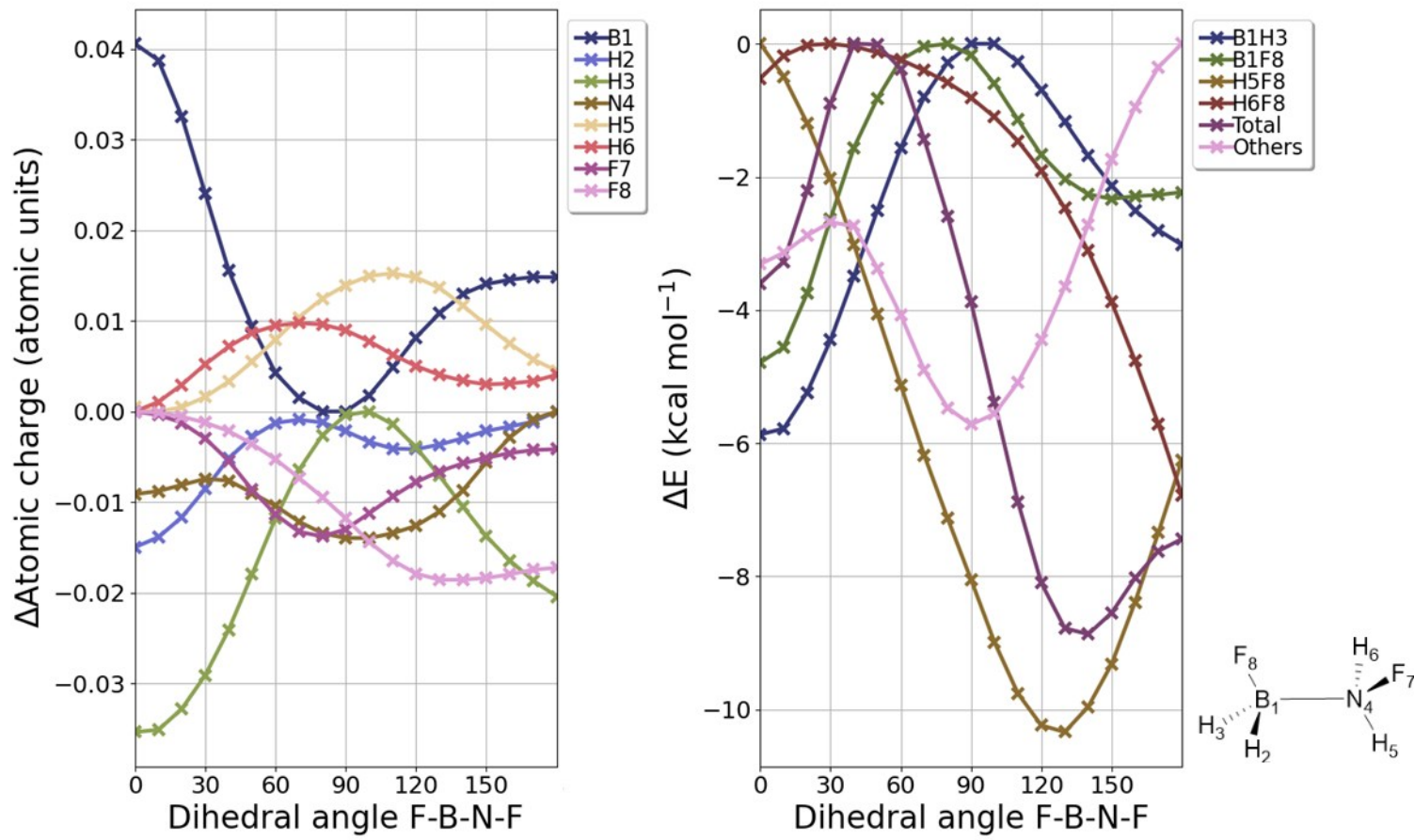


Figure S46. Atomic charges and natural Coulomb electrostatic (NCE) energy curves for $\text{FBH}_2\text{NH}_2\text{F}$ calculated at the M06-2X/6-311++G(3df,2p) level.

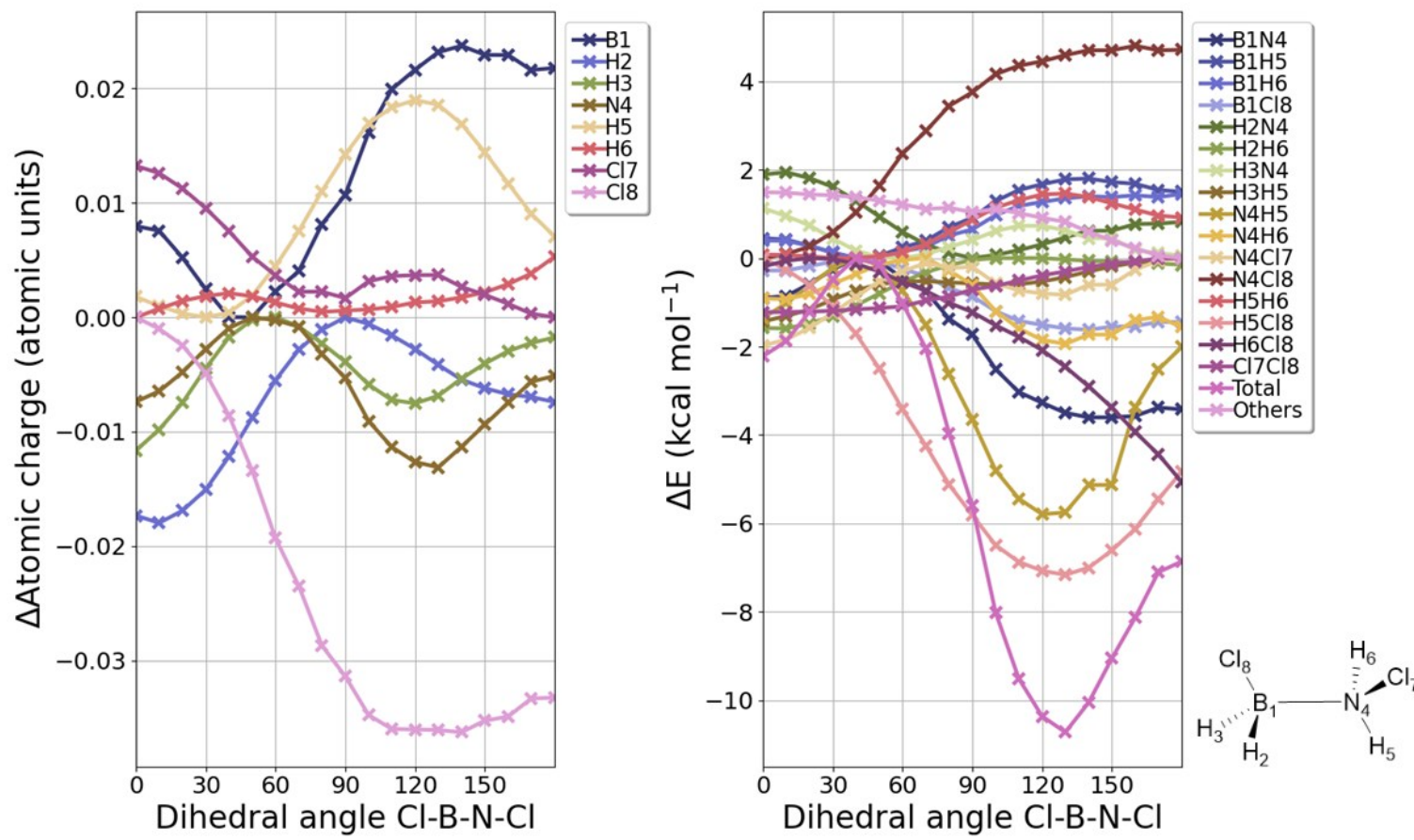


Figure S47. Atomic charges and natural Coulomb electrostatic (NCE) energy curves for $\text{CIBH}_2\text{NH}_2\text{Cl}$ calculated at the M06-2X/6-311++G(3df,2p) level.

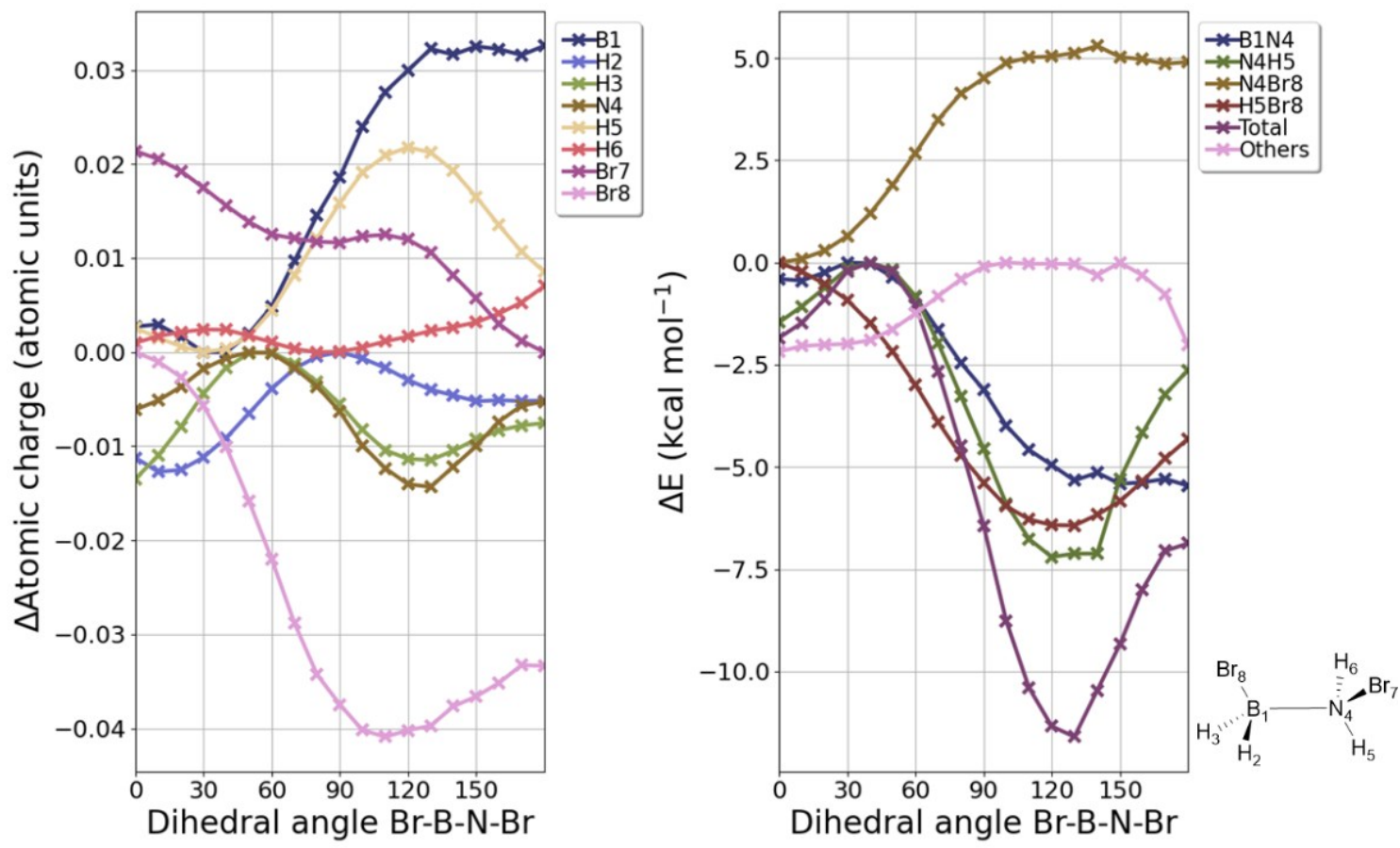


Figure S48. Atomic charges and natural Coulomb electrostatic (NCE) energy curves for $\text{BrBH}_2\text{NH}_2\text{Br}$ calculated at the M06-2X/6-311++G(3df,2p) level.

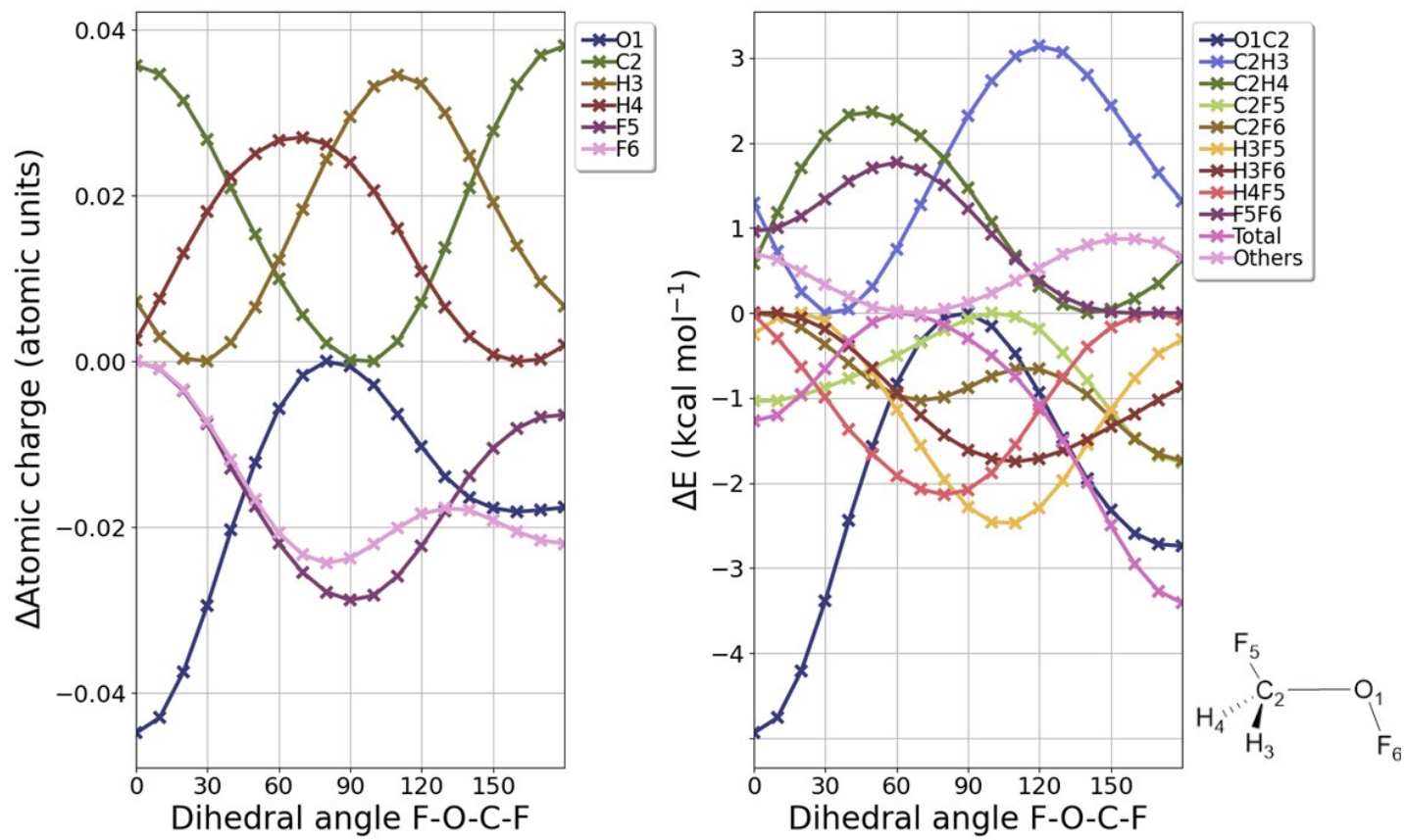


Figure S49. Atomic charges and natural Coulomb electrostatic (NCE) energy curves for FCH_2OF calculated at the M06-2X/6-311++G(3df,2p) level.

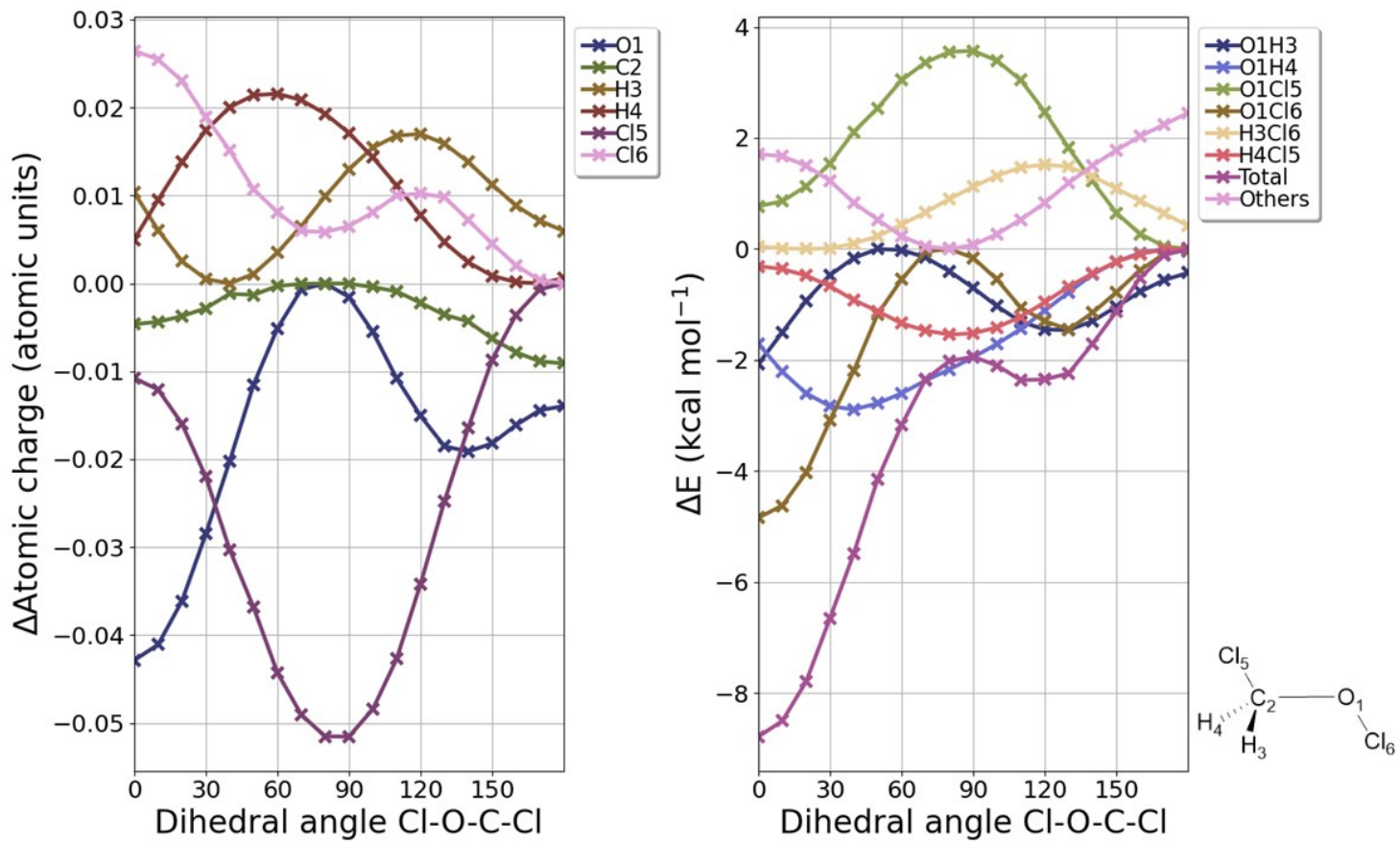


Figure S50. Atomic charges and natural Coulomb electrostatic (NCE) energy curves for ClCH2OCl calculated at the M06-2X/6-311++G(3df,2p) level.

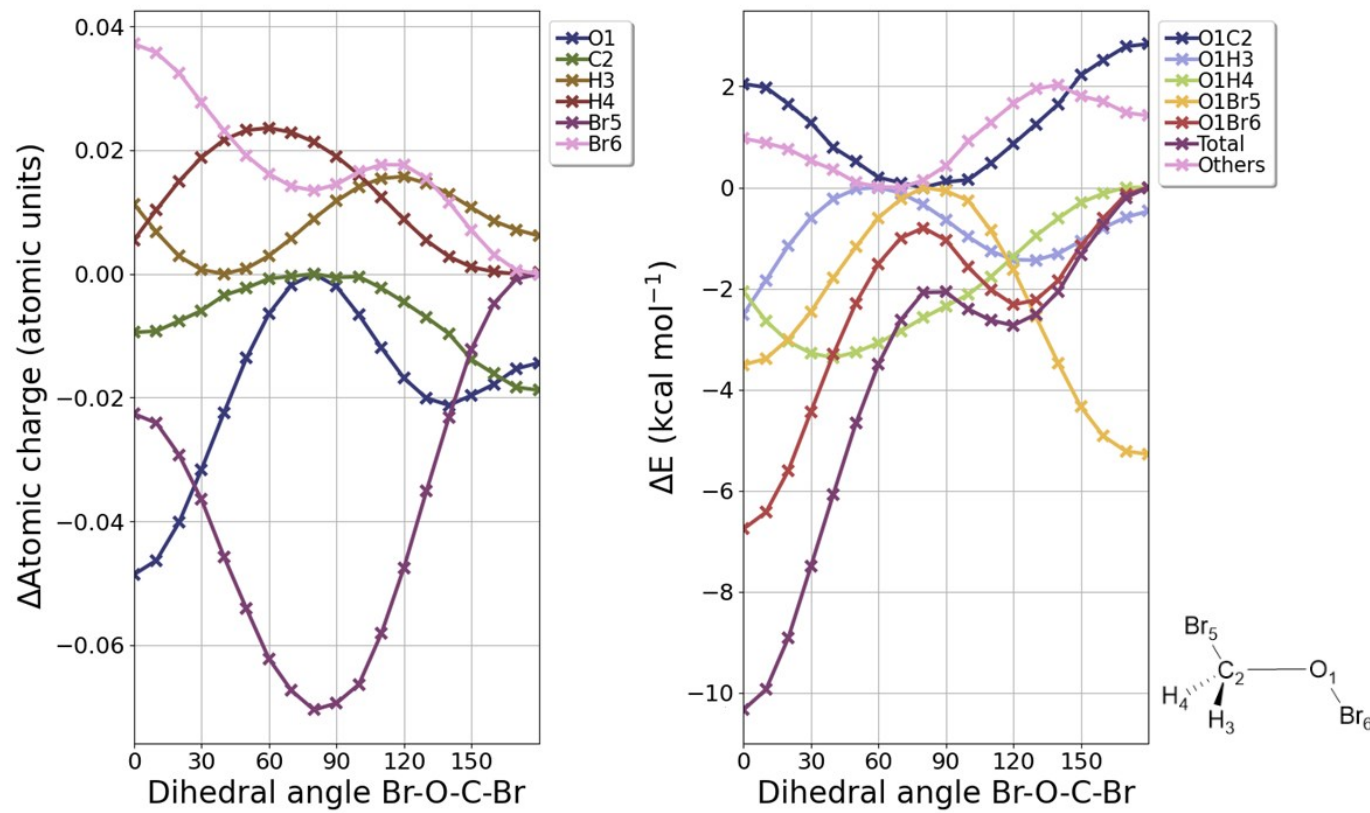


Figure S51. Atomic charges and natural Coulomb electrostatic (NCE) energy curves for BrCH_2OBr calculated at the M06-2X/6-311++G(3df,2p) level.

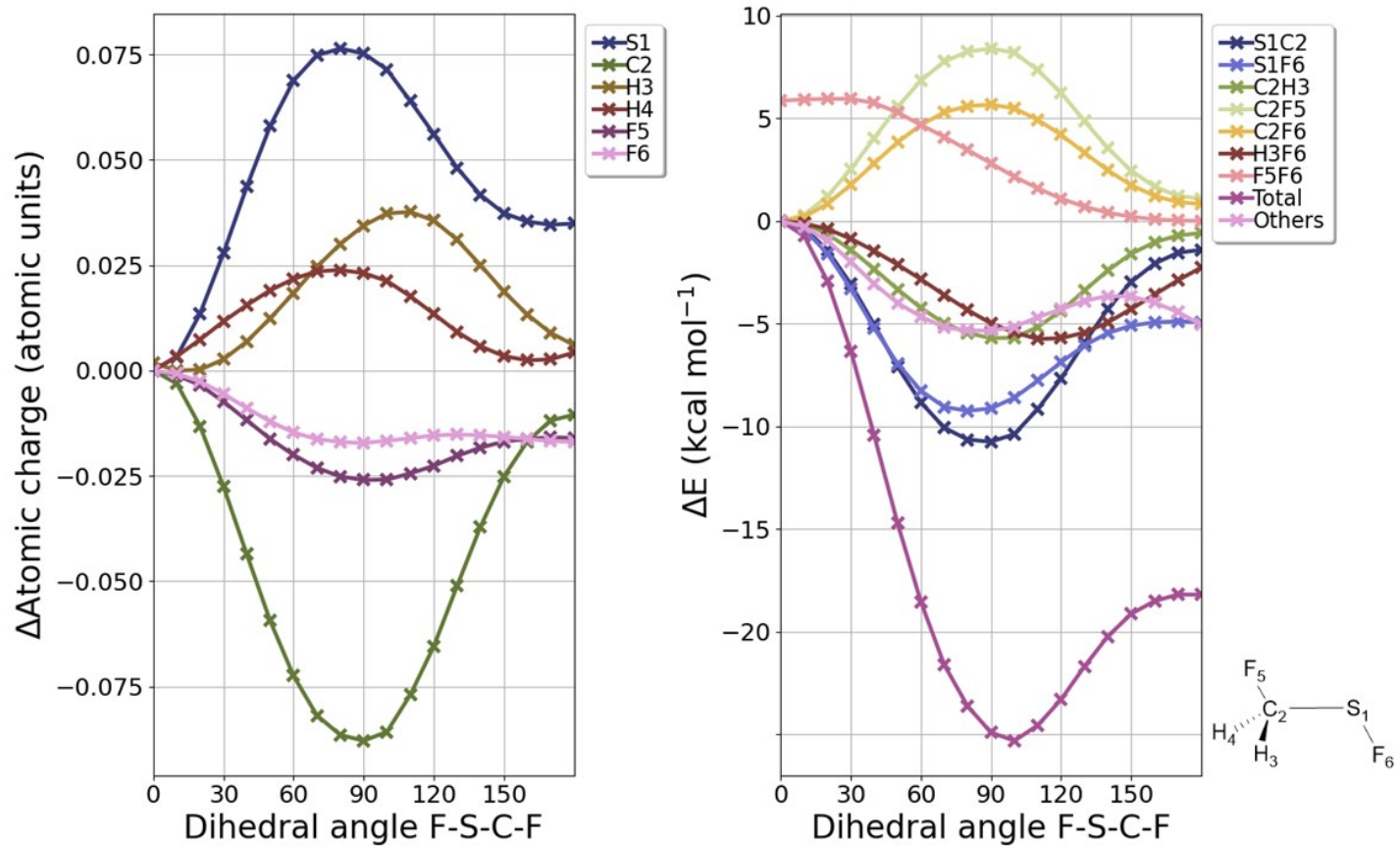


Figure S52. Atomic charges and natural Coulomb electrostatic (NCE) energy curves for FCH_2SF calculated at the M06-2X/6-311++G(3df,2p) level.

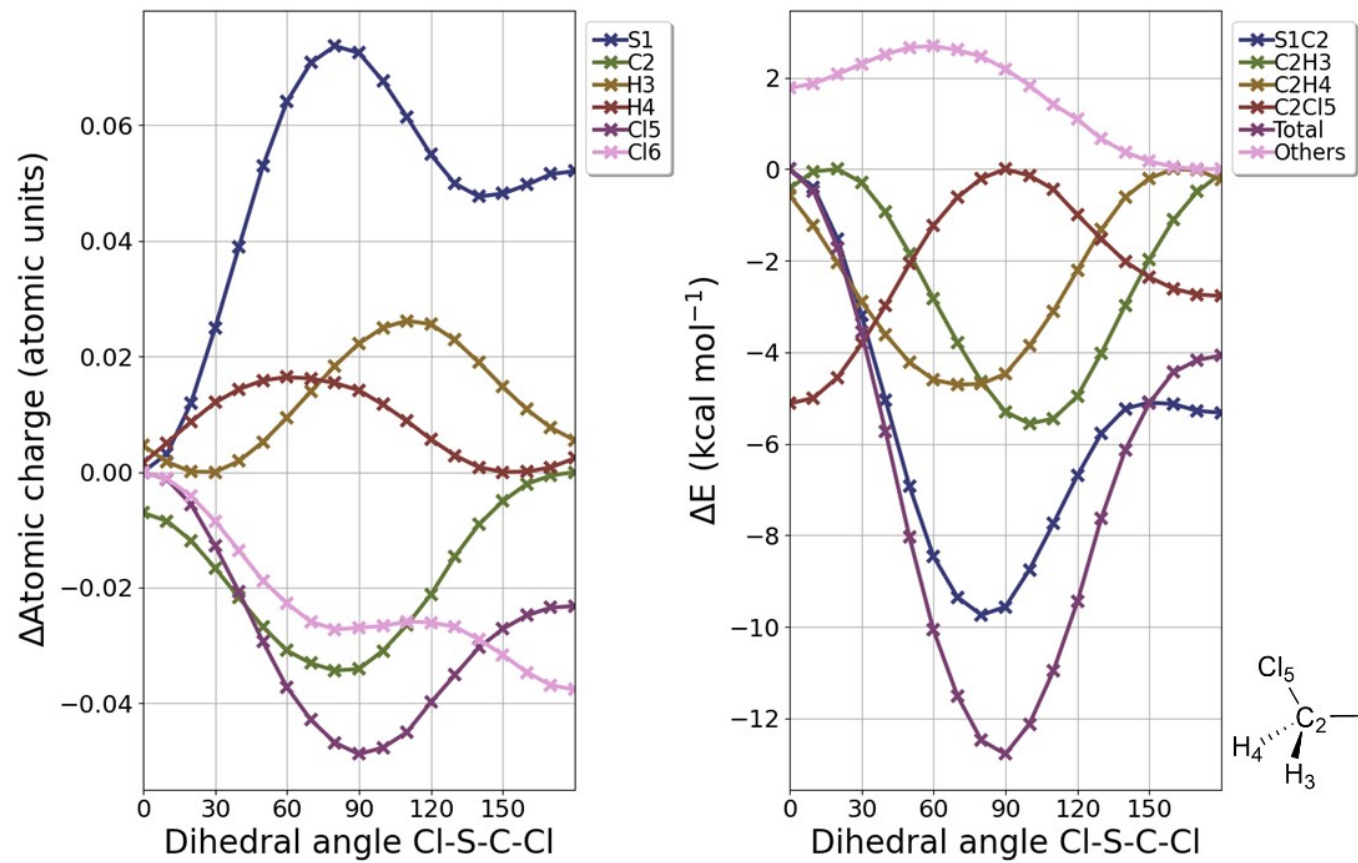


Figure S53. Atomic charges and natural Coulomb electrostatic (NCE) energy curves for ClCH_2SCl calculated at the M06-2X/6-311++G(3df,2p) level.

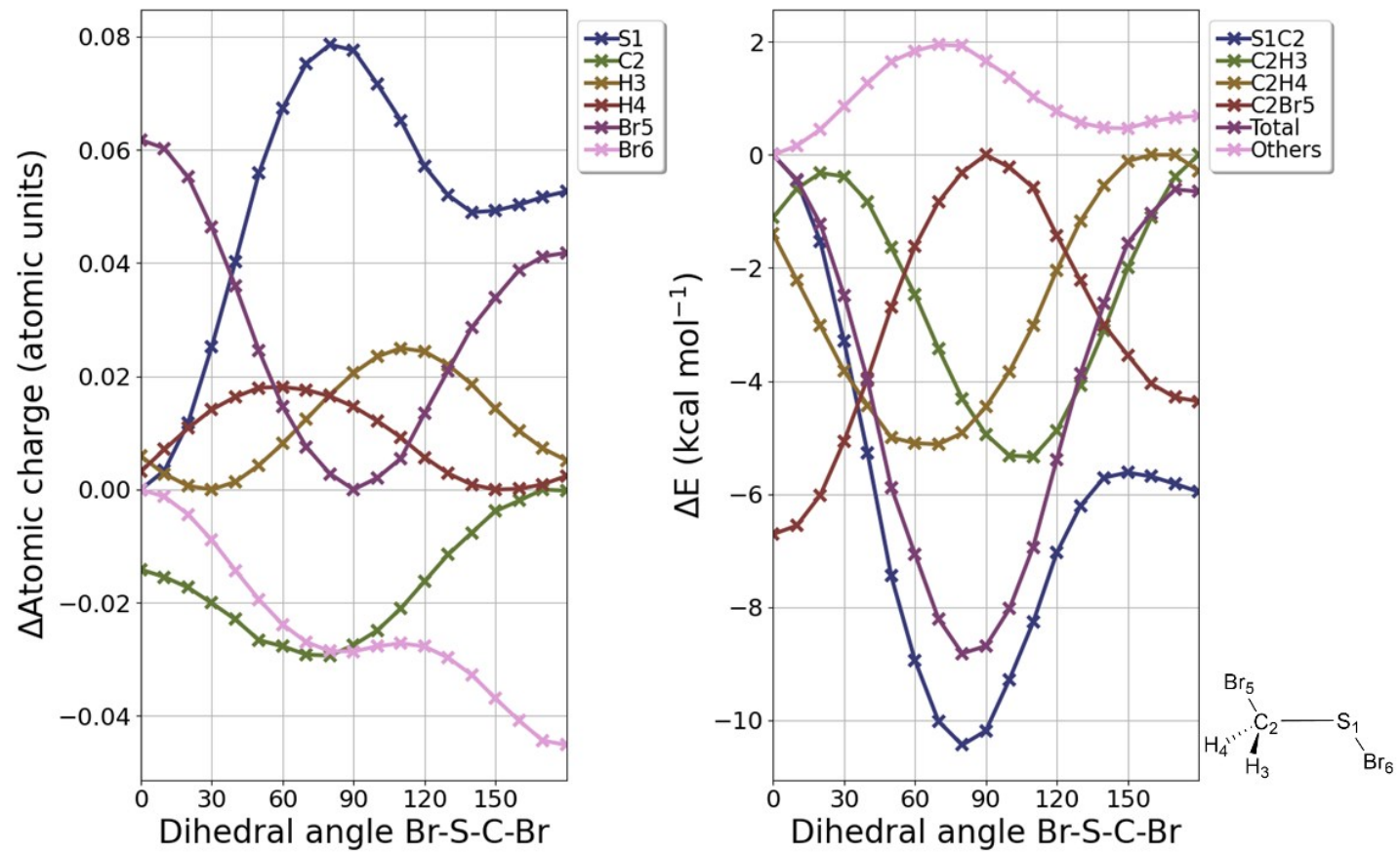


Figure S54 Atomic charges and natural Coulomb electrostatic (NCE) energy curves for BrCH_2SBr calculated at the M06-2X/6-311++G(3df,2p) level.

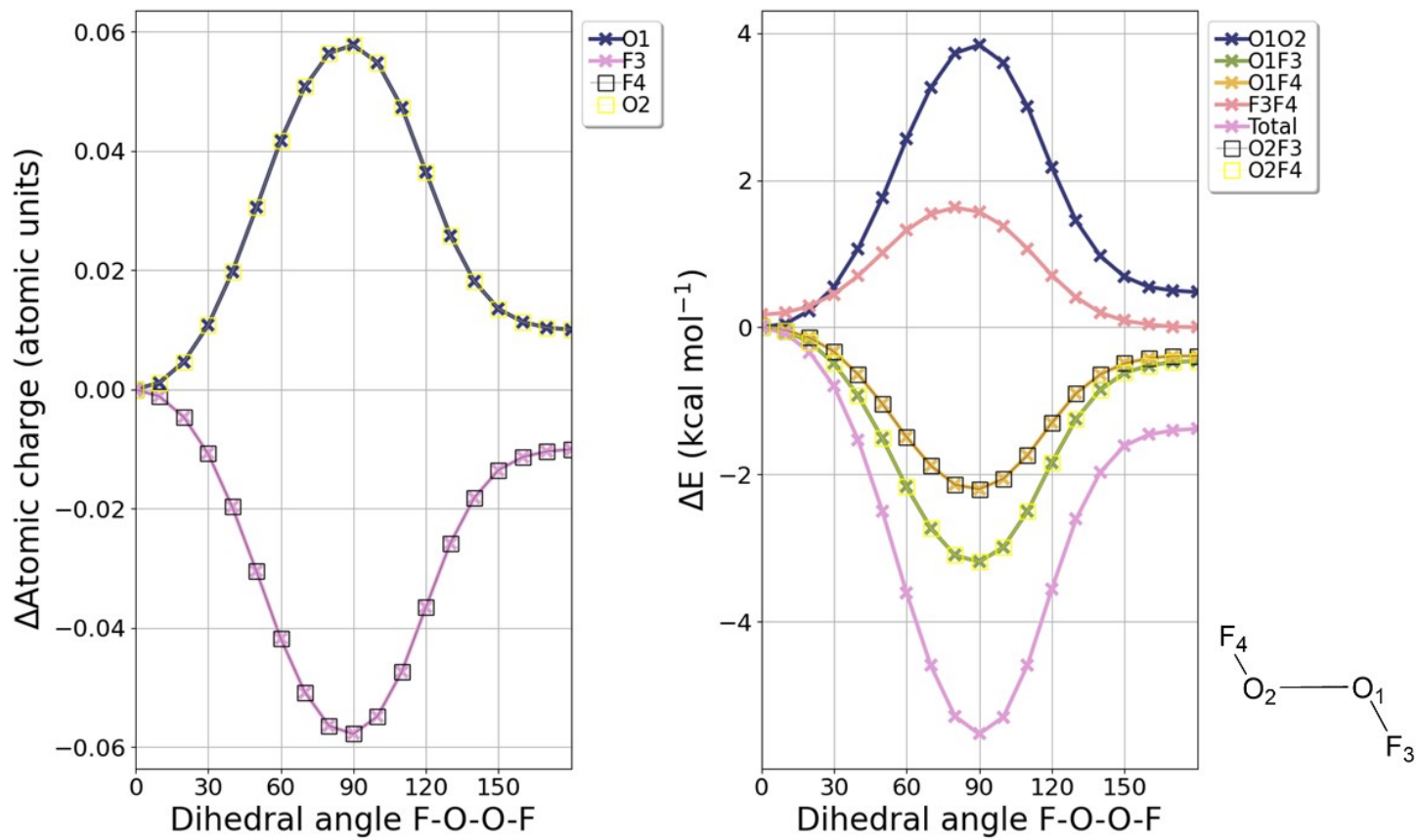


Figure S55. Atomic charges and natural Coulomb electrostatic (NCE) energy curves for FOOF calculated at the M06-2X/6-311++G(3df,2p) level.

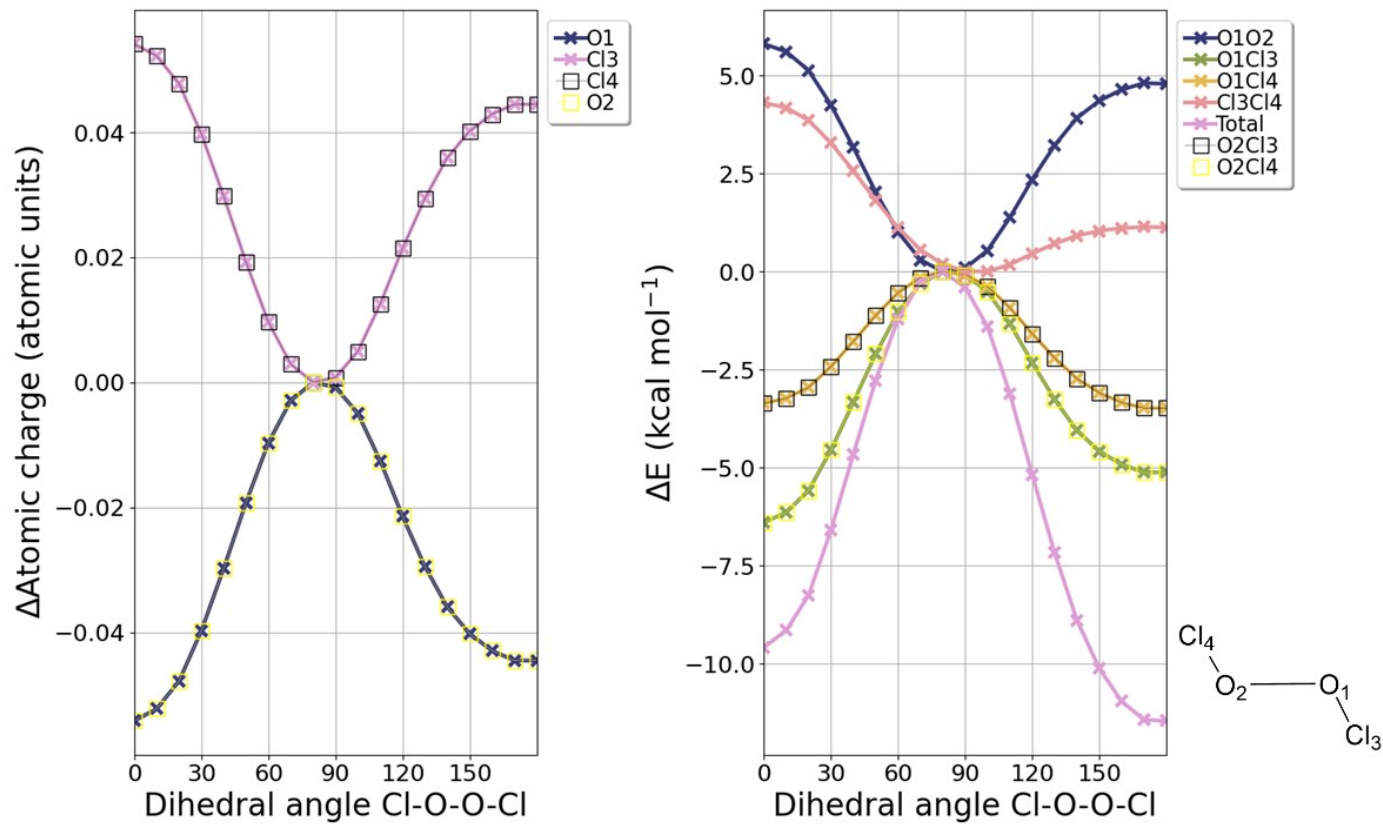


Figure S56. Atomic charges and natural Coulomb electrostatic (NCE) energy curves for ClOOCl calculated at the M06-2X/6-311++G(3df,2p) level.

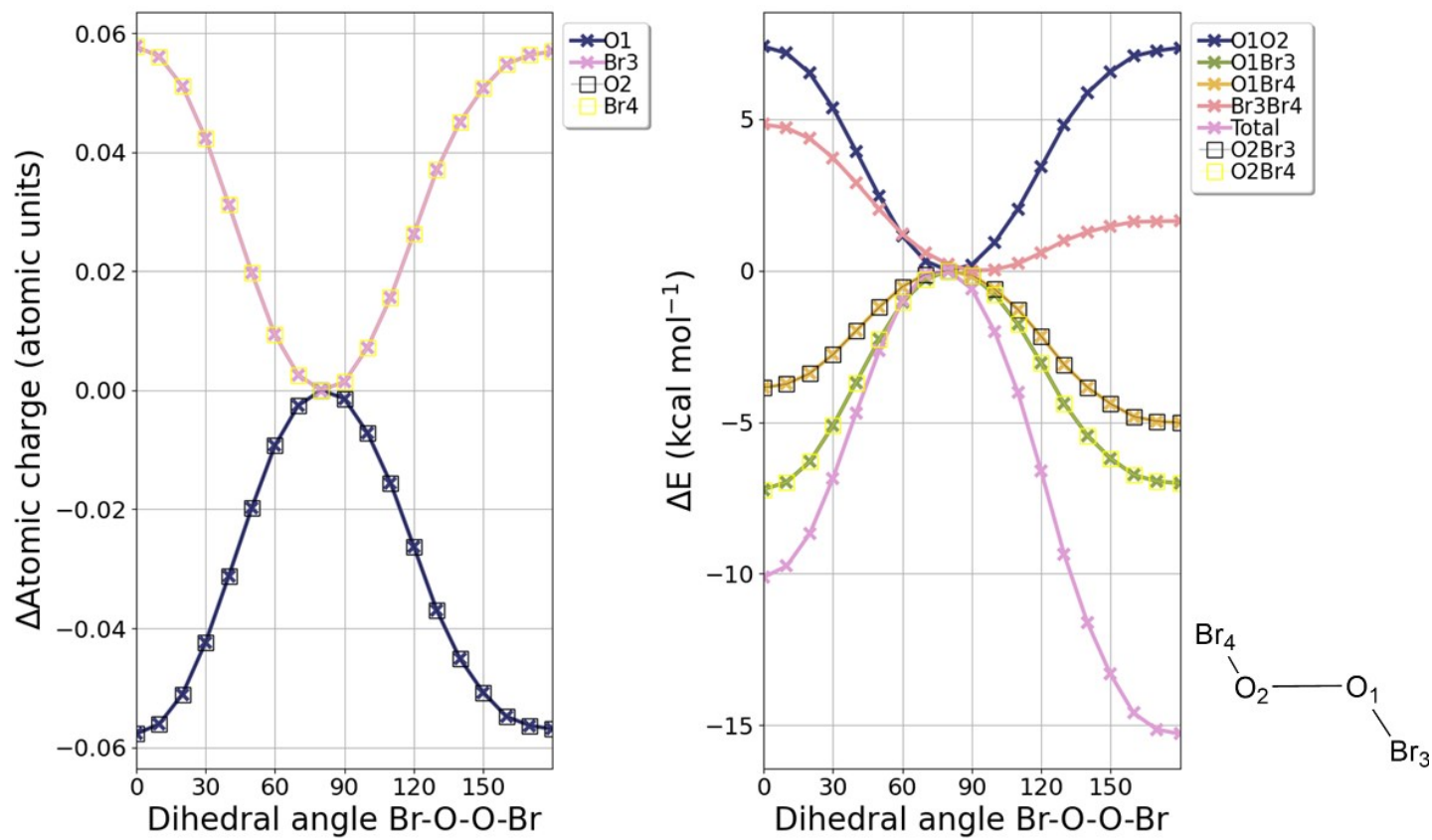


Figure S57. Atomic charges and natural Coulomb electrostatic (NCE) energy curves for BrOOBr calculated at the M06-2X/6-311++G(3df,2p) level.

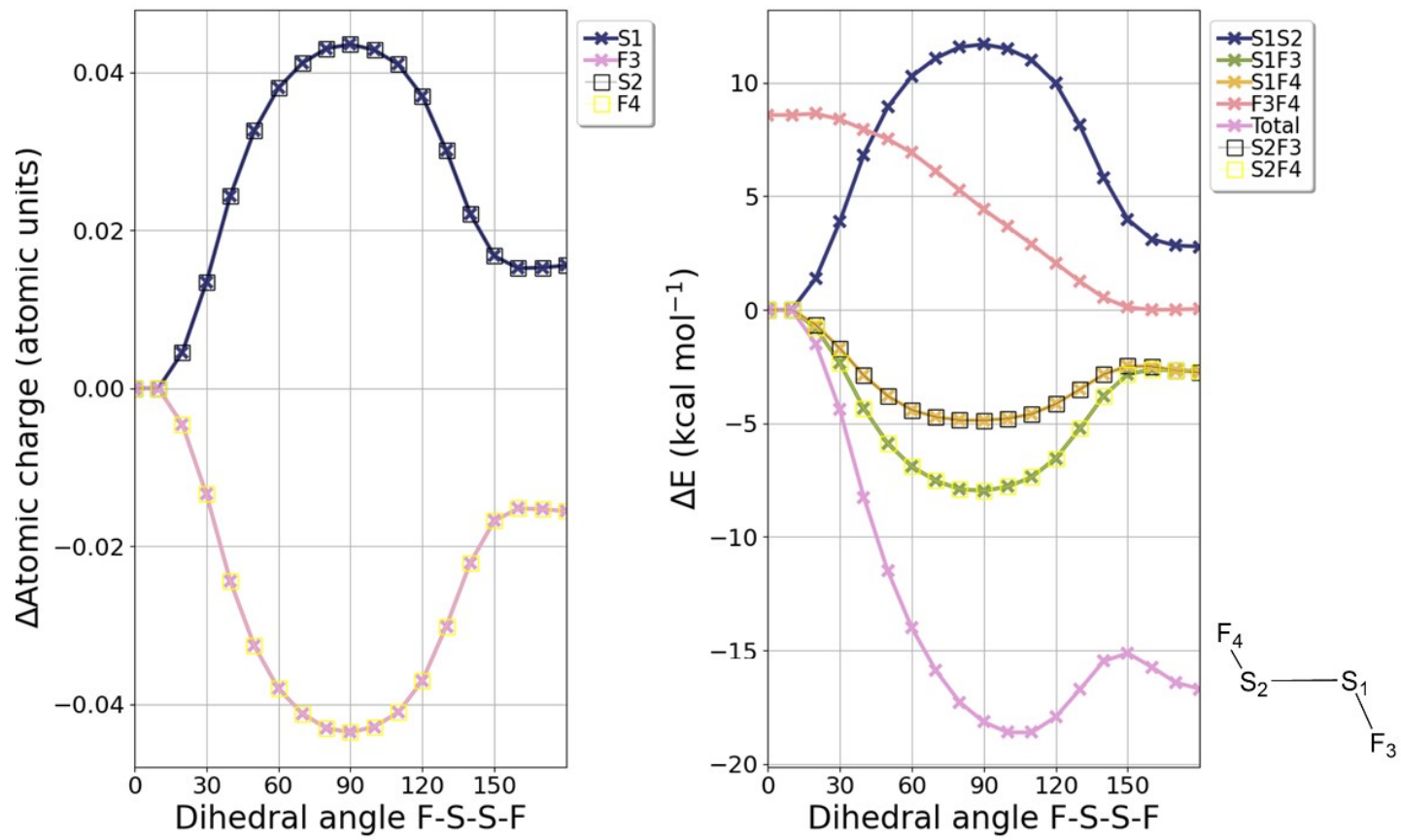


Figure S58. Atomic charges and natural Coulomb electrostatic (NCE) energy curves for FSSF calculated at the M06-2X/6-311++G(3df,2p) level.

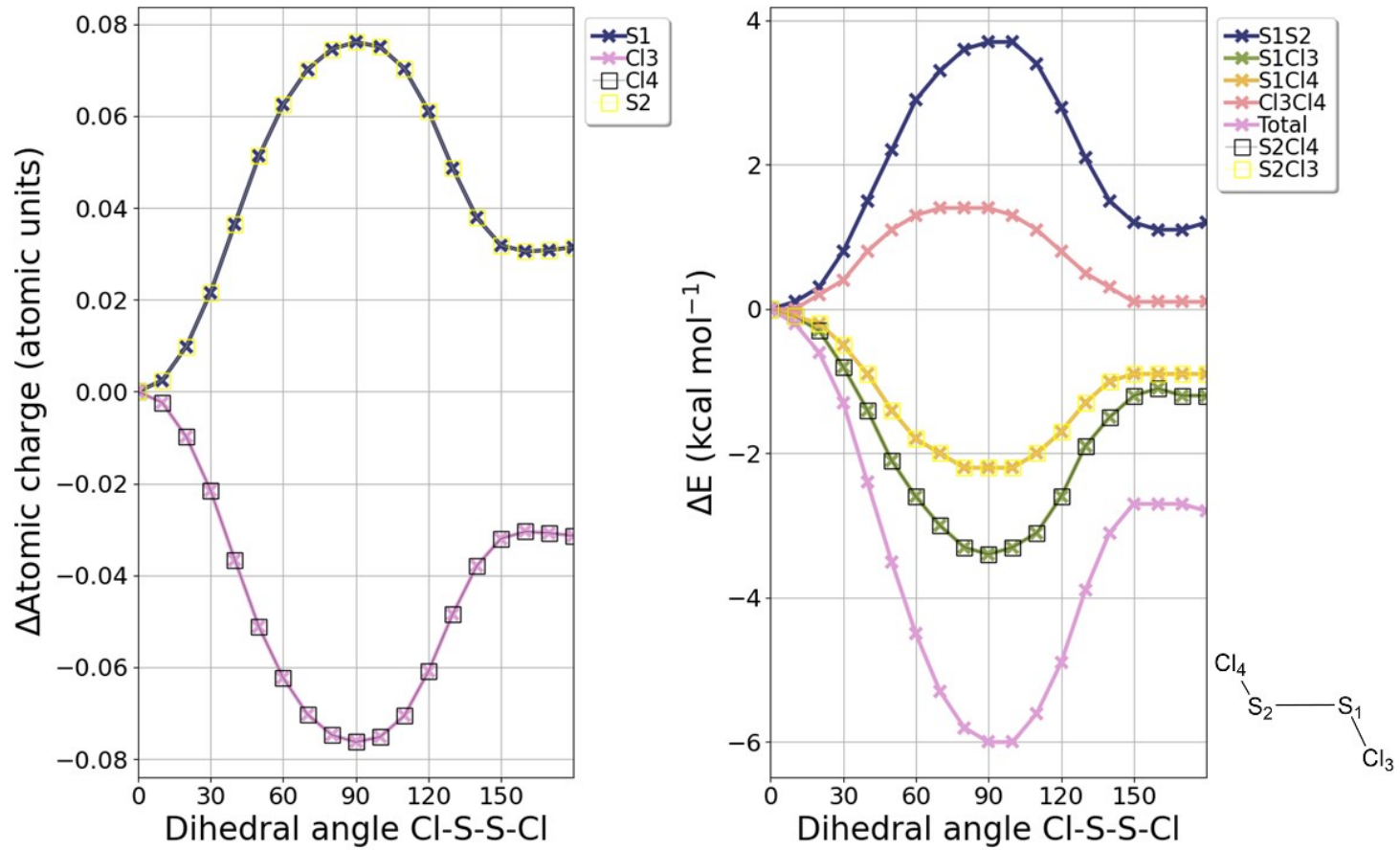


Figure S59. Atomic charges and natural Coulomb electrostatic (NCE) energy curves for ClSSCl calculated at the M06-2X/6-311++G(3df,2p) level.

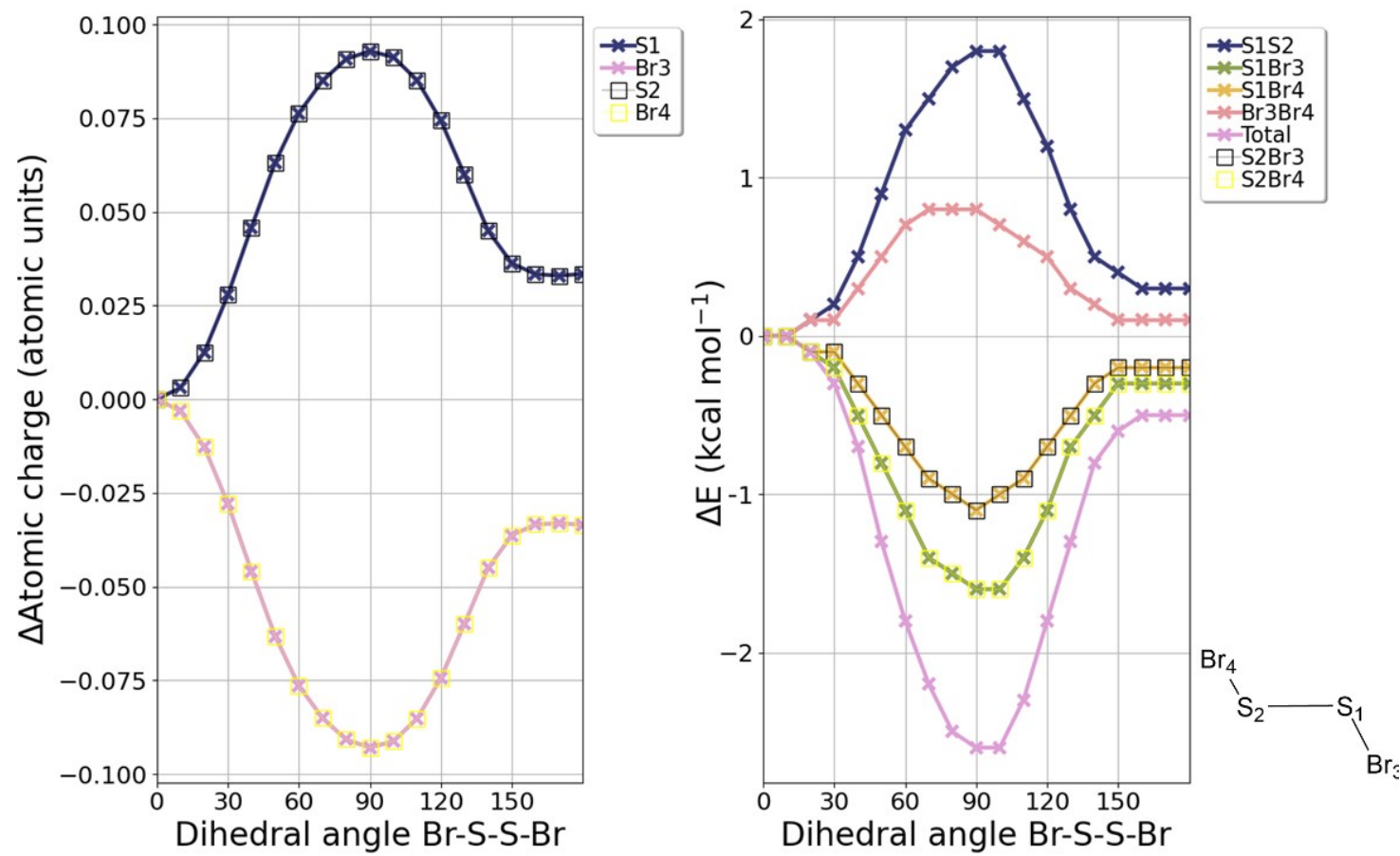
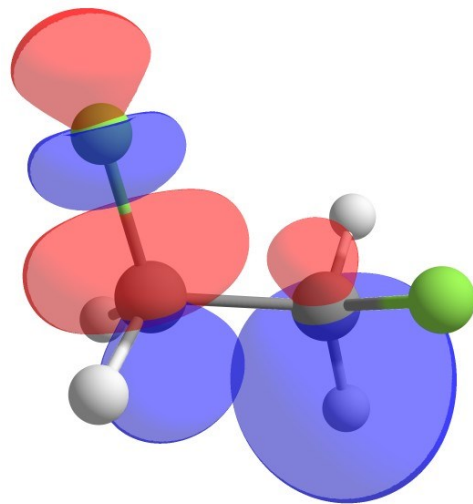
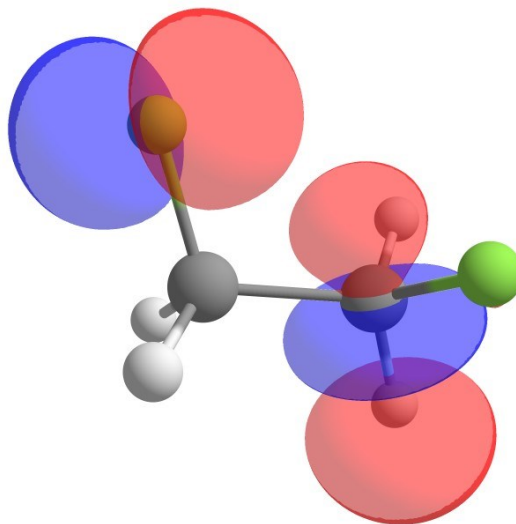


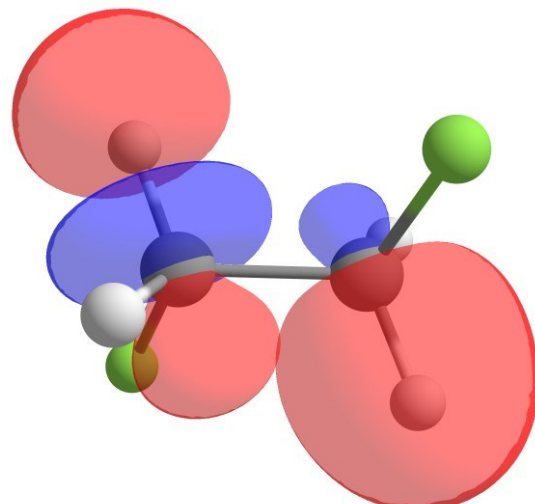
Figure S60. Atomic charges and natural Coulomb electrostatic (NCE) energy curves for BrSSBr calculated at the M06-2X/6-311++G(3df,2p) level.

a)

$$\sigma_{\text{CH}} \rightarrow \sigma^*_{\text{CF}}$$

b)

$$\text{LP}(2)\text{F} \rightarrow \sigma^*_{\text{CH}}$$

c)

$$\sigma_{\text{CH}} \rightarrow \sigma^*_{\text{CH}}$$

Figure S61. **a)** $\sigma_{\text{CH}} \rightarrow \sigma^*_{\text{CF}}$ and **b)** $\text{LP}(2)\text{F} \rightarrow \sigma^*_{\text{CH}}$ hyperconjugative interaction representations for the *gauche* and **c)** $\text{LP}(2)\text{F} \rightarrow \sigma^*_{\text{CH}}$ hyperconjugative interaction for the *anti* conformer of FCH₂CH₂F. All orbital isosurfaces were plotted with isovalues of 0.07 au.

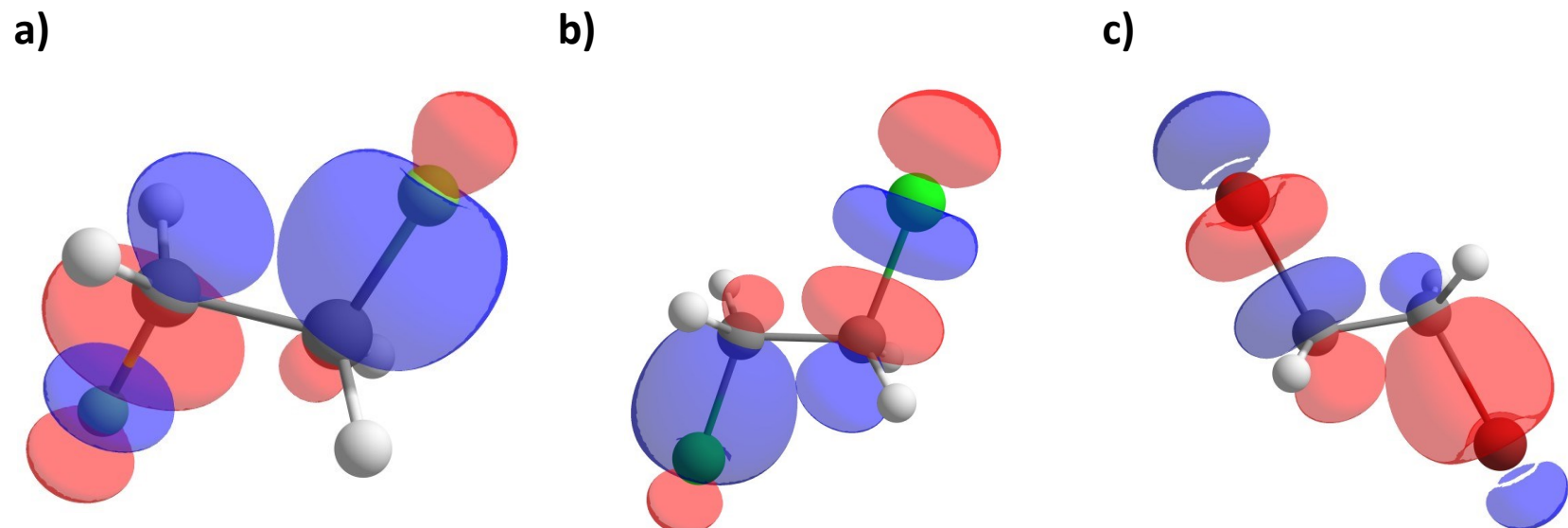


Figure S62. **a)** $\sigma_{\text{CF}} \rightarrow \sigma^*_{\text{CF}}$, **b)** $\sigma_{\text{CCl}} \rightarrow \sigma^*_{\text{CCl}}$ and **c)** $\sigma_{\text{CBr}} \rightarrow \sigma^*_{\text{CBr}}$ hyperconjugative interaction representations for the *anti* conformers of $\text{FCH}_2\text{CH}_2\text{F}$, $\text{ClCH}_2\text{CH}_2\text{Cl}$ and $\text{BrCH}_2\text{CH}_2\text{Br}$, respectively. All orbital isosurfaces were plotted with isovalue of 0.07 au.

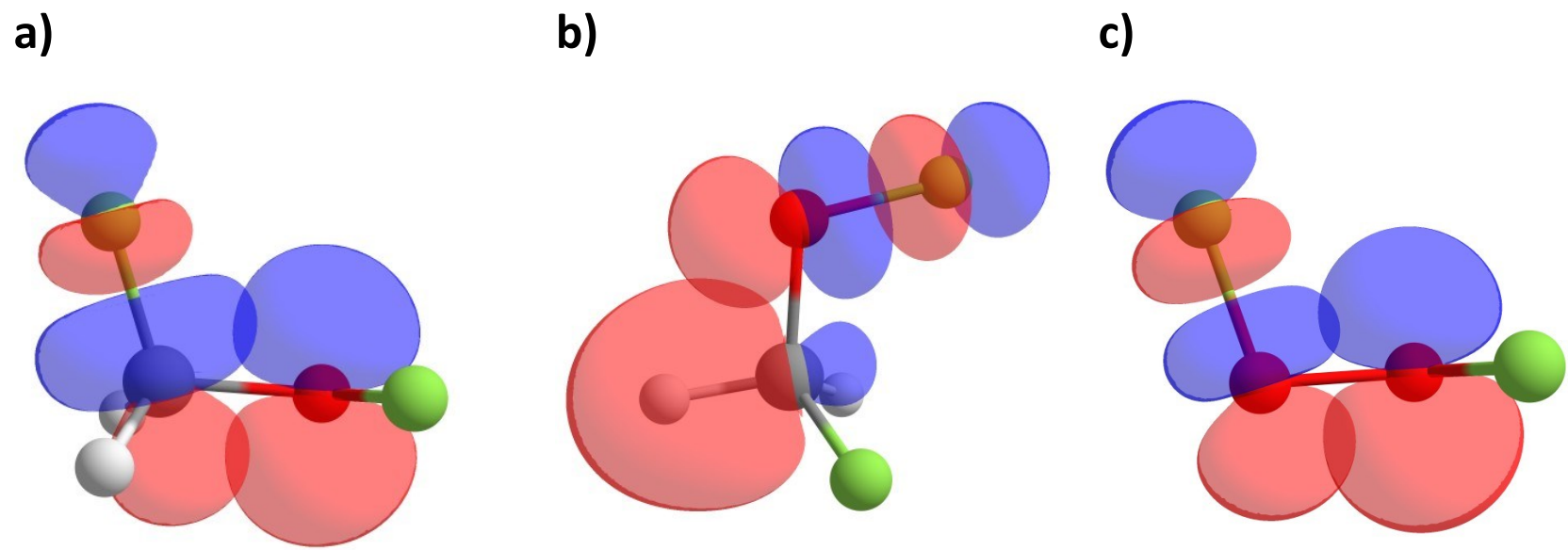


Figure S63. a) $\text{LP}(2)\text{O} \rightarrow \sigma^*_{\text{CF}}$ b) $\sigma_{\text{CH}} \rightarrow \sigma^*_{\text{OF}}$ hyperconjugative interactions for the *gauche* conformer of FCH_2OF and c) $\text{LP}(2)\text{O} \rightarrow \sigma^*_{\text{OF}}$ for the *gauche* conformer of FOOF . All orbital isosurfaces were plotted with isovalues of 0.07 a.u.

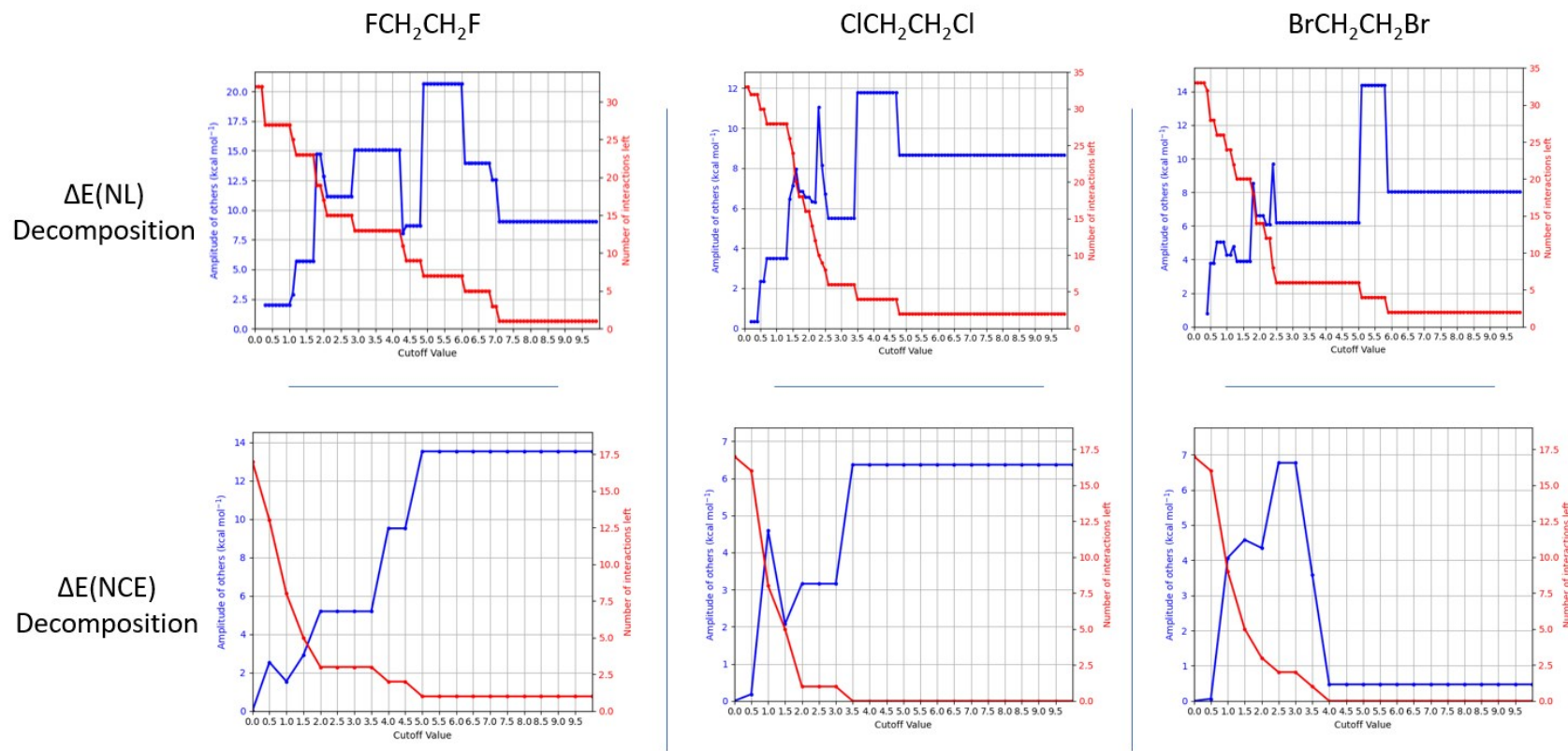


Figure S64. Number of remaining hyperconjugative interactions and the amplitude of the “Others” curve *versus* the cutoff value for the decomposition of hyperconjugative interactions and electrostatics interactions for $X\text{CH}_2\text{CH}_2\text{X}$ molecules.

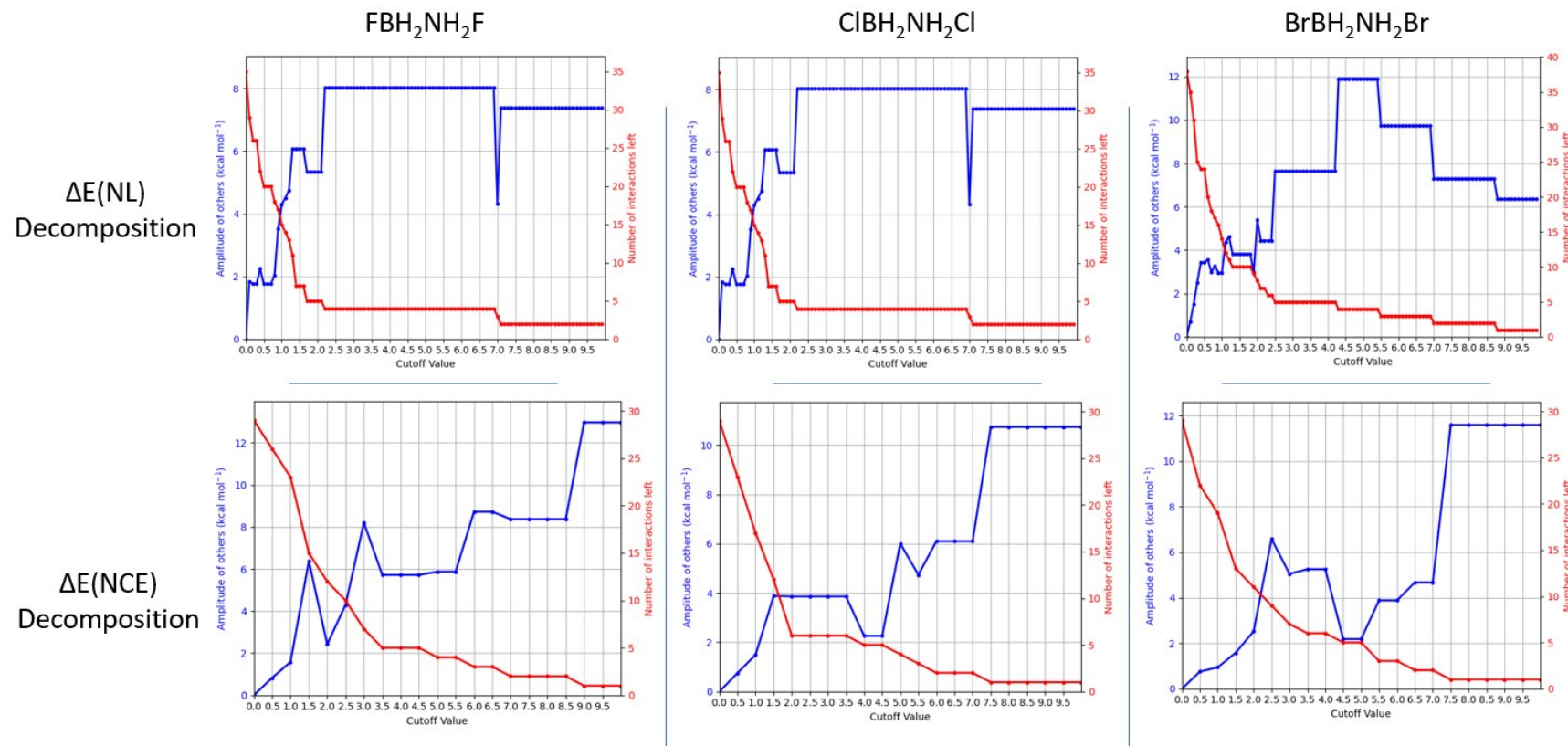


Figure S65. Number of remaining hyperconjugative interactions and the amplitude of the “Others” curve *versus* the cutoff value for the decomposition of hyperconjugative interactions and electrostatics interactions for XBH₂NH₂X molecules.

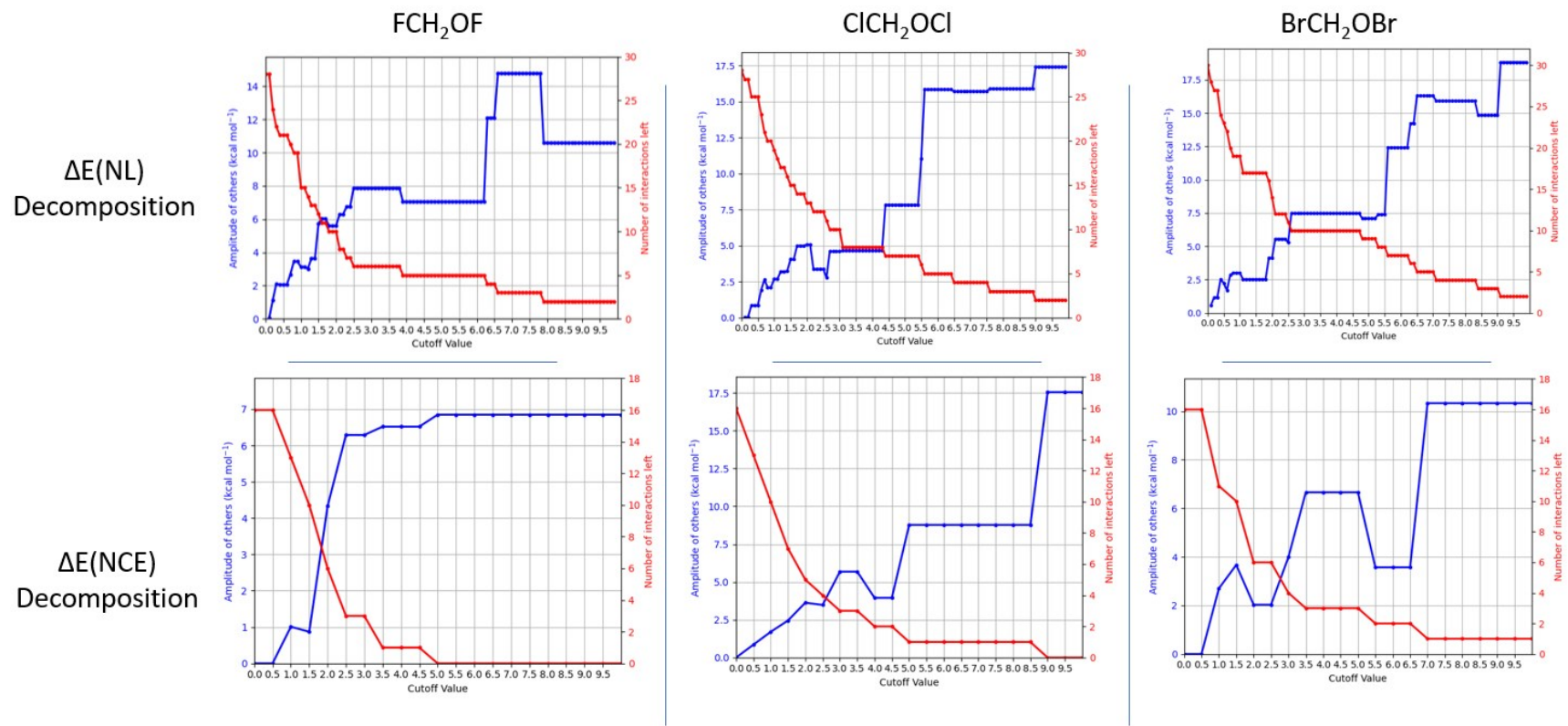


Figure S66. Number of remaining hyperconjugative interactions and the amplitude of the “Others” curve *versus* the cutoff value for the decomposition of hyperconjugative interactions and electrostatics interactions for XCH_2OX molecules.

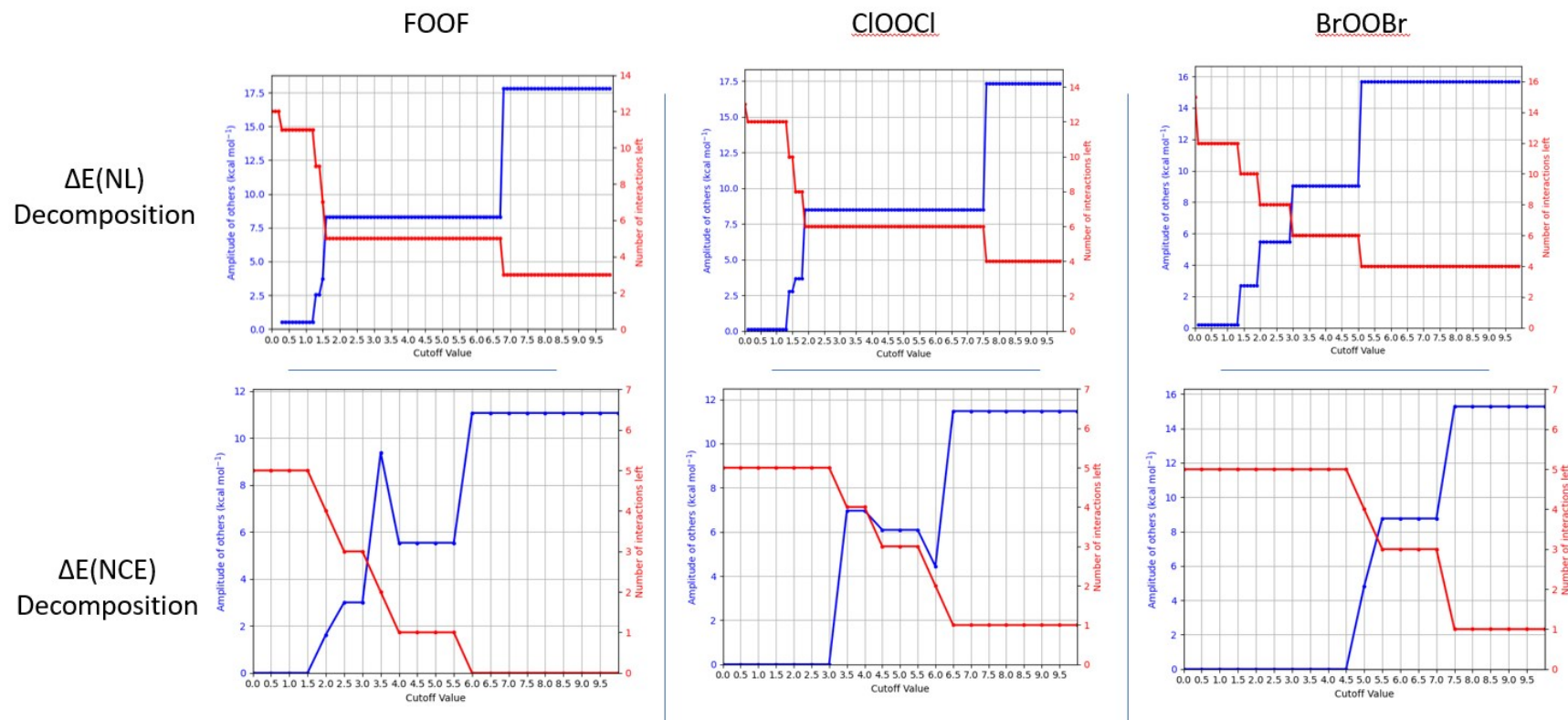


Figure S67. Number of remaining hyperconjugative interactions and the amplitude of the “Others” curve *versus* the cutoff value for the decomposition of hyperconjugative interactions and electrostatics interactions for XOOX molecules.

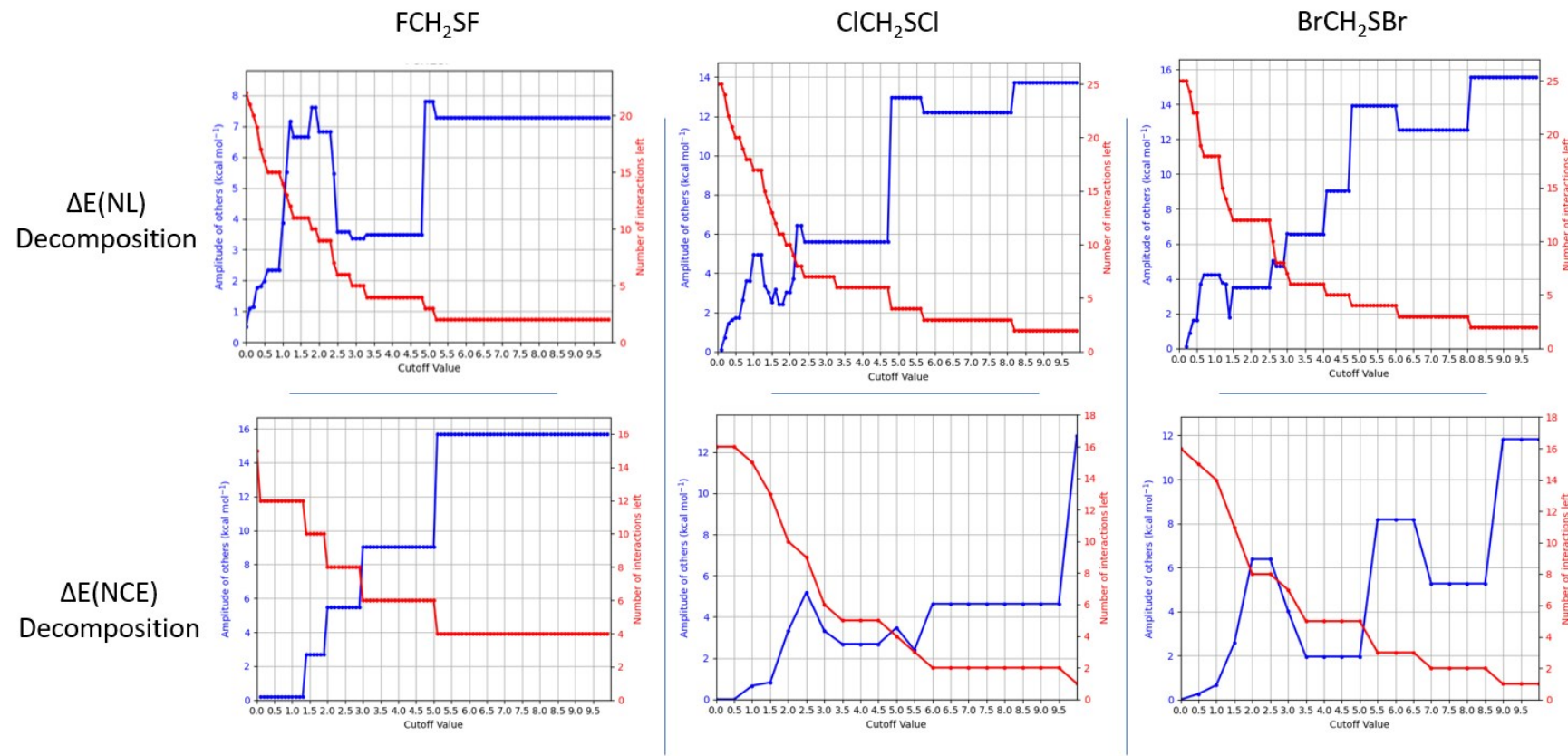


Figure S68. Number of remaining hyperconjugative interactions and the amplitude of the “Others” curve *versus* the cutoff value for the decomposition of hyperconjugative interactions and electrostatics interactions for XCH_2SX molecules.

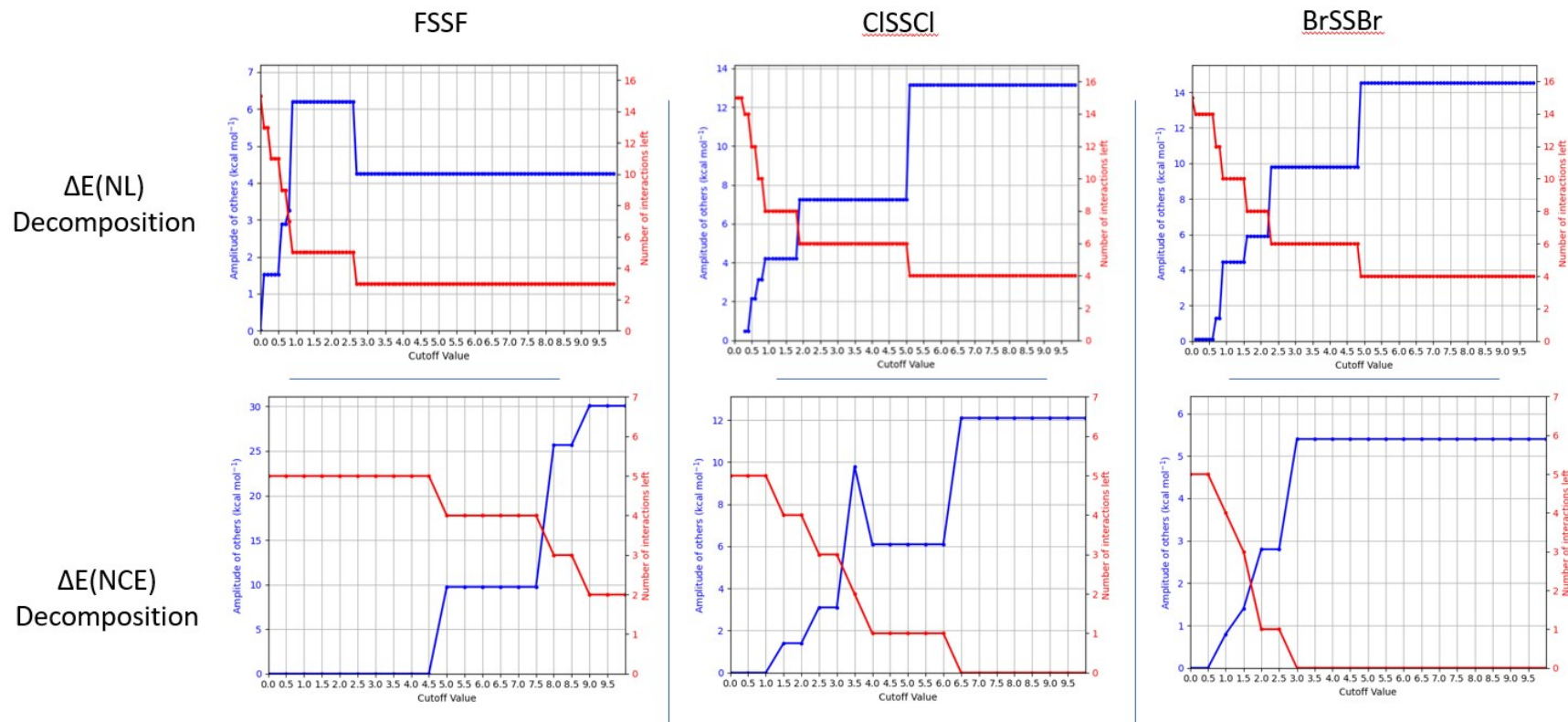


Figure S69. Number of remaining hyperconjugative interactions and the amplitude of the “Others” curve *versus* the cutoff value for the decomposition of hyperconjugative interactions and electrostatics interactions for XSSX molecules.



Figure S70. NBO deletion analysis calculated for CF_3OOCF_3 at the M06-2X/6-311++G(3df,2p) level

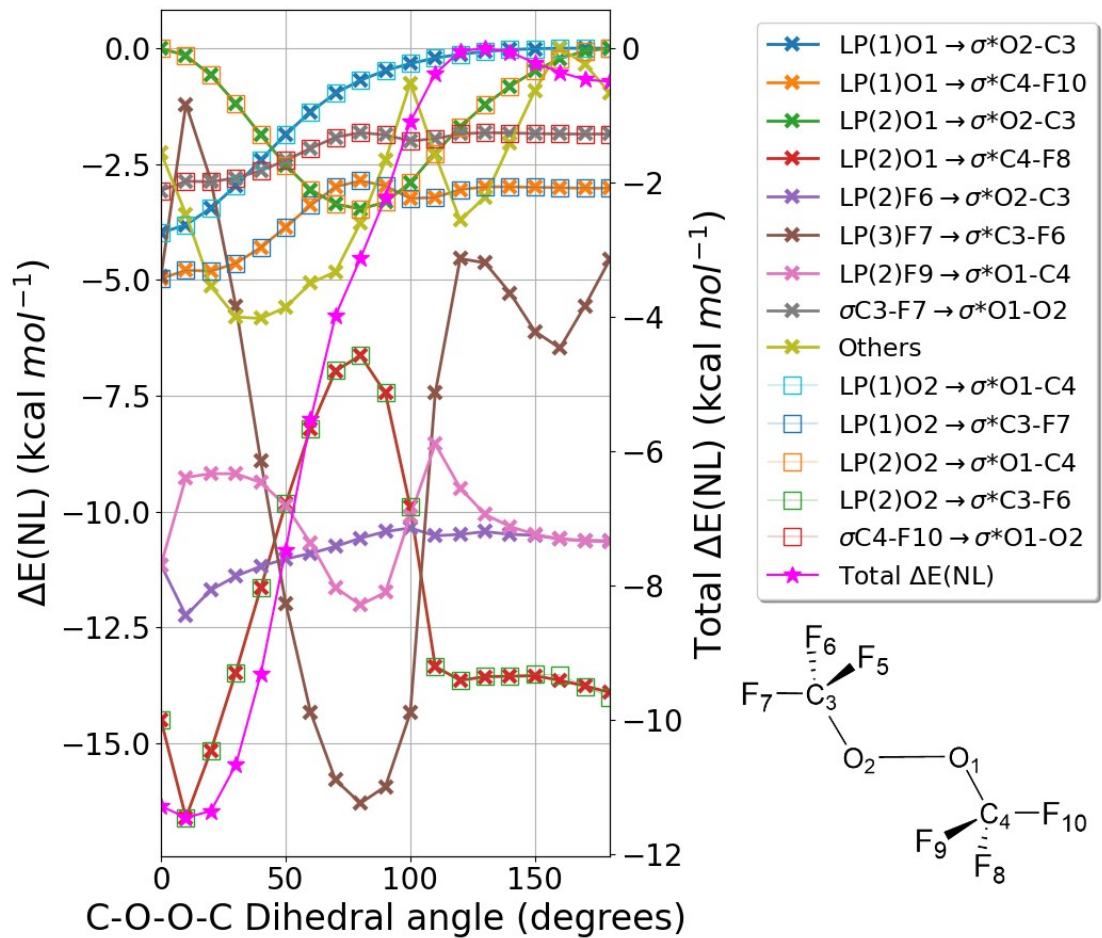


Figure S71. Hyperconjugation interaction energies for CF_3OOCF_3 obtained at the M06-2X/6-311++G(3df,2p) level using NBO analysis.

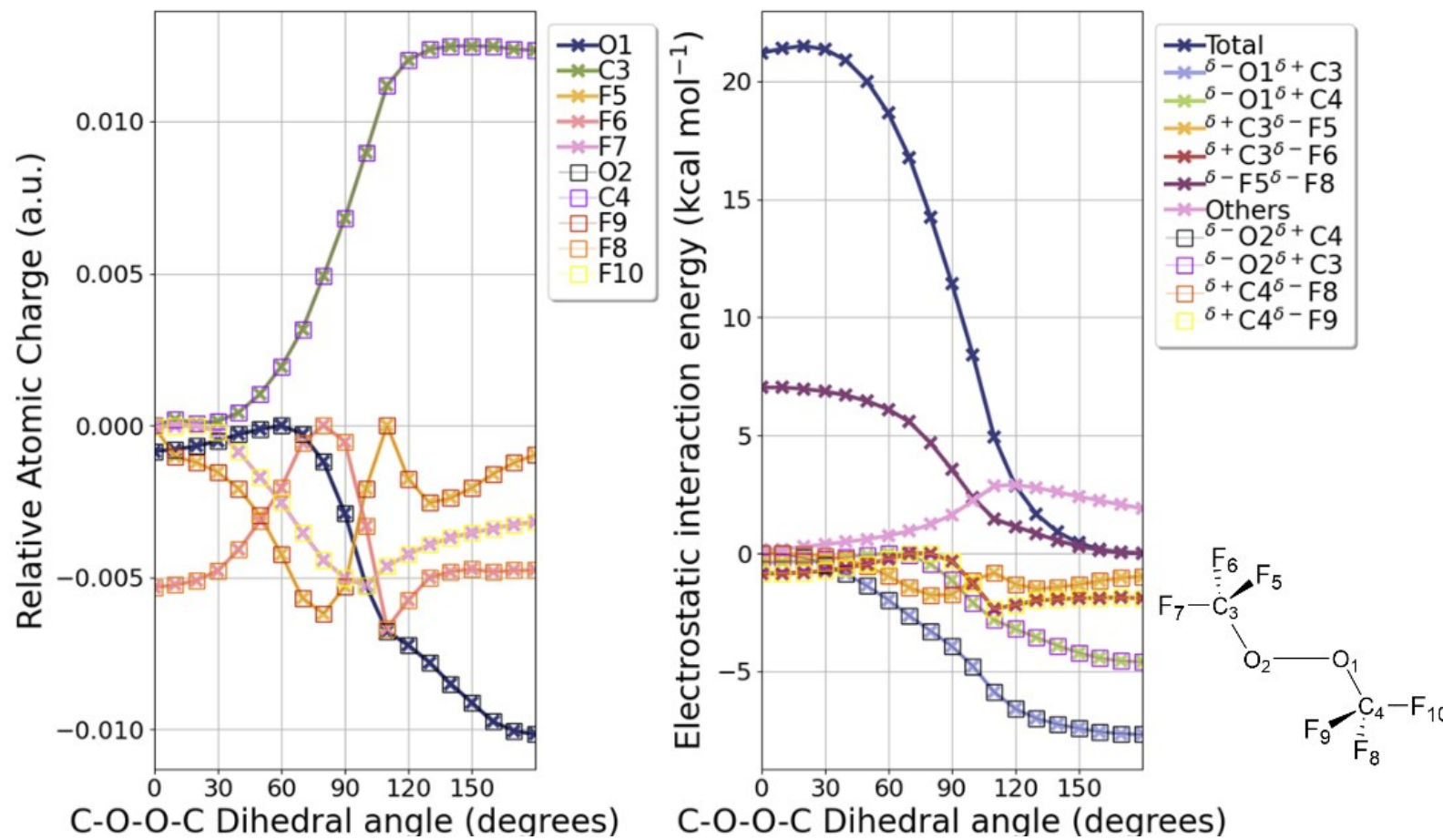


Figure S72. Atomic charges and natural Coulomb electrostatic (NCE) energy curves for CF_3OOCF_3 calculated at the M06-2X/6-311++G(3df,2p) level.